Histone deacetylase inhibitors reverse resistance to methylating agents: mechanisms in malignant melanoma and glioblastoma cells

Dissertation

Zur Erlangung des Grades

Doktor der Naturwissenschaften

Am Fachbereich Biologie

Der Johannes Gutenberg-Universität Mainz

Andrea Krumm geb. am 16. September 1986 in Wismar

Mainz, 2016

Dekan:

1. Berichterstatter:

2. Berichterstatter:

Tag der mündlichen Prüfung: 10. Februar 2016

Die vorliegende Arbeit wurde in der Zeit von April 2012 bis Dezember 2015 am Institut für Toxikologie der Universitätsmedizin Mainz angefertigt und wird am Fachbereich Biologie der Johannes Gutenberg Universität (D77) eingereicht.

Table of Contents

1 Summary

The aggressive characteristics of metastatic melanoma and glioblastoma necessitate DNA-damaging therapies, in particular with methylating agents such as Temozolomide (TMZ) or Dacarbazine (DTIC). However, the efficacy of therapy is limited by resistance factors such as DNA repair, DNA damage signaling and impaired apoptosis execution. Histone deacetylase (HDAC) inhibitors have proven antineoplastic as they are associated with cell cycle and apoptosis regulation as well as with DNA repair. Therefore, this study investigated whether HDAC inhibition enhances the efficacy of DNA damaging therapies in malignant melanoma and glioblastoma cell lines as well as its influence on DNA damage-resistance pathways.

First, it was shown that malignant melanoma cells express high levels of class I HDACs HDAC1, HDAC2 and HDAC3 in comparison to non-cancerous cells. Pre-treatment inhibition of these HDACs by valproic acid or Entinostat enhanced the apoptotic response of melanoma cells to the methylating agent TMZ, the chloroethylating agent Fotemustine and to ionizing radiation without sensitizing primary melanocytes. This work proposes that HDAC inhibition sensitizes melanoma cells to DNA damaging insults by downregulating proteins involved in homologous recombination (HR) repair of replication-dependently formed DNA double-strand breaks (DSBs), which leads to an increase in apoptosis. This is substantiated by the following observations obtained in this study: Inhibition of class I HDACs reduced the expression of the HR factors RAD51 and FANCD2 on transcript and protein level. The resulting functional impairment of HR decreased the repair of DSBs by this pathway and increased the sensitivity to PARP1 inhibition, which relies on HR derogation. Consequently, HDAC inhibition increased replication dependent DSB formation following TMZ exposure. The protective role of HR in melanoma TMZ toxicity was confirmed by RAD51 knockdown experiments. RAD51 knockdown cells were more susceptible to TMZ-induced apoptosis than the corresponding control lines.

In glioblastoma cells, half of the tested cell lines exhibited increased TMZ-induced cell death in combination with the HDAC inhibitor Entinostat. The findings support a possible mechanism whereby HDAC inhibition disrupts DNA damage signaling in glioblastoma cells and alters the cell cycle regulation in response to TMZ, leading to apoptosis. TMZ treatment activated the DNA damage signaling kinases ATM/ATR, whereas in combination with Entinostat, ATM/ATR activation was abolished. Similarly, TMZ-induced downstream signaling to checkpoint kinases (CHK1/CHK2) as well as the following p53 stabilization and expression of the cell cycle regulator $p21^{Cip1/Waf1}$ were abrogated in the presence of Entinostat. Further, HDAC inhibition protected from endoreplication upon TMZ-treatment and instead induced apoptosis in glioblastoma cells.

In conclusion, this work demonstrates that class I HDAC inhibitors are DNA damage sensitizers in cancer cells. This HDAC inhibitor-mediated sensitization is due to the impairment of RAD51 and

FANCD2 dependent HR repair in melanoma cells, or due to the premature shutdown of DNA damage signaling in glioblastoma cells. As inhibitors like valproic acid and Entinostat are well-tolerated in patients, the combination of adjuvant HDAC inhibition with methylating agents is a reasonable approach for improving therapeutic efficacy. Since acting on general DNA damage resistance pathways, HDAC inhibition might further provide a way for combination with genotoxic agents other than the common O^6-alkylating, thereby circumventing the major resistance factor O^6-methylguanine-DNA methyltransferase.

2 Introduction

2.1 Cancer

Cancer denotes malignant neoplasms of various origins, most frequently arising from prostate, breast, cervix, lung or colon that collectively caused 8.2 million deaths worldwide in 2012 (Stewart *et al.*, 2014). The reasons for its malignancy include unlimited proliferative capacity, resistance to cell death induction, genomic instability and the potential to metastasize. These features develop through inactivation of tumor suppressor genes (TSGs), which are typically responsible for cell cycle or cell death control, as well as by activation of oncogenes that drive proliferation (Hanahan and Weinberg, 2011). These alterations are the consequence of either changes of the base sequence of DNA (mutations), induced for instance by chemicals or radiation, or they originate from changes in gene expression caused by epigenetic means, which do not change the DNA sequence. Tumors can generally be staged by their size and invasiveness from stage I, which is localized and small, until stage IV, which describes an aggressive tumor linked to poor prognoses that has often metastasized to different parts of the body. Examples of two stage IV tumor types that resist therapy and therefore display low survival are malignant melanoma and glioblastoma multiforme (GBM).

2.1.1 Malignant melanoma

Cutaneous melanoma belongs to the five most frequently diagnosed cancers in Germany, out of which, approximately 7-8 % have metastasized and show low 5-year-survival rates ranging between 10-25 % (Kaatsch *et al.*, 2009/2010; Balch *et al.*, 2009). It develops from melanocytes that reside in the epidermal layer of the skin. There they produce the pigment eumelanin to protect epidermal cells against ultraviolet (UV) radiation-induced DNA lesions (Brenner and Hearing, 2008). Paradoxically, UV radiation is also the main risk factor for melanoma development, which predominantly affects fair-skinned populations (SEER - The Surveillance, Epidemiology, and End Results, 2015). This can be explained by lower eumelanin production in fair-skinned individuals and consequently lower protection against UV radiation (Brenner and Hearing, 2008; Vincensi *et al.*, 1998; Meredith and Sarna, 2006). The higher energy spectrum of sun-emitted UV radiation that reaches the earth's surface (namely, UVB) induces pre-mutagenic cyclobutane-pyrimidine dimers (CPD) that, if not repaired, are prone to be converted into so-called 'UV signature mutations' by DNA replication; predominantly cytosine-to-thymine-transitions (You *et al.*, 2001). The role of UV as the main reason for melanoma development is underlined by the finding that melanomas do not only bear the highest mutation load among cancers (Hodis *et al.*, 2012), but that the vast majority of them are C→T transitions. Genes commonly found modified by these mutations in melanoma cells are the cyclin-dependent-kinase-inhibitor 2A (*CDKN2A*) locus, tumor suppressor *TP53* or

different targets in the mitogen-activated protein kinase (MAPK) pathway (Hodis *et al.*, 2012; TCGA, 2015).

More than 20 % of melanomas carry a mutation in *CDKN2A* that encodes for two proteins, both of them controlling the G1/S cell cycle checkpoint: one of them, $p16^{INK4a}$, by inhibiting cyclin-dependent-kinase 4 and 6 (CDK4/CDK6) (Serrano *et al.*, 1993), the other, $p14^{ARF}$, by binding to and inhibiting the E3-ligase MDM2, which leads to stabilization of p53 (Stott *et al.*, 1998). Another 20 % of melanomas harbor a mutation in *TP53* (Hodis *et al.*, 2012).

The MAPK pathway regulates proliferation, differentiation and apoptosis in response to various activators like cytokines, growth factors or DNA damage. It refers to a phosphorylation cascade that can be activated by small GTPases of the rat sarcoma (RAS) family. One member, *NRAS*, is mutated in approximately 20 % of melanomas, which leads to more effective GTP-binding, lower intrinsic ATPase activity and therefore higher activation of its target proteins, namely rapidly accelerated fibrosarcoma (RAF) kinases. The B-RAF-kinase plays a pivotal role in melanoma as its gene is mutated in 50-60 % of melanomas, yielding a constitutively active protein (Hodis *et al.*, 2012). Since activation of the MAPK pathway is a common feature of melanoma, leading to increased cell proliferation and survival, its targeting is a novel therapy approach that will be discussed in 2.1.1.1.

Even though mutations fundamentally account for oncogenic transformation in melanomagenesis, epigenetic changes also play an important role. These comprise genome-wide DNA hypomethylation and loss of 5'hydroxymethylcytosine (Lian *et al.*, 2012), an intermediate of active DNA demethylation, both of which are prognostic and diagnostic markers for melanoma. Despite the genome-wide decrease in DNA methylation, promoter specific methylation increases for certain genes, leading to the suppression of the corresponding gene product. This applies, for instance, to the DNA repair gene O^6-methylguanine-DNA methyltransferase (*MGMT*) that is silenced in 38 % of melanomas (Hassel *et al.*, 2010) and removes therapy-induced DNA lesions. However, its impact on therapy outcome is still under debate (Hassel *et al.*, 2010; Tuominen *et al.*, 2015).

2.1.1.1 Therapy of metastatic melanoma

Currently, melanoma therapy aims at manipulating two novel targets i.e. the MAPK pathway and the immune response. B-RAF inhibitors like Vemurafenib or Dabrafenib interfere with the mutated, constitutively active B-RAF protein and show an increase in progression free survival of 3.5 months for patients with B-RAF-mutated tumors compared to patients treated with chemotherapy (Chapman *et al.*, 2011; Hauschild *et al.*, 2012). Additionally, inhibitors of mitogen-activated kinase kinases (MEK inhibitor) derogate the MAPK pathway and show a promising additional increase in progression free survival of three months in combination with B-RAF inhibition in B-RAF-mutated disease (Larkin *et al.*, 2014; Robert *et al.*, 2015).

In order to stimulate the immune response against melanoma cells, two drugs are being used that block receptors on T cells that negatively regulate T cell proliferation (Hodi *et al.*, 2010; Topalian *et al.*, 2014). Therefore, these drugs are also applicable in the treatment of B-RAF wild type (wt) tumors. Combination of both, the CTLA-4 antagonist Ipilimumab and PD-1 antagonist Nivolumab, resulted in a median progression free survival of 11 months, which is comparable to that of a combination of B-RAF inhibitor and MEK inhibitor and was observed irrespective of B-RAF status (Larkin *et al.*, 2015).

Despite the success of novel therapies, rapid development of resistance against these drugs (Flaherty *et al.*, 2012; Chapman *et al.*, 2011; Hauschild *et al.*, 2012; Hodi *et al.*, 2010; Topalian *et al.*, 2014) tempered expectations and required the subsequent use of chemotherapeutics, primarily with the methylating agents Dacarbazine (DTIC), Temozolomide (TMZ) or the chloroethylating agent Fotemustine (FM) (Dummer *et al.*, 2012). This makes alkylating agents a keystone in melanoma therapy, though resistance likewise reduces their efficacy. Mechanism of action and resistance to alkylating chemotherapeutics are discussed in 2.2 and 2.3.

In addition, radiation therapy is used in rare cases of symptomatic metastasis in the brain or near to bones (Dummer *et al.*, 2012).

2.1.2 Glioblastoma multiforme

GBM is a brain tumor belonging to neoplasms of glial cells (Glioma), which had an incidence of approximately 3/100 000 per annum in the United States between 2006 and 2010 (Ostrom *et al.*, 2013). GBM constitutes the major fraction of gliomas (54 %) (Ostrom *et al.*, 2013) and it is also the most aggressive with a median survival of 15 months (Stupp *et al.*, 2014a). It originates from oncogenic transformation of astrocytes and is highly invasive. Interestingly, only 10 % of GBM develop from lower grade astrocytomas (Ohgaki *et al.*, 2013), so-called secondary GBMs. In fact, most GBMs develop spontaneously *de novo* without any indications of precursor lesions (primary GBM). Both share a similar histology, but can be differentiated by genetic means, for instance mutations in isocytrate dehydrogenase (*IDH1/2*) are exclusively found in secondary GBMs (Ohgaki *et al.*, 2013). Genetic alterations differ greatly between primary and secondary GBMs, though they affect similar pathways that drive oncogenesis. Similar to melanomas, GBMs inactivate the G1/S cell cycle checkpoint thereby increasing proliferation. This is achieved by perturbing retinoblastoma protein (RB1) dependent S-phase gene regulation. This occurs in primary GBMs by homozygous deletions of *CDKN2A-p16*^{INK4a} and in secondary GBMs by promoter methylation mediated shutdown of *RB1* (Crespo *et al.*, 2015). Furthermore, alterations are also found in the p53 pathway (Brennan *et al.*, 2013). While secondary, and correspondingly less, GBMs harbor mutations in *TP53*, primary GBMs mainly loose *CDKN2A* and consequently p14^{ARF} expression leading to an uncontrolled degradation of p53 (Crespo *et al.*, 2015). Additional mechanisms whereby GBM cells increase their proliferation are the amplification of epidermal

growth factor receptor (EGFR) or its mutation, leading to a permanent activated state. This allows the cell to efficiently activate proliferative pathways like protein kinase B (AKT) or MAPK (Brennan *et al.*, 2013). GBMs further display a higher activity of the AKT pathway due to mutation or reduction of phosphatase and tensin homologue (PTEN) that physiologically abates AKT activation by dephosphorylation of phosphatidylinositol triphosphate, an attractor of AKT (Brennan *et al.*, 2013). As seen for PTEN, RB or MGMT, GBMs display characteristic mutations as well as epigenetic marks.

2.1.2.1 Therapy of Glioblastoma multiforme

Newly diagnosed GBM is removed by surgery, which removes an average 89 % of the tumor (Lacroix *et al.*, 2001) leading to symptomatic improvement and material for diagnostics. Only when more than 98 % of the tumor is resected, surgery is linked to a statistically significant improvement in patient survival (Lacroix *et al.*, 2001). Since it is impossible to remove the entire tumor burden, due to single cells invading the surrounding tissue, radiotherapy with concomitant TMZ-based chemotherapy is used. The MGMT promoter methylation status plays a significant role in therapy outcome (Stupp *et al.*, 2014a). Whereas patients with a methylated MGMT promotor respond with a median survival of 23.4 months in the combination treatment compared to 15.3 months with radiation alone, combination treatment of tumors with unmethylated MGMT promoter results in an minimal increase in median survival from 11.8 month to 12.6 month (Stupp *et al.*, 2009). Relapses might be treated with chloroethylating agents such as CCNU (Stupp *et al.*, 2014a).

2.2 Alkylating agents

Alkylating agents comprise a heterogeneous group of compounds that transfer alkyl groups to DNA. Exposure to environmental alkylating agents and endogenous alkylation of DNA seem to be rare events (Margison *et al.*, 2003; Rydberg and Lindahl, 1982). For clinical applications, agents that transfer the alkyl group via an S_N1 reaction to oxygens and nitrogens of DNA and RNA are predominantly used. Alkyl groups that are transferred by anti-neoplastic therapeutics are methyl- or chloroethyl-groups. Even though the mechanism of cytotoxicity differs greatly between the different alkyl groups, they are both able to block DNA replication either due to the induced lesion itself or due to toxic secondary lesions that form during their processing. They therefore target the fast-proliferating characteristic of tumor cells. This will be discussed in more detail in sections 2.2.1.1/2.2.2.1.

2.2.1 Methylating agents

Chemotherapeutics that transfer methyl groups to DNA include Procarbazine, Streptozotocin, DTIC and TMZ. As each molecule transfers one methyl group to its target they are referred to as mono-functional. DTIC requires metabolic activation by cytochromes P450, which catalyze its

demethylation to 5-(3-monomethyl-1-triazeno)imidazole-4-carboxamide (MTIC) (Reid *et al.*, 1999), whereas TMZ spontaneously hydrolyzes in aqueous solution (pH>7) to MTIC (Newlands *et al.*, 1997). Subsequent degradation of MTIC gives rise to the highly reactive methyldiazonium cation that reacts with nucleophilic sites of DNA, thereby transferring the methyl group (Figure 1).

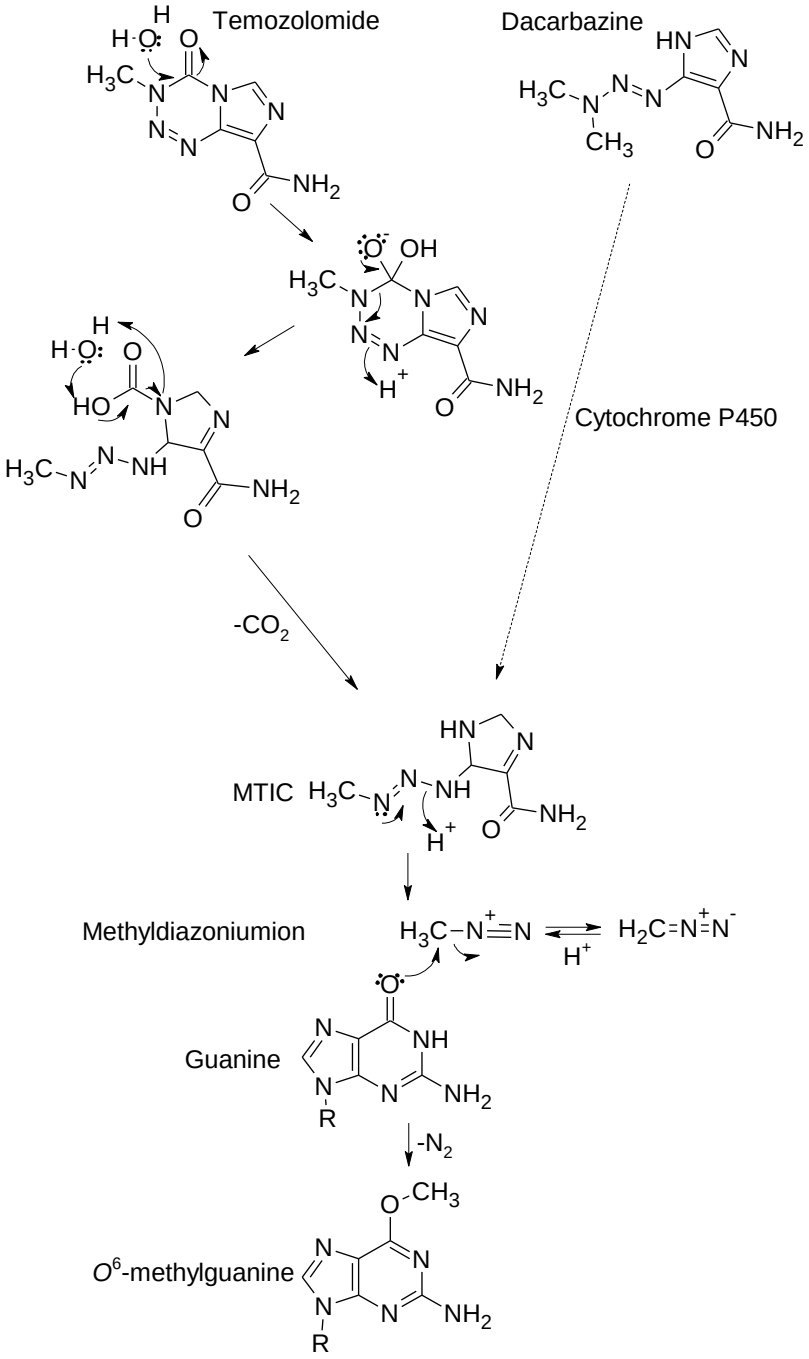

Figure 1 – Formation of O^6-methylguanine by TMZ and DTIC.
Hydrolysis of TMZ (left) and demethylation of DTIC (right) to MTIC followed by its degradation and transfer of the methyl group to guanine. Modified from (Newlands *et al.*, 1997; Reid *et al.*, 1999)

Out of the 13 targets in DNA that are methylated by monofunctional S_N1 methylating agents, the most frequently damaged site is *N*7-guanine (~70 %) forming *N*7-methylguanine (*N*7MeG), followed by *N*3-adenine (~10 %) forming *N*3-methyladenine (*N*3MeA). Both are regarded as harmless at clinical relevant doses, due to their efficient repair by base excision repair (BER) (2.3.1.2). In contrast, O^6-methylguanine (O^6MeG), which makes up only ~6-8 % of all induced DNA lesions (Drablos *et al.*, 2004; Beranek, 1990), is the most fateful lesion upon methylating agent exposure due to its high cytotoxic and mutagenic potential (Kaina *et al.*, 2007).

2.2.1.1 Toxicity of O^6-methylguanine

The most toxic lesion induced by clinically relevant S_N1 methylating agents is O^6MeG. If not repaired by MGMT (2.3.1.1.2), it is mutagenic during replication, forming mispairs with thymine at a ratio of 1:3 (Abbott and Saffhill, 1979; Choi *et al.*, 2006). O^6MeG opposite a misincorporated thymine might then be repaired by MGMT, converted from a G:C to an A:T transition during a second replication round or it might be recognized by mismatch repair (MMR) in an MGMT deficient and MMR proficient background. Processing by MMR generates single stranded DNA (ssDNA) intermediates (see 2.3.1.3) (Mojas *et al.*, 2007) and the missing strand is resynthesized in order to remove the mispair. However, since O^6MeG still exists in the template DNA, reinsertion of the wrong nucleotide may occur and repeatedly be processed by MMR. These futile MMR cycles might interfere with replication, if a replication fork encounters an ssDNA intermediate. This could lead to either a single-ended DSB if the fork collapses (Figure 2) or to a stall and regression of the replication fork. Re-initiation of DNA replication in both cases requires homologous recombination (HR), giving rise to sister chromatid exchanges (SCEs) (Roos *et al.*, 2009). If replication cannot be resumed by HR, cells undergo apoptosis. The demonstrated model of how O^6MeG exerts its cytotoxic effects is substantiated by strong experimental data. The MutSα complex has been shown to bind to O^6MeG-thymine as well as to O^6MeG-cytosine pairs (Duckett *et al.*, 1996). Consequently, O^6MeG-related apoptosis induction depends on MMR proficiency. Absence of MMR and accordingly prevention of ssDNA intermediates upon O^6MeG prevents induction of SCEs and chromosomal aberrations (Branch *et al.*, 1993; Galloway *et al.*, 1995; Hickman and Samson, 1999; Kaina *et al.*, 1997; Vernole *et al.*, 2003). Further, apoptotic signaling and execution require at least two cell cycles of damage processing (Quiros *et al.*, 2010). Additionally, low doses of e.g. *N*-methyl-*N*'-nitro-*N*-nitrosoguanidine (MNNG), a methylating agent with similar chemistry to TMZ, lead to an accumulation of aberrations and SCEs whereas higher doses result in apoptosis induction (Kaina, 1985; Kaina and Aurich, 1985), which hints to a tolerable and HR-repairable load of O^6MeG that is exceeded at higher concentrations. The role of HR is also seen in cells with reduced HR capacity, which show increased sensitivity to S_N1-methylating agents (Quiros *et al.*, 2011; Roos *et al.*, 2009).

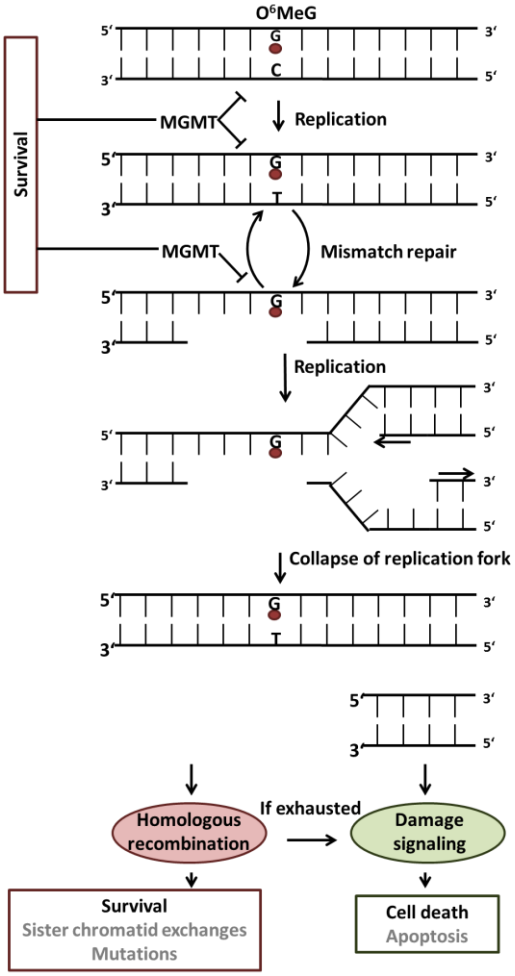

Figure 2 – Toxicity of *O*^{6}-methylguanine.
Processing of *O*^{6}-methylguanine and mechanisms involved in survival and cell death. Modified from (Fu *et al.*, 2012). Details are described in 2.2.1.1.

2.2.2 Chloroethylating agents

Another group of alkylating chemotherapeutics consists of chloroethylnitrosourea (CENU) derivatives that transfer chloroethyl groups onto DNA. The mono-functional S_N1-reacting agents Lomustine (CCNU) and Fotemustine (FM) are approved for second line therapy of GBM and metastatic melanoma, respectively. They spontaneously hydrolyze in aqueous solution to chloroethyldiazonium hydroxide that further decomposes into nitrogen and a chloroethyl carbonium ion, which reacts most notably with *N*7-guanine and *O*^{6}-guanine giving rise to *N*7-chloroethylguanine and *O*^{6}-chloroethylguanine, respectively (Ludlum, 1997; Bodell, 2009). Again, chloroethylation of the *O*^{6}-guanine position exhibits the highest biological relevance as it firstly rearranges to *N*1-*O*6 ethenoguanine and further to a *N*1-guanine-*N*3-cytosine interstrand crosslink ([ICL], Figure 3) (Tong *et al.*, 1982). Even though dG-dC crosslinks represent only ~3 % of CENU-induced adducts, its replication blocking action is responsible for the cytotoxicity of these anti-neoplastic agents (Bodell *et al.*, 1986).

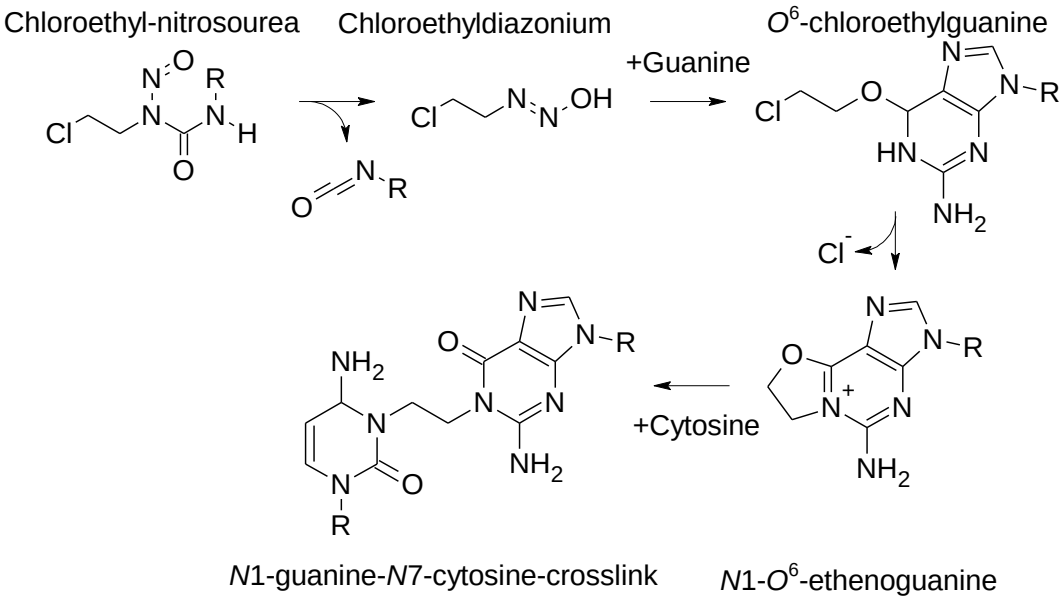

Figure 3 – Interstrand crosslink formation by CENUs.
See text for details (2.2.2). Modified from (Ludlum, 1997).

2.2.2.1 Toxicity of chloroethylating agents

The toxic effect of chloroethylating agents relies on their DNA crosslinking nature. ICLs prevent opening of the DNA strand and, therefore, DNA replication and RNA transcription. In contrast to methylating agents, CENUs induce DSBs in the first S-phase after treatment, suggesting that the collapse of the replication fork at the ICL is responsible. These DSBs trigger either apoptotic or necrotic cell death (Nikolova *et al.*, 2012; Batista *et al.*, 2007). Resistance to chloroethylating agents is mediated primarily by MGMT, since it removes the O^6-alkylation before the crosslink can form (Ludlum, 1990). Furthermore, repair pathways for ICLs (2.3.1.6) modulate sensitivity of cells to CENUs. These include HR, the Fanconi anemia (FA) pathway and nucleotide excision repair (NER) (Chen *et al.*, 2007a; Nikolova *et al.*, 2012; Batista *et al.*, 2007; Barckhausen *et al.*, 2014). Indeed, in melanoma cells it has been shown that even a single treatment with the CENU FM can upregulate the lesion-recognizing complex of DDB2 and XPC, leading to a long-lasting resistance phenotype (Barckhausen *et al.*, 2014).

2.3 Resistance to alkylating agents

2.3.1 DNA repair

The removal or reversal of DNA damage is an essential cellular function which ensures physiological survival in a constantly threatening environment. These damages comprise modifications of the nucleobases, breaks in the sugar-phosphate backbone or errors that are introduced during replication. Most of the cells' DNA damage is endogenously formed e.g. by erroneous replication, spontaneous hydrolysis of bases or by reactive oxygen species (ROS) formed

during oxidative phosphorylation in the mitochondria, (De Bont and van Larebeke, 2004). Only a minor part of DNA damage is exogenously induced by sources like UV radiation or components of food or tobacco smoke (De Bont and van Larebeke, 2004). In order to deal with these damages, the cell developed a network of repair mechanisms, which remove specific lesions and back-up systems thereof. In cancer, DNA repair plays a dual role as impairment of repair increases the number of mutations and genomic instability, which drives oncogenic transformation (Goode *et al.*, 2002). Secondly, DNA repair determines therapy sensitivity to DNA damaging treatment. Mechanisms that deal with alkylating agent induced lesions are described in the next sections.

2.3.1.1 Direct damage reversal

2.3.1.1.1 Oxidative dealkylation

ALKBH2 and ALKBH3 belong to the group of Fe(II)/α-ketoglutarate dependent dioxygenases and remove methyl groups from *N*1-methyladenine and *N*3-methylcytosine by hydroxylation of the methyl group that subsequently allows for the spontaneous release of formaldehyde and the unmodified base (Sedgwick, 2004). Both lesions are induced by S_N1 alkylating agents at a minor fraction of 0.6-1.3 %, but they are potentially toxic, as was shown in *E.coli* (Shrivastav *et al.*, 2010).

2.3.1.1.2 Alkyltransferases

The human MGMT protein removes alkyl groups from the O^6-position of guanine and the O^4-position of thymine (Sassanfar *et al.*, 1991). Therefore, MGMT screens the DNA for these alkylation events and then transfers the alkyl group onto an internal cysteine. This results in inactivation of MGMT and a conformational change of the protein, which allows it to be recognized by ubiquitin ligases. After ubiquitination it is degraded by the proteasome (Lindahl *et al.*, 1982; Srivenugopal *et al.*, 1996). Accordingly, MGMT works stoichiometrically and is referred to as a 'suicide enzyme'. Due to its importance in repairing O^6-alkylations, which represent the cytotoxic lesions of alkylating anticancer therapy, MGMT expression, activity and regulation has extensively been studied. This revealed heterogeneous MGMT activity inter-individually as well as between different tissues. Overall, the highest activity was found in liver and the lowest in brain and lung tissues (Margison *et al.*, 2003; Christmann *et al.*, 2011). Likewise, cancers show a heterogeneous expression of MGMT, though some tumors (e.g. 38-50 % of metastatic melanomas and GBMs) silence MGMT expression by promoter methylation, which increases their response to alkylating agents (Hassel *et al.*, 2010; Brennan *et al.*, 2013).

2.3.1.2 Base excision repair

Modifications to nucleobases are excised by proteins of the base excision repair (BER) pathway, which finally leads to a replacement of 1-10 nucleotides (Figure 4 a). Base modifications that are repaired by BER are bases that are oxidized by endogenous ROS, alkylated bases arising from

endogenous or therapy-induced alkylations and spontaneously deaminated bases that, in the case of cytosine, result in uracil-incorporated DNA. Repair is initiated by excision of the damaged base via hydrolysis of the *N*-glycosylic bond that is carried out by damage specific DNA glycosylases and leaves an apurinic/apyrimidinic site (AP site). Besides substrate specificity, DNA glycosylases differ in their enzymatic activity: the uracil-removing uracil DNA glycosylases (UDGs) or the *N*3MeA and *N*7MeG-excising *N*-methylpurine-DNA glycosylase (MPG) are monofunctional and solely bear glycosylase activity leaving an intact sugar-phosphate backbone missing only the base. Bifunctional glycosylases like the 8-oxoguanine-removing 8-oxoguanine glycosylase (OGG1) display an additional lyase activity, allowing cleavage of the sugar-phosphate backbone 3' to the AP-site leaving a 5'phosphate and modified 3' ends. This requires further processing by either AP-endonuclease 1 (APE1) or polynucleotide kinase 3'-phosphatase (PNKP) to yield a 3'hydroxylgroup. For AP sites generated by monofunctional glycosylases, APE1 incises 5' to the AP site also producing a 3'hydroxyl group and leaving a 5'deoxyribose phosphate at the other side of the nick. Irrespective of varying 5'structures, polymerase β (POL β) inserts the appropriate nucleotide to the 3' end. POL β additionally bears a phosphodiesterase function which hydrolyzes unmodified 5'ends, thereby making it a substrate for DNA ligase I (LIG I), which ligates both ends. In this case only one nucleotide is exchanged, which is referred to as 'short-patch BER'. If the 5' end is modified (oxidized, reduced), polymerase δ or polymerase ε, with the help of replication factor C (RFC) and proliferating cell nuclear antigen (PCNA), continue inserting up to 10 nucleotides, which is referred to as 'long patch BER'. This leads to a displacement of the original strand by the newly synthesized strand, which is cleaved by flap endonuclease (FEN1) so that ligation via LIG I can occur.

One additional protein mediates BER though lacking enzymatic activity: X-ray repair cross-complementing protein (XRCC1) recruits and stimulates factors like APE1, POL β or polynucleotide kinase 3-phosphatase (PNKP). It further interacts with poly (ADP-ribose) polymerase 1 (PARP1), a protein required for the detection of DNA single-strand breaks (SSB), which are also repaired by the end-processing proteins, polymerases and ligases of the BER pathway (Svilar *et al.*, 2011; Fortini and Dogliotti, 2007; Krokan and Bjoras, 2013; Caldecott, 2007).

BER is of particular importance for S_N1-methylating agent induced DNA lesions, as it efficiently removes the most abundantly induced *N*7MeG and *N*3MeA lesions, which both exhibit either indirect or direct toxic and mutagenic properties, respectively (Engelward *et al.*, 1998; Tudek, 2003; Park and Ames, 1988).

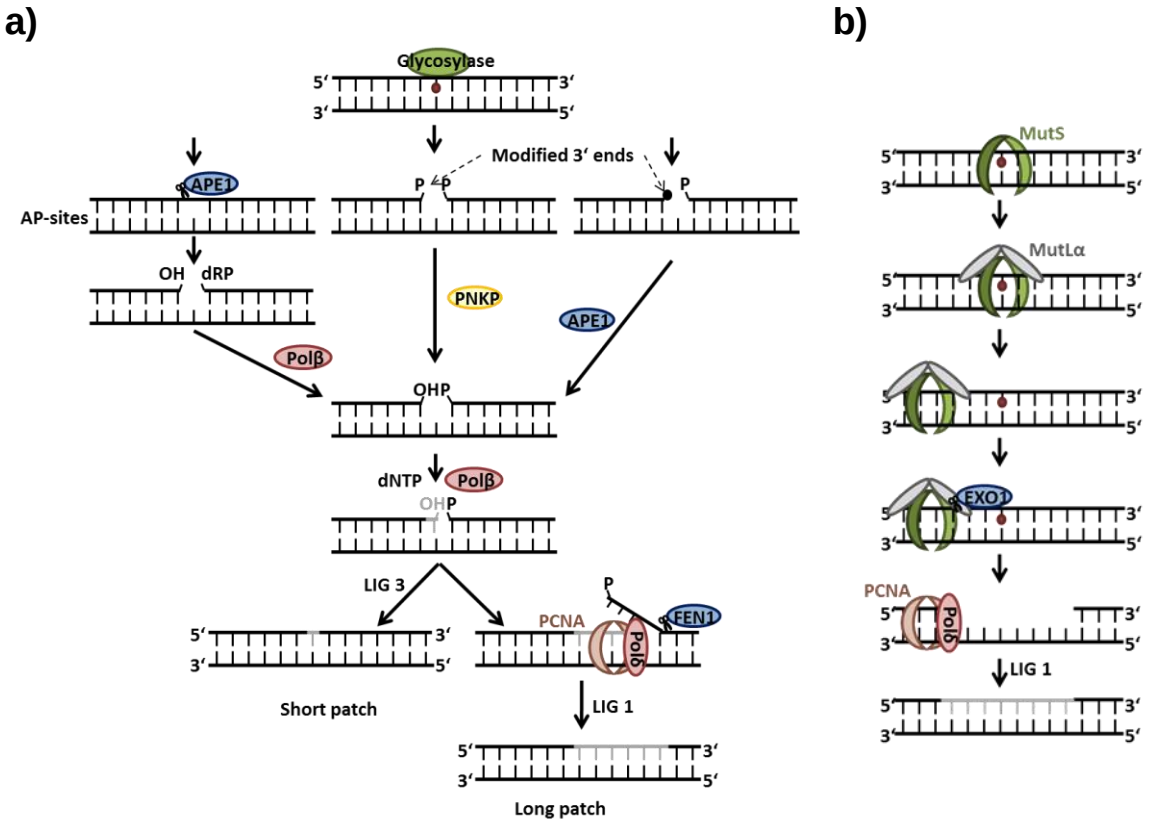

Figure 4 – Mechanism of base excision (a) and mismatch DNA repair (b).
Pathways are described in detail in the text (base excision repair 2.3.1.2, mismatch repair 2.3.1.3).

2.3.1.3 Mismatch repair

Substrates that are processed by MMR are base pairings that do not follow Watson-Crick pairing. These include mismatches introduced either by erroneous nucleotide insertion by DNA polymerases during DNA synthesis or by insertion of nucleotides opposite damaged and mispairing bases. This applies to 8-oxoguanine, which mispairs with adenine as well as to O^6MeG, which mispairs with thymine and is a prerequisite for cytotoxicity and mutagenicity of methylating agents as described earlier (2.2.1.1). Further, loops that build due to insertions or deletions (insertion/deletion loops – IDL) are detected by the MMR machinery (Fishel *et al.*, 1994). Substrate recognition relies on MutS heterodimers, which in case of mispairs consists of MSH2 and MSH6 (MutSα) and for IDLs with more than four nucleotides consists of MSH2 and MSH3 (MutSβ) (Genschel *et al.*, 1998). All subunits exhibit ATPase function, which allows scanning of DNA substrates and is inhibited by the exchange of ADP→ATP upon substrate recognition. This exchange induces a conformational change to a sliding clamp. The clamp complexes with a second heterodimer consisting of MLH1 and PMS2 (MutLα), which bears ATPase and endonuclease enzymatic activity. This allows displacement to nicks between Okazaki fragments on the lagging strand 5' to the mismatch and interaction between MutLα and exonuclease 1 (EXO1), whose 5'-3' exonuclease function removes the newly synthesized fragments including the lesion. In the leading

strand, the endonuclease function of MutLα is required to incise into the continuous strand and to generate a 5' end lying 5' of the mismatch for EXO1, which excises the mismatch. Detailed knowledge of how strand discrimination occurs and where incision takes place are still lacking. It is estimated that PCNA, which interacts with MutSα and MutLα dimers, dictates orientation and allows strand discrimination. Upon excision of up to a thousand nucleotides, the replication machinery, including POLδ, RFC and PCNA, resynthesizes the lacking strand, which is then re-ligated by LIG I (Li, 2008; Kunz *et al.*, 2009; Jiricny, 2013) (Figure 4 b).

The crucial role of MMR in TMZ-induced O^6MeG is discussed in 2.2.1.1.

2.3.1.4 Nucleotide excision repair

NER removes 22-30 nucleotides surrounding a helix-distorting DNA lesion (Figure 5 a). These are mainly the UV-induced CDPs and the less abundant 6-4 pyrimidine pyrimidone photoproducts (6-4 PP) (Sugasawa *et al.*, 2001; Scrima *et al.*, 2008). Further substrates arise from reaction of DNA with epoxide intermediates during detoxification of polycyclic aromatic hydrocarbons as they can be found in tobacco smoke and food. NER can be initiated in two ways: global genome repair (GG-NER), which recognizes lesions in the whole genome and transcription coupled repair (TC-NER), which is limited to actively transcribed genes. In GG-NER, xeroderma pigmentosum complementation group C (XPC) binds to a small single-stranded piece of DNA opposite the actual lesion caused by lesion-related impaired base pairing. This also explains the role of GG-NER in repair and especially in recognition of 'bulky lesions' induced, for example, by platinum drugs or other crosslinking agents (Clement *et al.*, 2010). As CDPs do not display a high affinity substrate for XPC itself, DDB2 takes over the generation of single-stranded DNA by binding to CPDs, introducing a kink in the damaged strand and ssDNA in the opposite strand. Once XPC has bound, it recruits the multiprotein complex transcription factor IIH (TFIIH) and its subunits XPB and XPD mediate strand opening, unwinding as well as lesion verification. Next, XPA and RPA stabilize the structure and organize assembly with XPG endonuclease responsible for 3' incision and ERCC1-XPF endonuclease responsible for 5' incision. Only if both nucleases are present, ERCC1-XPF incises 5' to the lesion, leaving a 3' hydroxyl group. The 3' end is used by POLδ or POLε for DNA-resynthesis, which is supported by PCNA and RFC. In the 3' direction from the lesion, XPG incises and releases a DNA fragment of 22-30 nucleotides, including the damaged base(s). Further, it generates a 5' phosphate that serves as the ligation site for LIG I on the newly synthesized strand (Schärer, 2013; Marteijn *et al.*, 2014).

Initiation of TC-NER requires recognition of lesion-stalled RNA polymerase II (RNAPII) by the Cockayne syndrome (CS) proteins CSB and CSA, which are responsible for NER protein recruitment. Translocation of RNAPII ('backtracking') allows binding of the NER factors (TFIIH, XPA, XPF, XPG) that accomplish lesion excision as described for GG-NER (Vermeulen and Fousteri, 2013).

NER is capable of removing methylating agent induced *N*3MeA and *N*7MeG as well as supporting recognition and repair of chloroethylating agent-induced ICLs (Plosky *et al.*, 2002; Wood, 2010). Furthermore, NER has been shown to repair O^6-guanine methylation/ethylation lesions (Bronstein *et al.*, 1992; Samson *et al.*, 1988).

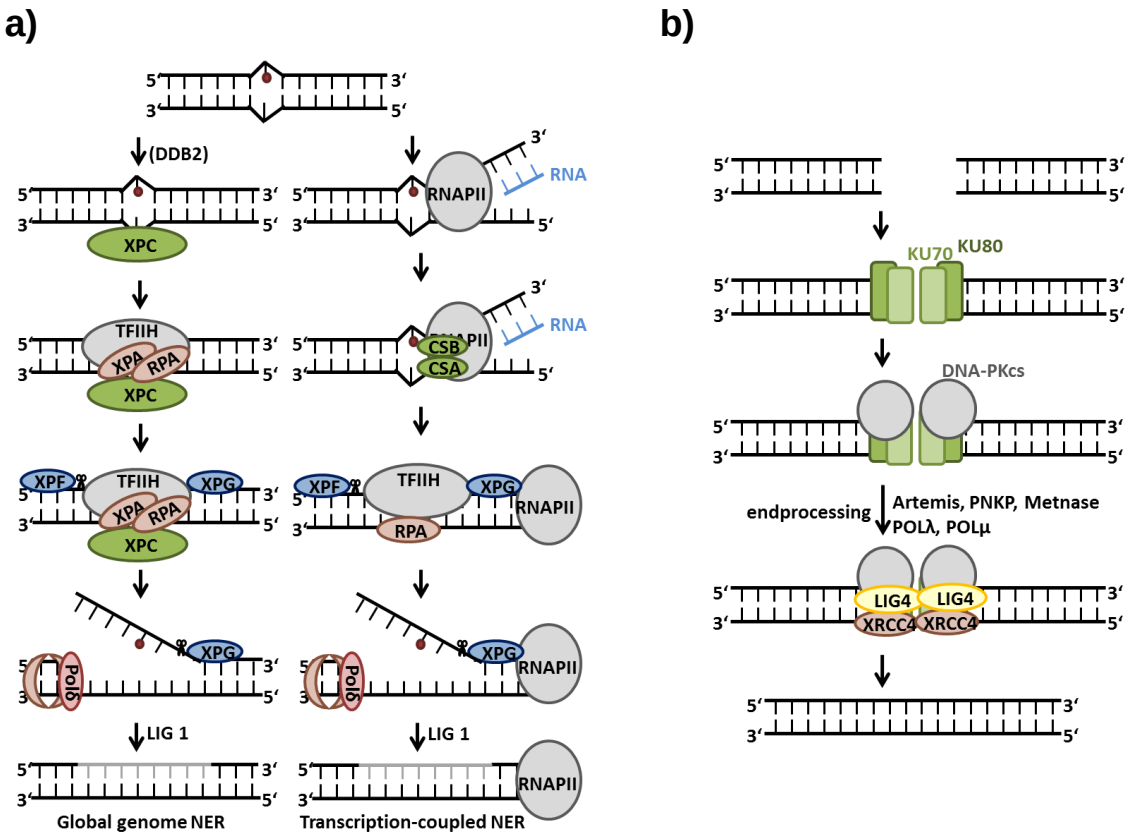

Figure 5 – Mechanism of nucleotide excision repair (a) and non-homologous end joining (b). Pathways are described in detail in the text (nucleotide excision repair - 2.3.1.4, non-homologous end-joining - 2.3.1.5.1).

2.3.1.5 DNA double-strand break repair

Breakage of both strands of the DNA helix considerably threatens and challenges a cell, since this potentially leads to mutations, chromosomal aberrations or induction of cell death. DNA double-strand breaks (DSB) can be induced exogenously by ionizing radiation originating from radioactive natural isotopes, medical procedures like X-rays and cancer treatments, or endogenously during replication e.g. when the replication fork meets damaged DNA (Pfeiffer *et al.*, 2000; van Gent *et al.*, 2001).

2.3.1.5.1 Non-homologous end joining

In mammalian cells, re-ligation of two DNA double-strand break ends induced by ionizing radiation occurs predominantly by non-homologous end joining (NHEJ), which does not require homology (Mao *et al.*, 2008; Beucher *et al.*, 2009). This is initiated by binding of a heterodimer consisting of KU70 and KU80 to the DSB ends, so that each end is encircled by one dimer,

protecting it from degradation and keeping both ends in proximity to each other (Walker *et al.*, 2001; Downs and Jackson, 2004) (Figure 5 b). The dimer serves as a scaffold, as it recruits and binds many NHEJ factors. Interaction of the KU proteins (KU70 and KU80) with DNA-dependent protein kinase catalytic subunit (DNA-PKcs) establishes kinase activity of the complex, which allows autophosphorylation and phosphorylation of additional NHEJ proteins (Davis *et al.*, 2014). The complex also regulates access of further factors to the DNA. As ends of DSBs, especially upon IR, often bear modified nucleotides, end-modifying enzymes, nucleases and polymerases clean them for relegation. The lyase activity of KU70 removes 5' altered nucleotides and abasic sites, leaving a 5' phosphate (Roberts *et al.*, 2010). Further, PNKP helps generating ligateable ends with its 5' kinase and 3' phosphatase activity leading to the required 3' OH and 5' P end. However, these proteins do not recognize all possible end alterations like for instance overhangs or hairpins, which are processed by the DNA-PKcs activated 5'-3' exonuclease Artemis or by the endonuclease Metnase (Ma *et al.*, 2002; Beck *et al.*, 2011). Another way of overcoming overhangs is to insert new nucleotides, which is carried out by POL λ or POL μ. For ligation of the cleaned ends, another complex containing XRCC4 and LIG IV is required, which finally seals the break (Lieber, 2010; Waters *et al.*, 2014; Zhang *et al.*, 2014).

A DSB repair mechanism that is independent of KU70/80 and LIG IV is termed alternative end joining (alt-EJ). Damage is therein recognized by PARP1 which recruits XRCC1 and LIG III. Processing of the ends is executed by the MRE11, RAD50, NBS1 (MRN) complex and C-terminal interacting protein CtIP (explained in 2.3.1.5.2), or by the polymerase POL β (Mladenov and Iliakis, 2011).

2.3.1.5.2 Homologous recombination

Homologous recombination (HR)-mediated repair of DSBs differs from NHEJ as it makes use of homologous sequences preferably on sister chromatids. It is therefore regarded as error free, but limited to the late S and G2 phase of the cell cycle (Figure 6). HR plays a minor role in repair of DSBs induced by IR. It essentially contributes to resolution of replication coupled errors like stalled replication forks and repairs one-ended DSBs resulting from replication fork-encountered SSBs in the DNA template (Arnaudeau *et al.*, 2001; Petermann and Helleday, 2010). DSB repair by HR is initiated by end resection for generation of 3' overhangs. Therefore, the MRN complex binds to the broken DSB ends and end processing is initiated by MRE11's 3'-5' exonuclease and single-strand DNA endonuclease activity. This enables bidirectional resection of the 5' strand and, if necessary, removal of modified nucleotides (e.g. protein bound DNA ends). This is followed by interaction of MRN with the endonuclease CtIP that primarily acts on 5' flaps and 5' branched structures (Sartori *et al.*, 2007; Makharashvili *et al.*, 2014). This leads to 3' overhangs which can be extended by the 5'-3' exonuclease EXO1 (Symington, 2014). The resulting 3' single stranded ends are bound by RPA, which protects them from formation of secondary structures and from

nucleolytic attacks. Central proteins in HR are RAD51 and its paralogs as they enable homology search and strand invasion. Since RAD51 forms filaments on single-stranded DNA, replacement of RPA is required. This is mediated by the RAD51 paralogs (XRCC3, XRCC2, RAD51D, RAD51C, RAD51B) and most importantly by BRCA2. The latter displaces RPA by RAD51 at ssDNA and promotes RAD51 filament formation (Liu *et al.*, 2010; Thorslund *et al.*, 2010). The 3' RAD51-nucleofilament then aligns with dsDNA of the sister chromatid for homology search. For yeast or *E.coli*, homology of 15 nucleotides is sufficient to stimulate invasion of the double-strand and displacement of the complementary strand, resulting in the displacement-loop (D-Loop) (Qi *et al.*, 2015) The 3' end of the (broken) invaded strand can serve as a primer for DNA synthesis by POL δ, which uses the intact DNA strand as the template (Li *et al.*, 2009; Sebesta *et al.*, 2011). The resulting structure can be dissolved in two ways. In the synthesis-dependent strand annealing (SDSA) pathway, the newly synthesized 3' end dissociates from the D-Loop as this translocates in the direction of synthesis and collapses. The end then re-anneals with the second, resected 3' overhang of its original complementary strand. In the double-strand break repair (DSBR) pathway, the second 3' end, which is resected, but has not invaded, anneals with the displaced strand of the template DNA which allows for its strand extension. Upon gap-filling, ligation of ends results in a double Holliday junction that can be dissolved in two ways: first, it can be dissolved by help of the helicase function of the Bloom syndrome protein (BLM) which migrates the two junctions to each other and topoisomerase TOP3α dissolves the resulting hemicatenane. Secondly, structure specific endonucleases, GEN1 or SLX1-SLX4, can resolve the junctions, leading to either crossover or non-crossover products (Svendsen and Harper, 2010; Li and Heyer, 2008; Jasin and Rothstein, 2013).

Furthermore, HR provides a way of repairing one-ended DSBs. They result from SSBs, which are encountered by a replication fork or by a stalled replication fork that is then converted into a DSB by MUS81-EME1 (Hanada *et al.*, 2007; Petermann and Helleday, 2010). The broken end is resected to invade a homologous region (sister chromatid) analogous to repair of two-sided DSBs to resume replication (Llorente *et al.*, 2008; Petermann and Helleday, 2010).

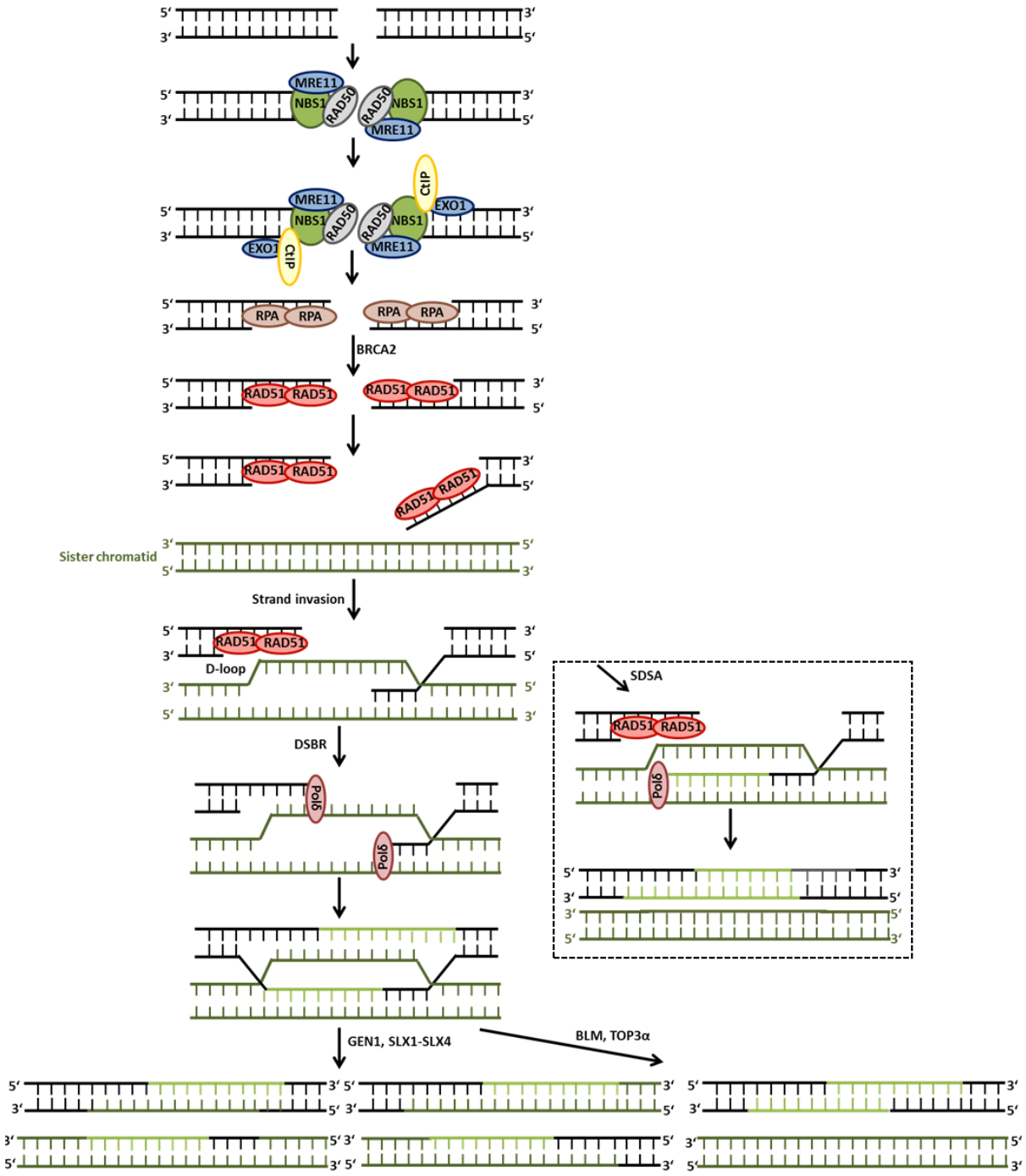

Figure 6 – Mechanisms of homologous recombination-mediated double-strand break repair. Overview of end resection and strand invasion during homologous recombination (upper part). Processing by double-strand break repair (DSBR – lower left) and resolution of a double Holliday junction by specific endonucleases leading to non-crossover (left) or crossover products (middle), or resolution by BLM helicase and TOP3α (right). Insert: Processing via synthesis dependent strand annealing. Detailed description is found in the text (2.3.1.5.2).

2.3.1.6 Interstrand crosslink repair

Covalent linkage of the two strands of a DNA double helix is induced exogenously by a variety of anti-cancer drugs, including platinum based drugs, mitomycin C (MMC), chloroethylating agents and also through endogenous processes, e.g. by aldehyde metabolites. This leads to a block of the

essential cellular functions transcription and replication and therefore demands repair. ICLs can be recognized throughout the whole cell cycle by the NER protein XPC in the case that the crosslink distorts the DNA (Muniandy *et al.*, 2009) or by CSB (Enoiu *et al.*, 2012) if met by RNAPII. Further, the presence of the ERCC1-XPF nuclease and of the translesion polymerases REV1 and POLζ has been demonstrated to confer ICL-resistance. This indicates a repair mechanism whereby ERCC1-XPF unhooks the ICL by incision in proximity to the lesion and subsequent gap filling by TLS. Nevertheless, ICL repair in G1 is insufficient and most lesions are processed when encountered during replication. Proteins belonging to the FA complementation group initiate replication dependent repair. The replication fork-encountered ICL is first recognized by FANCM, which mediates fork regression resulting in a chicken foot structure. Next, protomers of the heterodimer of FANCD2 and FANCI are monoubiquitinated by the FANCL subunit of the FA core complex (FANCA, FANCB, FANCC, FANCE, FANCF, FANCG and FANCL). Monoubiquitinated FANCD2 recruits nucleases that promote, most likely, dual incision and unhooking of the ICL. This involves the structure specific endonucleases SLX4-SLX1, XPF-ERCC1 and MUS81-EME1, as well as the Fanconi-associated nuclease (FAN1) which exhibits 5'-3' exonuclease function. This allows HR-mediated restart of the replication fork, which proceeds across the unhooked lesion with the help of the translesion polymerases REV1 and POLζ. The unhooked lesion is then removed enzymatically by NER or spontaneously by hydrolysis (Deans and West, 2011; Walden and Deans, 2014; Clauson *et al.*, 2013).

2.3.1.7 Translesion Synthesis

In contrast to the aforementioned mechanisms, translesion synthesis does not repair lesions, but enables DNA synthesis across the lesion. The replicative DNA polymerase is exchanged for a low-fidelity DNA polymerase of the type Y family, which additionally lack proofreading exonuclease function. Upon nucleotide insertion opposite the damaged strand, the nascent strand is extended by POLζ for some nucleotides before replicative polymerases complete synthesis. Though being error-prone, TLS prevents collapse of the replication fork and thereby DNA breaks (Sale, 2013).

2.3.2 DNA damage response and cell death

2.3.2.1 DNA damage response

Upon DNA damage induction, e.g. by chemotherapeutics, a network of signaling cascades regulates the cellular response. This comprises recruitment of repair factors, induction of cell cycle arrest, and induction of cell death or differentiation. Two central transducing damage-activated kinases are Ataxia telangiectasia mutated (ATM) and Ataxia telangiectasia and Rad3 related (ATR). The inactive dimerized ATM is activated at sites of MRN-bound DNA ends by autophosphorylation and monomerization (Bakkenist and Kastan, 2003; Lee and Paull, 2005). Activation of ATR takes place in a complex with ATR interacting protein (ATRIP), which binds

RPA-bound single-stranded DNA at resected DSBs or stalled replication forks and promotes subsequent trans-autophosphorylation of ATR (Zou and Elledge, 2003; Ball *et al.*, 2005). Both kinases phosphorylate the histone variant H2AX at serine 139, which regulates retention of DNA repair proteins at the damage site and chromatin organization. As phosphorylated H2AX (γH2AX) spans a region of megabases around a DSB and accordingly thousands of H2AX (Bonner *et al.*, 2008; Rogakou *et al.*, 1999), their immunochemical staining provides a detection method for DSBs. Further critical substrates of ATM and ATR are the checkpoint kinases CHK1 and CHK2, which arrest the cell cycle at different checkpoints (G1-S transition, G2-M transition) by inactivation of cell division cycle phosphatases 25 (cdc25) or by phosphorylation of p53 and subsequent induction of $p21^{Cip1/Waf1}$. Depending on the damage degree and the cells' phenotype, CHK activation also leads to apoptosis or senescence induction (Ciccia and Elledge, 2010).

For O^6-alkylating agents, activation of ATM/ATR and CHK1/2 has been shown. ATR was reported to play the major role in preventing TMZ-induced apoptosis, whereas ATM triggers TMZ-induced autophagy. Phosphorylation of the ATM and ATR downstream target H2AX was observed upon alkylating agent treatment, which for chloroethylating agents appeared earlier than for methylating agents, most likely because of the requirement of O^6-lesion processing. Similarly, methylation and chloroethylation induce a G2/M arrest, which again, for O^6MeG, occurs later, following two rounds of replication (Eich *et al.*, 2013; Knizhnik *et al.*, 2013; Nikolova *et al.*, 2012; Quiros *et al.*, 2010).

2.3.2.2 Apoptosis

Programmed cell death by apoptosis is a way of eliminating cells in the course of cell turnover, embryonic development or severe damage (Wyllie *et al.*, 1980) without causing inflammation (Huynh *et al.*, 2002). It is morphologically characterized by cell and nucleus shrinkage, membrane blebbing and finally by the generation of apoptotic bodies containing cell organelles that are subject to macrophage ingestion (Kerr *et al.*, 1972). Furthermore, degradation of proteins and DNA are intracellular markers of apoptosis, which are mediated by effector caspases-3 and -7 (cysteinyl-aspartate specific protease) that cleave proteins and activate the caspase activated DNase (CAD) (Enari *et al.*, 1998). Two classical ways of effector caspase activation are described: an intrinsic (mitochondrial) pathway which starts with mitochondrial outer membrane permeabilization by oligomerization of the BCL-2 family members BAX and BAK followed by cytoplasmic release of cytochrome C and second mitochondria-derived activator of caspases (SMAC). Cytochrome C binds to apoptosis protease activator protein (APAF-1), resulting in a conformational change of APAF-1 and its heptamerization, which is required for cleavage and activation of the initiator Caspase-9. SMAC contributes to apoptosis by disabling inhibitor of apoptosis proteins (IAP), inhibitors of caspases. For extrinsic activation of apoptosis, extracellular ligands bind to transmembrane death receptors like FASR to trigger their trimerization and subsequent recruitment of its cytoplasmic adaptor protein FAS-activated death domain (FADD). The death inducing

signaling complex (DISC) recruits procaspase-8, which dimerizes and is trans-autoactivated by cleavage that can, in turn, activate caspase-3.

These two classical activation paths converge at the caspase-8 substrate BH3-interacting domain death agonist (BID), whose truncated form interacts with BAX and consequently mediates mitochondrial outer membrane permeabilization (Fuchs and Steller, 2015; Elmore, 2007).

Both pathways of apoptosis induction (intrinsic and extrinsic) have been reported for alkylating agents and are dependent on cell type, p53 status and the agent used. Whereas p53 competent glioblastoma can activate both pathways upon methylating agents, p53 mutant cells are restricted to intrinsic activation. On the other hand, p53 wild-type melanoma cells are also impaired in receptor-mediated apoptosis induction by methylating agents. For chloroethylating agents, p53 status is also essential, though it rather predicts recognition and repair of ICLs and therefore mediates resistance to apoptosis (Batista *et al.*, 2007; Barckhausen *et al.*, 2014; Roos *et al.*, 2007; Naumann *et al.*, 2009; Roos *et al.*, 2011).

2.3.2.3 Necrosis and Necroptosis

Necrosis and Necroptosis are cell death pathways sharing similar characteristic cell morphology, i.e. cytoplasmic swelling and breakage of the cell membrane which results in release of the cell content into its environment, and therefore, local inflammation. Necrosis occurs upon physical damage of a cell and is not regulated. On the other hand, necroptosis is inducible by binding of extracellular ligands to membrane-receptors, which leads to activation of receptor-interacting serine/threonine protein kinase 1 (RIPK1), promoting membrane perforation in a regulated manner (Fuchs and Steller, 2015; Galluzzi and Kroemer, 2008).

2.3.2.4 Senescence

Senescence is a cellular state of permanent cell cycle arrest that the cell enters due to telomere-shortening, DNA damage or oncongene activation. Senescent cells are viable, but non-proliferating and resistant to apoptosis induction. They are characterized by a consistent upregulation of CDK inhibitors $p21^{Cip1/Waf1}$ or $p16^{INK4a}$, expression of β-galactosidase and senescence-associated heterochromatin foci (Campisi and d'Adda di Fagagna, 2007; d'Adda di Fagagna, 2008). Similar to autophagy, it is not clear whether senescence is beneficial or detrimental in therapy, since senescent cancer cells have been shown to re-enter the cell cycle post-treatment (Wang *et al.*, 2013; Roberson *et al.*, 2005).

Upon TMZ treatment, melanoma and glioblastoma cells enter a senescent-like state (Mhaidat *et al.*, 2007; Hirose *et al.*, 2001a; Hirose *et al.*, 2001b; Knizhnik *et al.*, 2013).

2.3.2.5 Autophagy

Cytoplasmic components and organelles can be degraded by autophagy. The process is initiated by the engulfment of cytoplasmic components in a double-membrane vesicle (autophagosome) that fuses with lysosomes, resulting in the digestion of the autophagosome content. Autophagy is induced upon different kinds of stress, like nutrient starvation or DNA damage (He and Klionsky, 2009). However, it is still being debated whether autophagy is a cell death mechanism, if it only accompanies cell death, or if it provides a cell survival function under stress scenarios (Codogno and Meijer, 2005).

In glioma cells, autophagy was induced upon TMZ and displayed a protective mechanism, since autophagy inhibition increased apoptosis induction (Lin *et al.*, 2012; Kanzawa *et al.*, 2004; Knizhnik *et al.*, 2013).

2.4 Histone deacetylases

Histone deacetylases catalyze the removal of acetyl groups from acetylated lysines in post-translationally modified proteins and oppose the activity of histone acetyl transferases (HAT). Based on phylogenetic development and sequence similarity, HDACs are subdivided into four classes: class I (HDAC1, HDAC2, HDAC3 and HDAC8), class IIa (HDAC4, HDAC5, HDAC7 and HDAC9), class IIb (HDAC6 and HDAC10) and class IV (HDAC11). Class I, II and IV HDACs are zinc (Zn^{2+})-dependent HDACs, whereas class 3 HDACs, or synonymously Sirtuins (SIRT1-7), are dependent upon nicotinamide adenine dinucleotide (NAD^{+}) (Gregoretti *et al.*, 2004; Yang and Seto, 2007). Their substrates are histones as well as non-histone proteins. Histones are nuclear proteins forming the nucleosome core, around which, the DNA is wrapped to provide compaction. The acetylation of histone tails impacts directly on chromatin structure by two means: acetylated lysines in histone tails are not positively charged like non-modified lysines, which decreases the interaction between negatively charged DNA phosphate backbone and positively charged histone tails (Hong *et al.*, 1993). Secondly, acetylation of histone 4 at lysine 16 (H4K16ac) inhibits chromatin compaction into 30 nm fibers, most likely by disrupting the interaction of the positively charged lysine with an acidic patch of histone 2A (H2A) in a neighboring nucleosome (Shogren-Knaak *et al.*, 2006; Tremethick, 2007). An indirect mechanism of HDACs on transcription has been described: HDACs are parts of multiprotein transcriptional repressor complexes like mSin3, N-CoR or CoREST (Hayakawa and Nakayama, 2011). On the other hand, HATs are associated with transcriptional activators like the HAT p300 with the transcription factor IID (Pazin and Kadonaga, 1997; Struhl, 1998). These features indicate a better accessible DNA for transcription factors and transcriptionally active chromatin in the absence of HDAC activity. Indeed, transcription is regulated by histone acetylation and histone acetylation is, therefore, regarded as an epigenetic mechanism. However, upon inhibition of HDACs (retained

acetylation), the number of genes upregulated is similar to those downregulated (Peart *et al.*, 2005; Bolden *et al.*, 2013). This might be explained by the histone-independent activity on thousands of non-histone substrates. These include post translational modifications on proteins such as HDACs, HATs, methyltransferase, demethylases, E3-ligases, chromatin remodelers, cell cycle regulators, DNA repair proteins and others (Choudhary *et al.*, 2009). Even though only a minor part of these acetylations has been characterized as to their function, protein acetylation is already linked to a variety of effects including protein localization, enzyme activity, protein stability and interactions with other proteins or DNA (Spange *et al.*, 2009).

2.4.1 Histone deacetylases and cancer

Given the plethora of cellular functions that are affected by acetylation and inevitably by HDACs, it is not surprising that they are associated with different diseases, including neurological and immunological diseases as well as cancer (Falkenberg and Johnstone, 2014). Contrary roles of HDACs in cancer have been described: studies investigating genetically modified mice showed that specific knockdown/knockout of HDAC1 and/or HDAC2 in thymocytes or lymphoid stem cells and progenitors promotes and accelerates the development of hematological tumors (Heideman *et al.*, 2013; Dovey *et al.*, 2013; Santoro *et al.*, 2013). Furthermore, loss of Hdac3 in mouse liver was associated with genomic instability, a cancer hallmark, and with the development of hepatocellular carcinomas (Bhaskara *et al.*, 2010). On the other hand, elevated expression of class I HDACs in human solid tumors, including prostate, colorectal cancer, lung adenomas, liver or breast cancer, is associated with decreased disease free or overall survival (Weichert *et al.*, 2008a; Weichert *et al.*, 2008b; Krusche *et al.*, 2005; Minamiya *et al.*, 2011; Rikimaru *et al.*, 2007). Based on this, HDAC inhibitors have been developed as potential cancer therapeutics and have been attributed a variety of anti-tumorigenic effects.

2.4.2 Histone deacetylase inhibitors

Based on their chemical structure, HDAC inhibitors are divided into hydroxamic acids (Dacinostat, Vorinostat), cyclic peptides (Romidepsin), aliphatic acids (sodium butyrate, valproic acid [VPA], used in this research) and benzamides (Entinostat [MS-275] used in this research, Mocetinostat) all of which generally act by binding the catalytic Zn^{2+} and interacting with the lipophilic tube lying between the active site and the surface of the HDAC (Bieliauskas and Pflum, 2008; Finnin *et al.*, 1999; Bressi *et al.*, 2010). Due to characteristics like size and polarity, HDAC inhibitors have different selectivities, ranging from pan-inhibition (Dacinostat) to the selective inhibition of HDAC1, HDAC2 and HDAC3 for example with MS-275 (Bradner *et al.*, 2010).

2.4.2.1 Valproic acid

VPA is a short chain fatty acid used for the treatment of epilepsy and bipolar-disorder and was shown to inhibit all class I HDACs (1; 2; 3 and 8) (Bradner *et al.*, 2010; Göttlicher *et al.*, 2001).

The anti-epileptic activity relies on VPA's ability to penetrate the blood-brain-barrier and to increase levels of the inhibitory neurotransmitter γ-aminobutyrate by preventing its degradation and promoting its synthesis (Mesdjian *et al.*, 1982; Nau and Loscher, 1982). The therapeutic serum concentration lies between 0.3 mM and 0.7 mM, which is sufficient to inhibit HDAC activity *in vitro* and *in vivo* (Bradner *et al.*, 2010; Bug *et al.*, 2005). Adverse effects caused by VPA are neurological and gastrointestinal in origin, namely dizziness, drowsiness, insomnia, nausea or vomiting (Nanau and Neuman, 2013).

2.4.2.2 Entinostat (MS-275)

MS-275 is a benzamide HDAC inhibitor of HDAC1, HDAC2 and HDAC3 at *in vitro* inhibitory concentrations < 1 µM (Bradner *et al.*, 2010). Currently MS-275 is under investigation in clinical phase I-III trials, primarily against hematological cancers, breast and lung cancer in monotherapies as well as combination therapies, e.g. with DNA-methylation interference by 5-azacytidine (http://clinicaltrials.gov/, 2015). Yet, initial phase I and II studies revealed that plasma concentrations from 5-350 nM can be achieved and that nausea, vomiting and fatigue were common adverse effects that occurred especially at high doses (Ryan *et al.*, 2005; Hauschild *et al.*, 2008; Kummar *et al.*, 2007).

2.4.2.3 Histone deacetylase inhibitors and cancer therapy

Early *in vitro* studies ascribed anti-neoplastic effects of HDAC inhibitors to the activation of apoptosis and growth arrest. *In vivo* studies expanded the anti-tumorigenic effect of HDAC inhibition as they were shown to act anti-angiogenic. A summary of the manifold consequences of HDAC inhibition is given in Figure 7.

Apart from the anti-neoplastic effects of HDAC inhibitors on their own, the following effects of HDAC inhibitors justify combination approaches with conventional therapy options that in a preliminary study has already been proven to be beneficial for two melanoma cell lines (Barckhausen, 2012).

2.4.2.3.1 Histone deacetylase inhibitors and apoptosis

HDAC inhibitors induce apoptosis via the intrinsic and extrinsic pathway in tumor cells (Bolden *et al.*, 2013; Brazelle *et al.*, 2010; Zhang *et al.*, 2004; Kerr *et al.*, 2012; Gillespie *et al.*, 2006). An established mediator is p53, which is acetylation-dependently stabilized and therefore capable of inducing pro-apoptotic BCL-2 members and repressing anti-apoptotic *BCL*-genes, which is often observed in HDAC-induced apoptosis (Juan *et al.*, 2000; Brazelle *et al.*, 2010; Bolden *et al.*, 2013; Zhang *et al.*, 2004). However, HDAC inhibitor-induced mitochondrial apoptosis is not limited to p53-wild-type cells as HDAC inhibitors also induce apoptosis in p53-deficient tumor cells (Vrana *et al.*, 1999; Sonnemann *et al.*, 2014). Death receptor-mediated apoptosis is inducible by HDAC inhibitors, which is also independent of the cell's p53 status and is commonly explained by an

upregulation of death receptors (DR5, FAS) and their respective ligands (TNF-related apoptosis-inducing ligand [TRAIL], FAS-Ligand) (Insinga *et al.*, 2005; Nebbioso *et al.*, 2005). Actual cell death execution may result from a combination of the aforementioned pathways, depending on cell type and genetic background, whereas other transformed cells are refractory to HDAC inhibitor-induced cell death (Fantin and Richon, 2007).

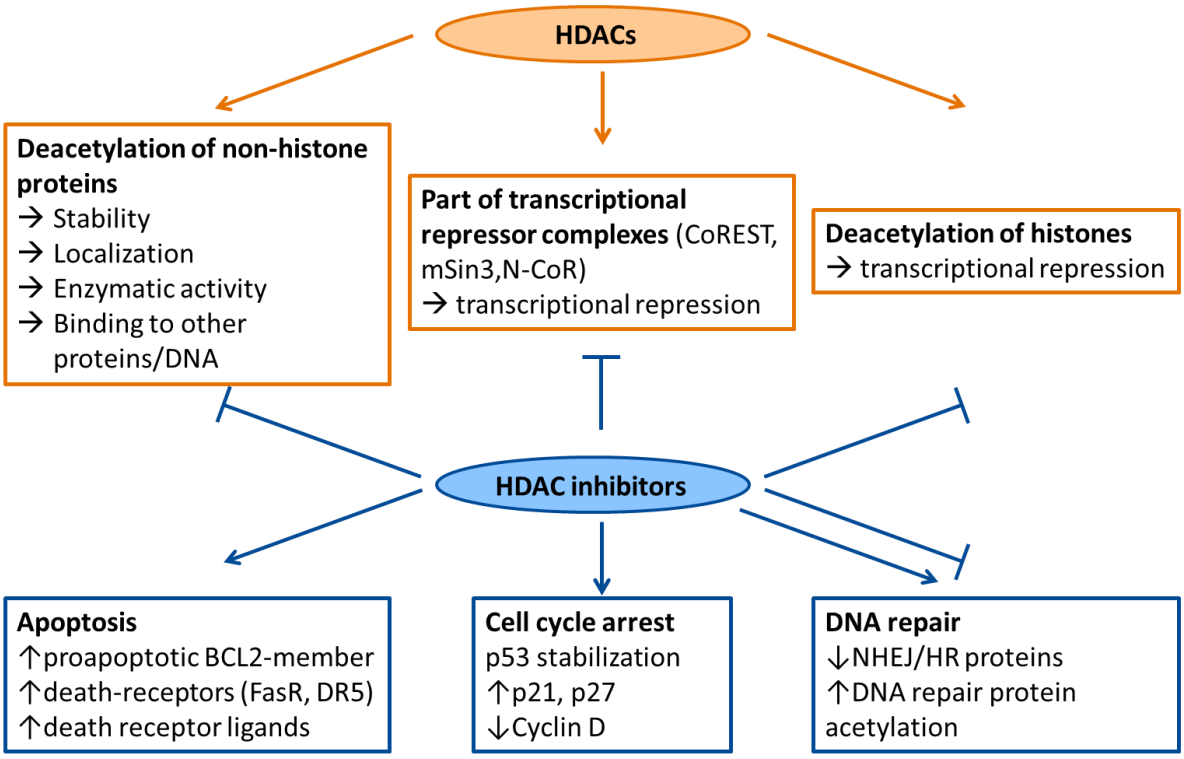

Figure 7 – Overview of histone deacetylase function and effects of histone deacetylase inhibitors. Detailed descriptions are given in the text (2.4).

2.4.2.3.2 Histone deacetylase inhibitors and cell cycle

In addition to the aforementioned effects of HDAC inhibitors on apoptosis, HDAC inhibitors were also shown to arrest cells at the G1/S or the G2/M cell cycle checkpoint. Retention of cells in G1 is mediated by an induction of the cyclin-dependent kinase inhibitors (CDKI) $p21^{CIP1/WAF1}$ and $p27^{KIP1}$ and a decrease in the G1-S-mediating cyclin D. HDAC inhibitors induce $p21^{CIP1/WAF1}$ by either p53 or SP1 transcription factor (Rosato *et al.*, 2003; Finzer *et al.*, 2001; Zhao *et al.*, 2006; Huang *et al.*, 2000; Sandor *et al.*, 2000; Newbold *et al.*, 2014), which then acts as an inhibitor of cyclin D:CDK4/6 and cyclin E:CDK2 complexes to halt cells from entering and progressing through S-phase. Cyclin D seems to be downregulated by HDAC inhibitors by acetylation of its transcription factor NF-κB or by proteasomal degradation of Cyclin D (Hu and Colburn, 2005; Alao *et al.*, 2006). Even though G2/M arrests were likewise reported upon HDAC inhibition, its underlying mechanism is still unclear. It has been reported that transcriptional downregulation of

mitosis-promoting cyclin B is responsible for G2 arrest (Noh and Lee, 2003). Other reasons for the HDAC inhibitor mediated G2/M arrest are related to Aurora kinases, which are involved in mitotic chromatin condensation. HDAC inhibition either downregulates Aurora kinases or the lack of histone 3 (H3) deacetylation reduces Aurora kinase substrates, both of the mechanisms would lead to the prevention of mitosis and an induction of a G2 arrest (Cha *et al.*, 2009; Li *et al.*, 2006).

2.4.2.3.3 Histone deacetylase inhibitors and DNA repair

Owing to the differential effects of protein acetylation, HDAC inhibitors mediate their influence on DNA repair by three mechanisms: chromatin remodeling, transcriptional regulation of DNA repair genes and post-translational acetylation of DNA repair proteins. Several studies indicate that HDAC inhibitors transcriptionally downregulate the NHEJ proteins KU70, KU80 and DNA-PK and/or the HR proteins RAD51 and BRCA2, which increases radio-sensitivity of cancer cells (Adimoolam *et al.*, 2007; Blattmann *et al.*, 2010; Kachhap *et al.*, 2010; Chinnaiyan *et al.*, 2005; Munshi *et al.*, 2005; Munshi *et al.*, 2006).

The repair of damaged heterochromatic DNA requires accessibility of repair factors to the damaged sites. Thus, histone modifications were suspected to support DNA repair as they regulate the opening of chromatin. Indeed, acetylation of histone 3 at lysine 56 (H3K56/H3K56ac) was found to contribute to reassembling of nucleosomes after completion of DNA repair or replication in yeast. Further, defects in H3K56 acetylation lead to a higher sensitivity of yeast to DNA damaging agents (Li *et al.*, 2008; Chen *et al.*, 2008; Masumoto *et al.*, 2005). In human cells, the role of H3K56 acetylation in the DNA damage response is unclear. Some studies show an increase of H3K56 acetylation by CBP/p300 HAT upon DNA damage induced by hydroxyurea, γ-radiation or MMS (Das *et al.*, 2009; Vempati *et al.*, 2010) that is reversed by class I or class III HDACs. Others have observed that H3K56ac is deacetylated by HDAC1 and HDAC2 upon DNA damage (Tjeertes *et al.*, 2009; Miller *et al.*, 2010). Interference of deacetylation by siRNA knockdown of HDAC1 and HDAC2 or addition of the HDAC inhibitor sodium butyrate is associated with impaired NHEJ, prolonged checkpoint signaling and sensitization to DNA damage (Miller *et al.*, 2010).

Despite the knowledge of multiple acetylated DNA repair proteins, the role of specific acetylations remains widely unknown (Choudhary *et al.*, 2009). A summary of DNA repair proteins and the consequence of their acetylation are shown in Table 1.

Table 1 – Acetylation of DNA repair proteins and its function.

Protein	HDAC	HAT	Functional consequence	Reference
CtIP	SIRT6	?	Constitutively acetylated, removal upon damage promotes end resection	(Kaidi *et al.*, 2010)
Sae2 (yeast CtIP homolog)	Hda1, Rpd3	Gcn5	Acetylation mediates degradation by autophagy and impairs end resection	(Robert *et al.*, 2011)

MSH2	HDAC6	?	Overlapping acetylation and ubiquitylation sites are deacetylated and ubiquitylated by HDAC6 leading to decreased MSH2 half-life and MNNG resistance	(Zhang *et al.*, 2014)
MSH2	HDAC10	HBO1?	Acetylation stimulates repair	(Radhakrishnan *et al.*, 2015)
KU70	Sirtuins	CBP, PCAF	Acetylation induced upon UV at C-terminal linker, loss of interaction with BAX that is released to mitochondria to induce apoptosis	(Cohen *et al.*, 2004)
KU70	HDAC6	CBP, PCAF	KU70 acetylation interrupts FLIP-KU70 complex leading to FLIP proteasomal degradation and apoptosis	(Kerr *et al.*, 2012)
KU70	?	?	Acetylation prevents DNA binding and repair and sensitizes to DNA damage	(Chen *et al.*, 2007b)
NBS1	SIRT1	PCAF	Acetylation prevents NBS1 phosphorylation upon irradiation and increases sensitivity to irradiation	(Yuan *et al.*, 2007)
POLβ	?	p300	Acetylation impairs 5'dRP lyase activity	(Hasan *et al.*, 2002)
PCNA	?	CBP, (p300)	Acetylation upon UV-radiation promotes DNA synthesis and subsequent proteasomal degradation	(Cazzalini *et al.*, 2014; Hasan *et al.*, 2001)

2.5 Aim of the study

A cornerstone of cancer treatment is DNA damaging therapies. In the case of malignant melanomas and glioblastomas these comprise methylating and chloroethylating agents as well as ionizing radiation. However, since both tumor entities weakly respond to therapy, intervention remains mostly palliative. Research on tumor cells already revealed multiple mechanisms that protect them from DNA damage. These include DNA repair enzymes, which repair cytotoxic lesions, or dysregulation of apoptosis, preventing cells from dying. However, to date, these resistance factors are not therapeutically targetable. A possible way of reversing intrinsic resistance is provided by a class of small molecules that target histone deacetylases. High expression of HDACs is linked to a poor prognosis and their inhibition was shown to enhance the response of colon and lung cancer cells to ionizing radiation. Based on a preliminary study that suggested a synergistic effect of the methylating agent Temozolomide with the HDAC inhibitor valproic acid in two melanoma cell lines, this study is aimed at investigating the effect of HDAC inhibitors on DNA damaging insults. Since malignant melanoma and glioblastoma cells are remarkably resistant, the potential of HDAC inhibitors for alleviating this resistance in these cancer models will be examined here. The combination with methylating agents will be of utmost interest as methylating agents are an integral part of therapy for these tumors. The HDAC inhibitors VPA and Entinostat have been shown to be well tolerated by patients and will therefore be used to address the following questions.

- Is there a synergistic effect of HDAC inhibitors and DNA damaging therapies, in particular with the methylating agent Temozolomide, in melanoma or glioblastoma cells? Is there a mechanistic difference between possible synergistic effects in these tumor entities and consequently, is a possible synergistic effect limited to characteristic genotypes of the tumor entity?
- Do HDAC inhibitors target specific DNA damage resistance pathways in these cancer types? The influence of HDAC inhibitors on DNA repair, DNA damage signaling and apoptosis will be elucidated in detail.

3 Materials and Methods

3.1 Materials

3.1.1 Chemicals and Consumables

If not stated otherwise, chemicals used for this work were obtained from Carl Roth GmbH & CoKG (Karlsruhe, Germany) or Sigma-Aldrich (Steinheim, Germany). Plastic ware was obtained from Greiner BioOne GmbH (Frickenhausen, Germany) and Eppendorf AG (Hamburg, Germany). Cell culture reagents were obtained from Gibco/ThermoFisherScientific (Waltham, MA, USA).

3.1.2 Equipment

Description	Commercial Name	Supplier
^{137}Cs source	Gammacell 2000	Molsgaard medical, Copenhagen, Denmark
Analytical balances	Sartorius analytical	Sartorius, Göttingen, Germany
Blotting chamber	TransBlot Cell	Biorad, Hercules, CA, USA
Cell disruptor	Sonifier cell disruptor	Branson Ultrasonics, Danbury, CT, USA
Centrifuges	Hereaus Megafuge1.0	ThermoFisherScientific, Waltham, MA, USA
	Refrigerated, 5402	Eppendorf, Hamburg, Germany
	Microcentrifuge Sprout	Heathrow Scientific, Vernon Hills, IL, USA
CO_2 incubator	HeraCell	ThermoFisherScientific, Waltham, MA, USA
Electrophoresis chamber	Tetra Vertical Electrophoresis Cell	Biorad, Hercules, CA, USA
Flow cytometer	FACS CANTO II	BD Biosciences, Heidelberg, Germany
Freezer	ProfiLine 7082-577-00	Liebherr, Ochsenhausen, Germany
Heating block	Thermostat 5320	Eppendorf, Hamburg, Germany
Infrared imaging system	Odyssey 9120	LI-COR, Bad Homburg, Germany
Inverse microscope	Wilovert A	Hund, Wetzlar, Germany
Laminar flow cabinet	HERA safe	ThermoFisherScientific, Waltham, MA, USA
	Nuaire	NuAire, Plymouth, MN, USA
Laser scanning microscope	LSM 710	Carl Zeiss GmbH, Jena, Germany
Liquid scintillation analyzer	Tri-Carb 2100TR	Canberra-Packard, Dreieich, Germany
Microplate reader	Multiskan EX	ThermoFisherScientific, Waltham, MA, USA
Power supply	PowerPac HC	Biorad, Hercules, CA, USA
Refrigerator	Premium NoFrost	Liebherr, Ochsenhausen, Germany

Thermal Cycler	CFX96 C1000 Real-Time PCR Detection System	Biorad, Hercules, CA, USA
	T100 Thermal Cycler	Biorad, Hercules, CA, USA
Tissue disruptor	TissueLyser LT	Qiagen, Hilden, Germany
Ultra-low temperature freezer	Forma 905	ThermoFisherScientific, Waltham, MA, USA
UV-Vis-Spectrophotometer	NanoDrop 2000	ThermoFisherScientific, Waltham, MA, USA
Vortex mixer	VORTEX 1	VWR, Darmstadt, Germany
	Vortex-Genie	Bender & Hobein GmbH, Ismaning, Germany
Water bath	3044	Köttermann, Uetze/Hänigsen, Germany

3.1.3 Software

Name and version	Source
Ascent Software Version 2.6	ThermoFisherScientific, Waltham, MA, USA
BD FACSDIVA SOFTWARE (Version 6)	BD Biosciences, Heidelberg, Germany
Cell^A	Olympus Soft Imaging Solutions, Münster, Germany
CFX Manager software (Version 3.1)	Biorad, Hercules, CA, USA
ChemSketch 2012 (Version 14.01)	ACD/Labs, Toronto, ON, Canada
EndNote (Version 9.0.0)	Thomson Reuters, New York City, NY, USA
Flowing Software (Version 2.5.1)	Perttu Terho, http://www.flowingsoftware.com
ImageJ (Version 1.49)	Wayne Rasband, http://imagej.nih.gov
ModFit LT for Mac (Version 3.3.11)	Verity Sofware House, Topsham, ME, USA
PRISM 5 for Windows (Version 5.01)	La Jolla, CA, USA
Zen 2012 (blue edition)	Carl Zeiss GmbH, Jena, Germany

3.2 Methods

3.2.1 Cell Culture

Human malignant melanoma and glioblastoma cell lines were cultured in the appropriate cell culture medium (3.2.1.1) supplemented with 10 % fetal calf serum (FCS) in a humidified, 5 % CO_2 atmosphere at 37 °C. To prevent confluency, cells were passaged, according to proliferation characteristics of the cell line, 2-3 times a week in a ratio of 1:5-1:20 by washing with phosphate buffered saline (PBS), proteolytic detachment with trypsin (0.5 g/l, Sigma-Aldrich, Steinheim, Germany) in presence of ethylenediaminetetraacetic acid (EDTA) (0.2 g/l) and resuspension in FCS-containing medium. For cryopreservation, exponentially growing cells were likewise detached

and resuspended in FCS-containing medium. After sedimentation of the cells by centrifugation (4 min, 1000 x g), cells were resuspended in FCS-containing medium + 10 % dimethylsulfoxide (DMSO) for cryoprotection and 1.5 ml aliquots thereof were immediately transferred to a -80 °C deep freezer in a passive freezer containing isopropanol for retarded chilling. After 48 h, cells were transferred to liquid nitrogen for long-term storage. Cryopreserved cells were thawed at 37 °C in a water bath and diluted with FCS-supplemented medium. Cells were sedimented by centrifugation and the supernatant (containing medium, FCS and DMSO) was removed and replaced by the appropriate cell culture medium. Cells were allowed to recover for at least 7 days. Cell lines were cultured for a maximum of 2-3 months and were then replaced by a new cryopreserved batch. Before use of a new batch of cells for experiments, they were checked for mycoplasma using Venor®GeM Classic kit (minerva biolabs®, Berlin, Germany).

Primary melanocytes and culture reagents were obtained from Gibco/ThermoFisherScientific (Waltham, MA, USA). Melanocytes were kept in Medium 254 supplemented with 1 % human melanocyte growth supplement II at a humidified atmosphere at 37 °C, 5 % CO_2 and reduced oxygen content of 5 % in order to minimize oxidative stress. Medium was refreshed every 3 days. Melanocytes were passaged by washing them with PBS and detaching them with trypsin in the presence of EDTA. Trypsin was inactivated by addition of Trypsin neutralizer solution, which was subsequently removed by centrifugation. Cell sediment was then resuspended in growth medium.

3.2.1.1 Cell lines

Cell line	Medium	Source	Described in
Melanoma cell lines			
A375	DMEM	ATCC, Manassas, VA, USA	(Roos *et al.*, 2014; Gaddameedhi *et al.*, 2010)
A2058	DMEM	Dr. W. K. Kaufmann (Dept. of Pathology and Laboratory Medicine, University of North Carolina at Chapel Hill, NC, USA).	(Gaddameedhi *et al.*, 2010; Roos *et al.*, 2014)
SK-Mel187	DMEM		(Gaddameedhi *et al.*, 2010; Roos *et al.*, 2014)
Mel537	RPMI-1640		(Gaddameedhi *et al.*, 2010; Roos *et al.*, 2014)

D05	RPMI-1640	Prof. C.W. Schmidt (Cancer Immunotherapy, QIMR Berghofer Medical Research Institute, Brisbane, Queensland, Australia) via Prof. T. Wölfel (Hematology/ Oncology/ Pneumology, University Medical Center, Mainz, Germany)	(Barckhausen *et al.*, 2014; Naumann *et al.*, 2009)
G361	RPMI-1640	ATCC, Manassas, VA, USA	(Naumann *et al.*, 2009; Ji *et al.*, 2012)
Glioblastoma cell lines			
U87MG	DMEM	CLS, Eppelheim, Germany	(Batista *et al.*, 2007; Ishii *et al.*, 1999)
LN229	DMEM	ATCC, Manassas, VA, USA	(Batista *et al.*, 2007; Ishii *et al.*, 1999)
LN308	DMEM	Dr. M. Hermisson (Department of General Neurology, Hertie Institute for Clinical Brain Research, University of Tübingen, School of Medicine, Tübingen, Germany)	(Batista *et al.*, 2007; Ishii *et al.*, 1999)
LN428	DMEM		(Ishii *et al.*, 1999)

3.2.1.2 Treatments and irradiation

3.2.1.2.1 Histone deacetylase inhibitor treatment

Cells were seeded at an appropriate number, according to growth characteristics of the cell line 24 h before treatment to allow attachment. For pretreatment, VPA (sterile filtered stock solution of 100 mM in double distilled H_2O [ddH_2O]) or MS-275 (Selleckchem, Houston, TX, USA, stock solution of 5 mM in DMSO) was added and replaced every 48 h by exchange of medium containing the respective drug. Fast growing cells required passaging during 168 h pretreatments. One day before the end of the pretreatment period, cells were seeded for further treatment/irradiation, kept in HDAC inhibitor-containing medium, which was removed before further treatment. Controls were seeded, passaged and reseeded according to pretreated cells. For co-treatment, cells were likewise treated with HDAC inhibitor 24 h after seeding, but the drug remained in the medium also after further treatment, which occurred 1 h after HDAC inhibitor addition (Figure 8).

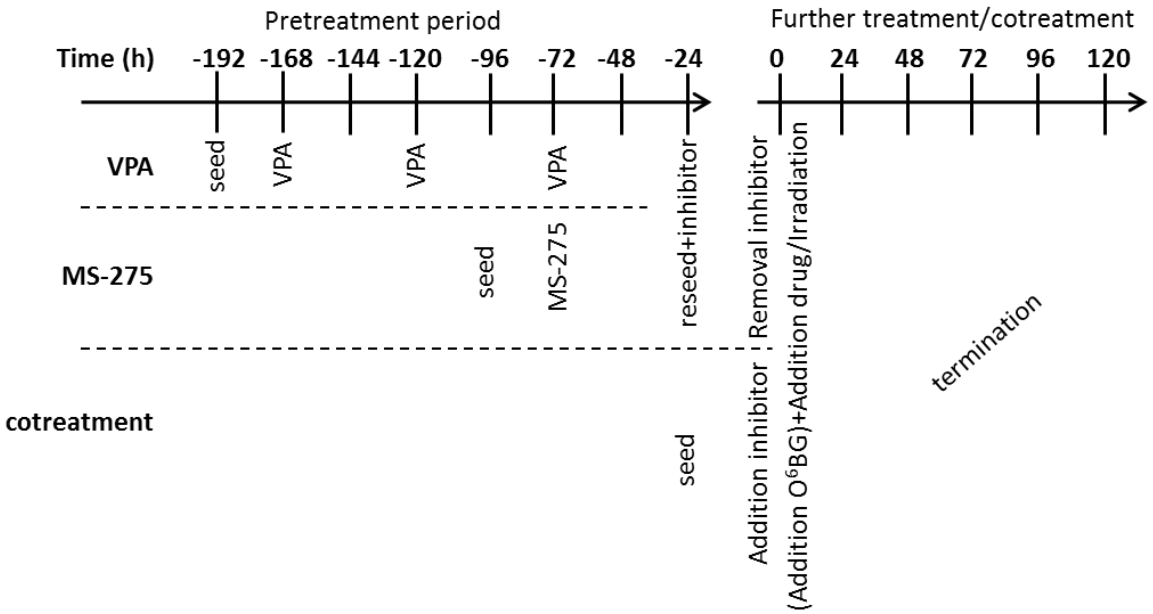

Figure 8 – Visualization of pre- and co-treatment scheme.
See text for details (3.2.1.2.1)

3.2.1.2.2 Treatment with alkylating agents

Unless otherwise stated, cells were seeded 24 h prior to treatment with 10 µM O^6-benzylguanine (O^6BG, 10 mM stock solution in DMSO) to deplete MGMT. In case of HDAC inhibitor pretreatment, medium was changed in order to remove the inhibitor before O^6BG addition. One hour after O^6BG, the alkylating agent was added. Temozolomide (Schering-Plough, Kenilworth, NJ, USA) was prepared by dissolving in DMSO and further diluting, 1:3, in sterile H_2O to 35 mM. Aliquots of 35 mM stock solution were stored at -80 °C until use. Fotemustine (Servier Research, International, Neuilly-sur-Seine, France) was dissolved immediately before use in ethanol to a 32 mM working solution.

3.2.1.2.3 Olaparib treatment

Olaparib (Selleckchem, Houston, TX, USA) was dissolved in DMSO to a 10 mM solution and stored in aliquots at -80 °C. It was added to pretreated cells after HDAC inhibitor removal by medium exchange.

3.2.1.2.4 Irradiation

Adherent cells were irradiated in medium with γ rays using a ^{137}Cs source.

3.2.1.3 Cell growth

Cells were seeded at a defined density of 50 000 cells in 60 mm cell culture dishes and allowed to attach 24 h before treatment. Number of cells was assessed every 24 h by counting using a

hemocytometer and cell numbers were related to pre-treatment number (0 h). Doubling times were calculated using PRISM software.

3.2.1.4 Colony Formation Assay

Cells were seeded in 60 mm cell culture plates at a defined density (200 cells for controls, 400 cells for 5 µM TMZ and 800 cells for 10 µM TMZ), resulting in approximately 50-200 colony forming units. After six hours incubation that allowed cell attachment and conditioning of the medium, cells were treated and allowed to grow to colonies for 10-14 days depending on the growth characteristics of the cell line. Then, growth medium was removed and cells were fixed with a methanol-acetic acid-water solution (1:1:8, V:V:V) for 30 min. Colonies were stained with 1.25 % Giemsa and 0.125 % Crystal violet for 15 min and subsequently rinsed with water. Stained colonies that contained at least 50 cells were counted for control and treatments. Clonogenic survival was calculated with respect to the seeding efficiency that was obtained from untreated samples.

3.2.1.5 Transfection

Stably transfected clones were generated by transfection of cells at a confluence between 60-80 percent. Knockdown of RAD51 was achieved using a shRAD51 sequence targeting RAD51 mRNA expressed by the pSUPER vector backbone (Quiros *et al.*, 2011). Antibiotic resistance for selection of positive clones was introduced by co-transfection with the pSUPER.neo plasmid with a lower plasmid amount (1.8 µg pSUPER-RAD51sh + 0.2 µg pSUPER.neo, plasmids gratefully received from Dr. Steve Quiros). The pDRGFP plasmid for flow cytometric detection of HR-mediated DSB repair (Pierce *et al.*, 1999) addgene #26475, plasmid gratefully received from Dr. Wynand Roos) provided the repair substrate and puromycin selector and 1 µg DNA was used for transfection. All transfections of cells were performed using the Effectene® transfection reagent (Qiagen, Hilden, Germany) according to manufacturer's protocol. One day after transfection, cells were re-passaged 1:6 and another 24 h later the selective antibiotic was added (G418 in A375-1.5 µM, Puromycin: A375-34.7, D05-9.3 µM). Upon colony formation, clones were selected and transferred to a 24 well plate and expanded for cryopreservation and testing. RAD51 knockdown was verified by western blotting.

Cells transfected with pDRGFP for HR activity measurement required transient transfection with an I-SceI expressing plasmid (pCβASceI, described in (Richardson *et al.*, 1998), addgene #26477, provided by Dr. Wynand Roos). Cells were transfected with 1 µg DNA using Effectene® transfection reagent (Qiagen, Hilden, Germany) according to the manufacturer's instructions.

All stably transfected cells were kept in selective antibiotic during culture, but not during the course of an experiment.

3.2.2 Flow cytometry analyses

3.2.2.1 Apoptosis and cell cycle detection

3.2.2.1.1 Propidium iodide staining

Propidium iodide enters ethanol-fixed cells and intercalates into DNA, which multiplies its fluorescence and therefore allows measurement of a cell's DNA content by flow cytometry. A typical cell cycle profile of unperturbed cells shows a G1 (2n) and G2-peak (4n). The G2-peak shows double the fluorescence intensity of the G1 peak and S-phase cells show fluorescence intensities between the G1 and the G2 peaks. Cells with a subdiploid DNA content are regarded as apoptotic due to DNA fragmentation and degradation during apoptosis (Nicoletti *et al.*, 1991; Krishan, 1975).

Cells were detached and combined with the cells in the supernatant medium and sedimented as described earlier. Then, cell sediments were resuspended in 20 µl PBS and fixed with ice-cold 80 % ethanol by adding 1 ml of the ethanol while vortexing. Samples were stored at –20 °C awaiting staining. To this end, 2 ml of PBS were added to the cell suspension and cells were sedimented by centrifugation (5 min, 1500 x g). Cells were resuspended in PBS containing RNase A (30 µg/ml working concentration, 10 mg/ml in H_2O stock concentration stored at -20 °C). RNA digestion was performed for 30 min at room temperature (RT). Propidium iodide (working concentration of 25 µM, stock concentration 50 µg/ml in PBS at 4 °C) was added to the cell suspension and kept in the dark and on ice until analysis by flow cytometry (maximum 30 min). Apoptosis measurement by Sub-G1 content was analyzed using BD FACSDiva™ software and cell cycle distribution was analyzed using ModFit LT™ software.

3.2.2.1.2 AnnexinV-FITC/Propidium iodide double-staining

An early event in apoptosis is flipping of phosphatidylserine from the inner cytoplasmic facing membrane to the outer cellular facing membrane, which marks the cell for phagocytosis by macrophages. AnnexinV binds to phosphatidylserine on the cell surface, but also to intracellular phosphatidylserine if the membrane integrity is lost. Membrane integrity is lost in cells undergoing necrosis or when apoptosis has progressed beyond the point where macrophages would have removed them from the cell population in a physiological environment. In order to discriminate between apoptotic cells and necrotic/late apoptotic cells the DNA intercalator PI is added to the cells. PI is excluded from viable cells but not from dead cells and, therefore, marks late apoptotic or necrotic cells (Vermes *et al.*, 1995).

Cells were detached and collected as described and washed with 1 ml PBS. For binding of AnnexinV-FITC, sedimented cells were resuspended in 50 µl binding buffer (10 mM 4-(2-hydroxyethyl)-1-piperazineethanesulfonic acid [HEPES] pH 7.4, 140 mM NaCl, 2.5 mM $CaCl_2$,

0.1 % bovine serum albumin [BSA]) containing 2.4 µl AnnexinV-FITC (Miltenyi, Bergisch Gladbach, Germany). After 20 min incubation on ice and in the dark, PI (in 430µl binding buffer) was added, yielding a final concentration of 1.5 µM PI. Cells were kept in the dark and on ice until flow cytometry analysis. Data were analyzed using BD FACSDiva™ software. Double-negative cells were regarded as viable, FITC-only positives were regarded as apoptotic and FITC/PI double-positives were regarded as late apoptotic/necrotic.

3.2.2.2 Homologous recombination assay

To measure the capacity of cells to repair DSBs by HR, cells with a stably integrated pDRGFP plasmid were used (see section 3.2.1.5). The plasmid bears two non-functional *GFP* genes: one truncated, the other containing a recognition site for I-SceI endonuclease. Upon introduction of an I-SceI expressing plasmid, the endonuclease cleaves the modified *GFP* gene leading to a DSB. If this is repaired by HR, with the use of the sequence of the truncated *GFP* gene, a functional GFP protein is generated, allowing analysis by flow cytometry. Cells were analyzed 48 h (A375) or 72 h (D05) after transfection with pCβASceI, which took into account their differences in proliferation rate. Cells were detached and washed with PBS and measured by flow cytometry. Data were analyzed with BD FACSDiva™ software.

3.2.3 Protein analysis

3.2.3.1 Protein extracts

3.2.3.1.1 Total protein extraction

Cells were detached, sedimented by centrifugation at 4 °C followed by medium removal and flash frozen in liquid nitrogen. Pellets were stored at -80 °C until protein extraction. For protein extraction, cells were resuspended in extraction buffer (20 mM Tris(hydroxymethyl)aminomethane [TRIS] HCl pH 8.5, 1 mM EDTA, 5 % glycerine, 1 mM β-Mercaptoethanol, 10 µM Dithiothreitol [DTT], 1 x protease inhibitor cOmplete™). For disruption, the suspension was sonicated on ice (three times 10 pulses at duty cycle 40 % and output control 4) and afterwards centrifuged (10 min, 4 °C, 16000 x g) to sediment remaining debris. The supernatant extract was stored at -80 °C.

For protein extraction from *in vivo* tumor samples, pieces of 2-4 mm^3 were disrupted in 1 ml extraction buffer (20 mM TRIS HCl pH 8.5, 1 mM EDTA, 5 % glycerine, 1 mM β-Mercaptoethanol, 10 µM DTT, 1 x protease inhibitor cOmplete™) by Qiagen Tissue Lyser and further sonicated and cleared from debris as described above.

3.2.3.1.2 Nuclear protein extraction

Cell pellets were collected as described, washed in PBS and stored at -80 °C until extraction. Cell pellets were resuspended in nuclear extraction buffer (20 mM TRIS HCl pH 8.5, 1 mM EDTA, 1 mM β-Mercaptoethanol, 10 µM DTT, 1 x protease inhibitor cOmplete™). In order to damage the

cell membrane, the suspension was repeatedly frozen (three times) in liquid nitrogen and thawed at 37 °C. To sediment the nuclei, suspensions were centrifuged at 4 °C, 16000 x g for 10 min. Pellets were resuspended in nuclear extraction buffer containing 5 % glycerol and were subsequently disrupted by sonication (three times 10 pulses at duty cycle 40 % and output control 4). Nuclear extract was separated from debris by centrifugation (4 °C, 16000 x g for 10 min) and stored at -80 °C until use.

3.2.3.1.3 Protein concentration determination

The protein concentration in extracts was measured by the Bradford method, which is based on an adsorption shift of free Coomassie Brilliant Blue to protein bound Coomassie Brilliant Blue (Bradford, 1976). A calibration curve of BSA (1 mg/ml in ddH_2O) was pipetted into a 96 well plate ranging from 0-6 µg BSA per well. Likewise, 10 µl of pre-diluted protein samples (1:5 in ddH_2O) were loaded on the plate and stained with 200 µl of Bradford reagent (8.5 % phosphoric acid, 4.75 % ethanol, 1 % Coomassie Brilliant Blue G250). Samples and calibration were performed in technical triplicates. After 10 min of incubation in the dark, adsorption was measured at 600 nm.

3.2.3.1.4 Protein extraction for phosphorylated and large proteins

For the analysis of large (> 200 kDa) or phosphorylated proteins, the cell monolayer was washed with PBS in the culture dish and the PBS was completely removed. Cells were lysed directly on the plate by addition of sodium dodecyl sulfate (SDS) sample loading buffer (62.5 mM TRIS HCl pH 6.8, 10 % glycerine, 5 % β-mercaptoethanol, 2 % SDS and 0.01 % bromophenol blue) with agitation and using a cell scraper. Lysates were transferred to microfuge tubes, sonicated (three times 10 pulses at duty cycle 40 % and output control 4) and stored at -80 °C until use.

3.2.3.1.5 Semi-quantitative measurement of protein concentration

Relative protein amounts of extracts obtained by direct lysis of cells in SDS-loading buffer (3.2.3.1.4) were determined by densitometry analysis of loading controls (β-Actin or ERK2) as measured after SDS polyacrylamide gel electrophoresis (SDS-PAGE), western blotting and detection (3.2.3.2 and 3.2.3.3). After quantification of loading controls by densitometry, the volume loaded onto gels was adjusted to obtain equal relative protein amounts. The absence of regulation of the loading control proteins by the treatment was verified by blots performed with Bradford-quantified protein extracts.

3.2.3.2 Sodium dodecyl sulfate polyacrylamide gel electrophoresis

SDS-PAGE allows separation of proteins by their size. SDS sample buffer was added to each sample (unless SDS sample buffer was used for cell lysis as described in section 1.2.3.1.4), denatured at 95 °C (for 3 min) or at 56 °C (for 5 min) for proteins >200 kDa. Depending on protein abundance, an amount of 30-80 µg of protein was loaded onto gels for electrophoresis. Proteins

were firstly concentrated in the stacking gel (126 mM TRIS HCl pH 6.8, 4 % Acrylamide/Bisacrylamide, 0.1 % SDS, 0.1 % ammonium persulfate, 0.1 % TEMED) and then electrophoretically separated in the separating gel (375 mM TRIS HCl pH 8.8, 5-15 % Acrylamide/Bisacrylamide, 0.1 % SDS, 0.05 % ammonium persulfate, 0.05 % TEMED). Electrophoresis was performed between 90 and 120 V in running buffer (50 µM TRIS, 384 mM glycin, 0.1 % SDS). Protein ladders (protein-marker IV, peqlab, Erlangen, Germany or Spectra™ Multicolor High Range Protein Ladder, ThermoFisherScientific, Waltham, MA, USA) were used in parallel to protein samples to allow size comparison after blotting.

3.2.3.3 Immunoblotting

Transfer of SDS-PAGE separated proteins onto a nitrocellulose membrane (Protran, Amersham, GE Healthcare, Dassel, Germany) occurred in blotting buffer (50 µM TRIS, 384 mM glycin, 20 % methanol) at a current of 80-300 mA for 3-18 h at 4 °C. Transfer was verified by ponceau staining (0.1 % Ponceau, 5 % acetic acid) for 2 min, which was removed by rinsing the membrane in ddH_2O. Following ponceau removal, non-specific antibody binding to the membrane was blocked by incubation of the membrane in 5 % BSA or 5 % fat milk free in TRIS-buffered saline with Tween (TBS-T) (20 mM TRIS HCl pH 7.6, 150 mM NaCl, 0.1 % Tween-20) for 60 min. Primary antibodies (3.2.3.4) were diluted in 5 % BSA or fat free milk in TBS-T and incubated with the membrane overnight at 4 °C. Unbound residual antibody was washed away by rinsing the membrane in TBS-T (three times for 5 min at RT). The appropriate secondary antibody (3.2.3.4) coupled to an infrared dye was diluted 1:10000 in TBS-T and incubated with the membrane for 3-5 h at RT in the dark. After binding of the secondary antibody to the primary antibody, the membrane was washed (three times for 5 min at RT) and the signal generated by the infrared dye coupled secondary antibody was detected with the LI-COR® Odyssee system that measures fluorescence. Relative protein levels were determined by densitometry analysis using ImageJ.

3.2.3.4 Antibodies

Antigen	Host	Dilution	Supplier
Primary antibodies			
Acetylated histone 3	Rabbit	1:1000	Merck Millipore, Billerica, MA, USA
Acetylated histone 4	Rabbit	1:2000	Merck Millipore, Billerica, MA, USA
ATR	Rabbit	1:1000	Cell signaling technology, Danvers, MA, USA
BAX	Mouse	1:500	Santa Cruz Biotechnology, Dallas, TX, USA
BCL-2	Mouse	1:1000	BD Pharmingen, Franklin Lakes, NJ, USA
CHK1	Mouse	1:1000	Cell signaling technology, Danvers, MA, USA
CHK2	Mouse	1:1000	Cell signaling technology, Danvers, MA, USA
ERK2	Mouse	1:1000	Santa Cruz Biotechnology, Dallas, TX, USA
FANCD2	Mouse	1:200	Santa Cruz Biotechnology, Dallas, TX, USA

HDAC1	Mouse	1:1000	Cell signaling technology, Danvers, MA, USA
HDAC2	Mouse	1:1000	Cell signaling technology, Danvers, MA, USA
HDAC3	Mouse	1:1000	Cell signaling technology, Danvers, MA, USA
HDAC8	Rabbit	1:1000	Santa Cruz Biotechnology, Dallas, TX, USA
HSP90	Mouse	1:1000	Santa Cruz Biotechnology, Dallas, TX, USA
KU80	Mouse	1:1000	GeneTex, Irvine, CA, USA
NOXA	Mouse	1:1000	Calbiochem/Merck Millipore, Billerica, MA, USA
p21$^{Cip1/Waf1}$	Mouse	1:1000	Cell signaling technology, Danvers, MA, USA
p53	Rabbit	1:1000	Santa Cruz Biotechnology, Dallas, TX, USA
pATM^{Ser1981}	Rabbit	1:1000	Cell signaling technology, Danvers, MA, USA
pATR^{Ser428}	Rabbit	1:1000	Cell signaling technology, Danvers, MA, USA
pCHK1^{Ser345}	Rabbit	1:1000	Cell signaling technology, Danvers, MA, USA
pCHK2^{Thr68}	Rabbit	1:1000	Cell signaling technology, Danvers, MA, USA
PCNA	Mouse	1:300	Calbiochem/Merck Millipore, Billerica, MA, USA
RAD51	Rabbit	1:5000	abcam, Cambridge, UK
RAD51D	Mouse	1:1000	Merck Millipore, Billerica, MA, USA
RPA p34	Mouse	1:1000	ThermoFisherScientific, Waltham, MA, USA
Talin-1	Rabbit	1:1000	Cell signaling technology, Danvers, MA, USA
β-Actin	Mouse	1:2000	Santa Cruz Biotechnology, Dallas, TX, USA
γH2AX	Rabbit	1:1000	Cell signaling technology, Danvers, MA, USA
Secondary antibodies			
IRDye anti mouse IgG 800CW	Donkey	1:10000	LI-COR, Lincoln, NE, USA
IRDye anti rabbit IgG 800CW	Donkey	1:10000	LI-COR, Lincoln, NE, USA
IRDye anti mouse IgG 680RD	Donkey	1:10000	LI-COR, Lincoln, NE, USA
IRDye anti rabbit IgG 680RD	Donkey	1:10000	LI-COR, Lincoln, NE, USA

3.2.3.5 Immunohistofluorescence

Paraffin-embedded melanoma samples from untreated patients were obtained from Dr. C. Loquai (Dermatology, University Medicine Mainz). Microtome sections were deparaffinized by Xylene extraction (three times 5 min at RT) and rehydrolized by incubation in solutions with decreasing ethanol dilutions (100 % three times for 3 min at RT, 95 %, 80 % both two times for 3 min at RT) and finally in ddH_2O for 5 min at RT. For antigen retrieval, sections were incubated in citrate buffer (10 mM sodium citrate pH 6) at 95 °C for 25 min, cooled down to RT and rinsed with TBS-T. Non-specific binding sites were blocked by incubating the sections in serum free protein block

(DAKO, Carpinteria, CA, USA) for 30 min at RT. Primary antibodies were diluted in TBS-T (HDAC1 1:6400, HDAC2 1:400), added onto the section and allowed to bind overnight at 4 °C in a humidified atmosphere. After washing away the first antibody with TBS-T (three times for 5 min), the secondary Alexa Fluor® 488-coupled anti-mouse antibody (LifeTechnologies, Carlsbad, CA, USA), diluted 1:1000 in TBS-T, was incubated on the section for 1 h at RT. The antibody was removed by washing with TBS-T (three times for 5 min) and the section was stained with nuclear stain TO-PRO®-3 (1 µM in TBS-T for 15 min, ThermoFisherScientific, Waltham, MA, USA). TO-PRO®-3 was rinsed away with TBS-T and the section was mounted in Vectashield (Vector Laboratories, Burlingame, CA, USA). Images were acquired using a laser scanning microscope together with the Zen software.

3.2.3.6 Immunofluorescence

For detection of γH2AX foci, cells were seeded on pretreated coverslips (10 min in diethylether, 5 min in 100 % ethanol, 5 min in 70 % ethanol, 5 min in dH_2O, 30 min in 1 M HCl and storage in 70 % ethanol). After treatment and incubation time, cells on coverslips were rinsed in PBS and fixed for 15 min in 3.7 % formaldehyde in PBS. Coverslips were washed with PBS (three times for 5 min) and then submerged in ice-cold 100 % methanol in which the samples were stored until staining (maximum 5 days). Cells on coverslips were washed with PBS (three times for 5 min) before non-specific binding was blocked with BSA (5 % in PBS/0.3 % Triton-X-100) for 1 h at RT. The γH2AX antibody (murine host, Merck Millipore, Billerica, MA, USA) was diluted 1:1000 in PBS/0.3 % Triton-X-100 and added to the coverslips. After incubation overnight at 4 °C, the primary antibody was removed by washing the coverslips with PBS (three times 5 min). The secondary anti mouse Alexa Fluor® 488 coupled antibody (1:1000 in PBS/0.3 % Triton-X-100, LifeTechnologies, Carlsbad, CA, USA) was added to the coverslips and the coverslips were incubated for 1 h at RT. Upon removal of secondary antibody by washing in PBS (three times for 5 min), nuclei were stained with TO-PRO®-3 in PBS/0.3 % Triton-X-100 for 15 min, rinsed, and coverslips were mounted in Vectashield (Vector Laboratories, Burlingame, CA, USA). Images were acquired with laser scanning microscope. Foci per cell were counted using the Cell A software.

3.2.3.7 MGMT activity assay

The *in vitro* measurement of MGMT activity in protein extracts (3.2.3.1.1) is based on the transfer of ^{3}H-labeled methyl groups from ^{3}H-MNU treated calf thymus DNA onto MGMT. Therefore the ^{3}H-DNA (10 µl, 80000 counts per minute) was incubated with 200 µg of total protein in reaction buffer (HEPES-KOH pH 7.8, 1 mM DTT, 5 mM EDTA) for 90 min at 37 °C. Transfer reactions were stopped by addition of trichloroacetic acid (13 %) and 200 µg BSA and DNA was heat-denatured (95 °C for 45 min). After precipitation of the protein (10 min, 14 000 4 °C), the sediment was washed three times with 5 % trichloroacetic acid and resuspended in 200 mM NaOH.

Using a liquid scintillation counter, remaining radioactivity was measured and was expressed as fmol (transferred radioactivity from ^{3}H-DNA) per mg of total protein (fmol/mg protein).

3.2.4 Gene expression

3.2.4.1 Real time polymerase chain reaction

Real time polymerase chain reaction (real-time PCR) enables the measurement of gene specific mRNA expression. Therefore, RNA was extracted from cell pellets stored at -80 °C using a silica column kit (NucleoSpin® RNA, Macherey-Nagel, Düren) according to the manufacturer's instructions. The RNA was eluted with RNase-free water and the concentration and purity was measured spectrophotometrically using absorbance at 260 nm for RNA concentration and its ratio to 280 nm and 230 nm to note contamination with proteins, EDTA and carbohydrates. One microgram of RNA was subjected to reverse transcription using Verso cDNA kit (ThermoFisherScientific, Waltham, MA, USA) with anchored oligo dT primers. The resulting cDNA in 20 µl was diluted to 50 µl and 4 µl of this dilution were used in the 16 µl PCR reaction (total cDNA dilution 1:6). Primers (forward and reverse, see 3.2.4.1.1) were added at a final concentration of 250 nM each. Primers for the housekeeping genes (*ERCC6* and *VIPAS39)*, obtained from primerdesign (Southampton, UK) were tested for non-regulation following experiment specific treatment. For amplification and measurement a mastermix (SensiMix SYBR® & Fluorescein Kit, Bioline, London, UK) containing a hot start DNA polymerase, dNTPs, $MgCl_2$ (final concentration 4 mM) and the SYBR® green fluorophore was used. Conditions for the PCR were 50 °C for 2 min, polymerase activation at 95 °C for 10 min, amplification cycles of 10 s at 95 °C denaturation, 20 s at 56 °C for annealing and elongation for 20 s at 72 °C. SYBR® green fluorescence was acquired after each cycle. After 45 cycles a melt curve analysis of the products was performed at temperatures ranging from 65 to 95 °C. Relative cDNA levels were analyzed using Bio-Rad CFX manager software.

3.2.4.1.1 Primer sequences

Gene	Orientation	Sequence	Supplier
RAD51	forward	ACGGTTAGAGCAGTGTGGC	Primers were obtained from Life Technologies, Carlsbad, CA, USA
	reverse	TGATCTCTGACCGCCTTTGG	
FANCD2	forward	CCTGGCGGGAAAGTCGAAA	
	reverse	GGTTGCTTCCTGGTTTTGGAG	
ATR	forward	ATGCAAACTCTCAAGCTCGG	
	reverse	TGAATCTTCTACTCCAGTCACAAA	

3.2.4.1.2 PCR array

The PCR array comprised about 180 gene specific primers, for the detection of genes implicated in cell cycle regulation, DNA repair and cell death as well as *ACTB* and *GAPDH* used as housekeeping genes, at a concentration of 625 nM on PCR plates. A mixture of cDNA (2 µg RNA input for synthesis, final dilution of cDNA 1:20), $MgCl_2$ (4 mM) and the master mix (see. 3.2.4.1) was added to the primers (final concentration 250 nM) and amplification occurred according to a slightly modified version of the previously described PCR protocol (see section 3.2.4.1). Here the annealing temperature was 55 °C.

3.2.5 Xenograft experiment

Animal experiment was conducted in accordance with the act for the protection of animals (Tierschutzgesetz) by FELASA-trained, Dr. K.-H. Tomaszowski, until mice were humanly sacrificed. Nude immune deficient male BALB/c nu/nu mice were obtained from Charles River (Wilmington, MA, USA) and housed in a pathogen free environment at 26 °C, a 12 h day/night cycle and watered and fed *ad libitum*.

For the induction of xenograft tumors, 6 x 10^6 Mel537 cells in PBS were subcutaneously injected into each flank (left and right) of the mouse. Mice were randomly grouped (six groups of three animals) and when tumor size [(W*H*L*π)/6] reached on average 100 mm^3 treatment was started. Animal groups received PBS only (control group) or VPA at doses of 200/275/350/425 or 500 mg/kg bwt (bodyweight – bwt) twice daily (in the mornings and nights, 10 h difference) for five days. The drug was injected intraperitoneally. Bodyweight and tumor size was monitored over the course of the experiment. The experiment was terminated 2 h after the last treatment by cervical dislocation and subsequent surgical harvesting of the tumor material, which was snap-frozen in liquid nitrogen and stored at -80 °C until protein extraction.

3.2.6 Statistics

Unless otherwise stated, data points show the means of at least three independent experiments and their standard deviation as error bars. For comparison of two groups the two-tailed unpaired t-test was used and the calculated *p*-values are displayed: *p*-value<0.05*, *p*-value<0.005**, *p*-value<0.001***. For statistical analysis and graph plotting PRISM software was used.

4 Results

4.1 Effect of histone deacetylase inhibition on the sensitivity of melanoma cells to genotoxic stress

Patients suffering from metastatic melanoma face low response rates as the cancer rapidly develops resistance to B-RAF inhibitors (in B-RAF mt tumors), immunotherapy and to irradiation or alkylating agent-based genotoxic therapies. This results in a low 5-year survival rate ranging between 10-25 % (Balch *et al.*, 2009). As HDAC inhibitors have proven antiproliferative and radiosensitizing in prostate cancer (Chen *et al.*, 2007b), lung cancer cells (Geng *et al.*, 2006) and other cancers (Blattmann *et al.*, 2010; Banuelos *et al.*, 2007), their impact on melanoma sensitivity towards routinely used alkylating agents was investigated.

4.1.1 Histone deacetylase expression in melanoma

The use of HDAC inhibitors in cancer therapy is based upon the correlation of HDAC overexpression with dismal prognoses, which has been shown for class I HDACs in solid tumors like colon and prostate cancer (Huang *et al.*, 2005; Wilson *et al.*, 2006; Halkidou *et al.*, 2004; Weichert *et al.*, 2008b). Expression levels of these HDACs, namely HDAC1, HDAC2, HDAC3 and HDAC8, in melanoma are incomplete and therefore required analysis.

Class I HDAC expression levels were assessed in six melanoma cell lines (A375, A2058, D05, G361, Mel537 and SK-Mel187) and compared to three non-cancerous cell samples (peripheral blood mononuclear cells-PBMCs, immortalized fibroblasts-VH10tert and primary melanocytes) by immunoblotting. HDAC1, HDAC2, HDAC3 and HDAC8 were expressed in all of the analyzed samples. HDAC expression in PBMCs was only detectable at higher intensity settings and therefore not included for further analysis. Though, differing between the cell lines, HDAC1, HDAC2 and HDAC3 protein levels were 2.5-3 fold higher in melanoma cells as compared to non-cancerous cells. In contrast, protein levels of HDAC8 were similar in cancer and non-cancerous cells (Figure 9 a and b). Further, HDAC1 and HDAC2 expression was verified in a melanoma sample by immunohistofluorescence. Both HDACs were positively stained and staining was limited to the nucleus as indicated by nuclear stain TO-PRO®-3 (Figure 9 c).

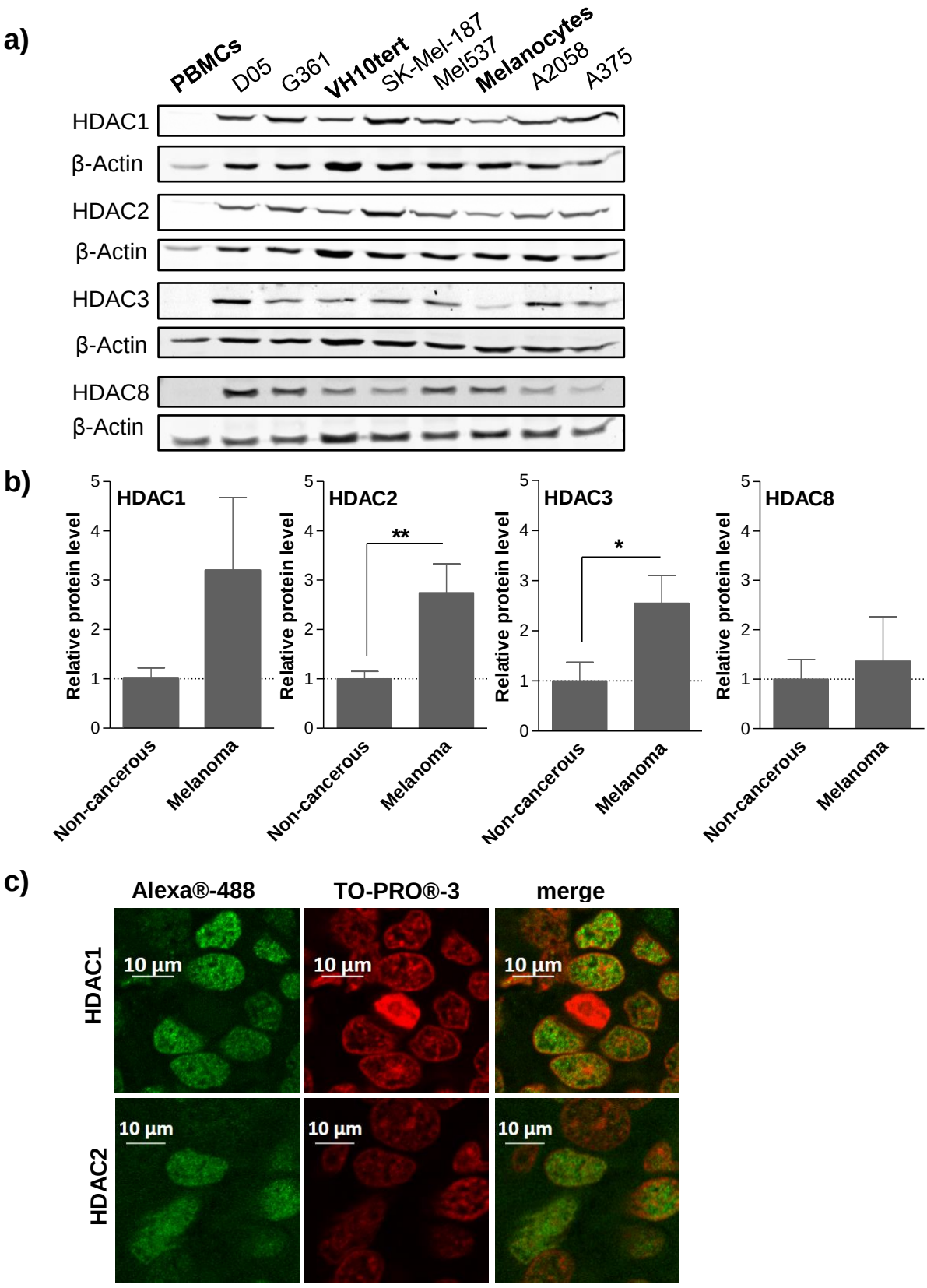

Figure 9 – Class I HDAC expression in melanoma cells.
Whole-cell protein extracts of melanoma cell lines (D05, G361, SK-Mel-187, Mel537, A2058 and A375) and non-cancerous cells (PBMCs, VH10tert and Melanocytes) that have been subjected to immunoblotting (**a**). HDAC-levels were quantified and normalized to β-actin and means of relative protein levels for melanoma cell lines and non-cancerous cells are displayed (**b**). Immunohistofluorescence staining of melanoma samples. HDACs are shown in green while nuclear stain (TO-PRO®) is shown in red (**c**).

4.1.2 Effect of HDAC inhibitors on melanoma cells

Having shown that HDAC1, HDAC2 and HDAC3 are upregulated in melanomas, their inhibition might be a reasonable approach for a possible adjuvant therapy. The short chain fatty acid VPA is an HDAC inhibitor that has been used for the therapy of epilepsy for more than fifty years and is well characterized in terms of adverse side effects and tolerance. VPA acts at a millimolar range and inhibits HDAC1, HDAC2, HDAC3 and HDAC8 (Phiel *et al.*, 2001; Göttlicher *et al.*, 2001; Bradner *et al.*, 2010). First, its functionality in melanoma cells was tested by analyzing histone acetylation. The six melanoma cell lines tested, show heterogenous basal acetylation of histone 3 (H3ac) and histone 4 (H4ac), but in all of them a 168 h treatment with VPA increased H3ac and H4ac levels, verifying the function of VPA as an HDAC inhibitor in these melanoma cells (Figure 10 a). In addition, VPA decreased the protein levels of HDAC1, HDAC2 and HDAC3 in all cell lines except for A2058 (S 1). MS-275 was selected as a second HDAC inhibitor due to its selectivity to HDAC1, HDAC2 and HDAC3 (Bradner 2010), as these showed the highest expression compared to non-cancerous cells in the melanoma cell lines used. Treatment of melanoma cell lines (D05, A375) with MS-275 dose-dependently increased H3ac, showing the susceptibility of melanoma cell lines to this HDAC inhibitor (Figure 10 b).

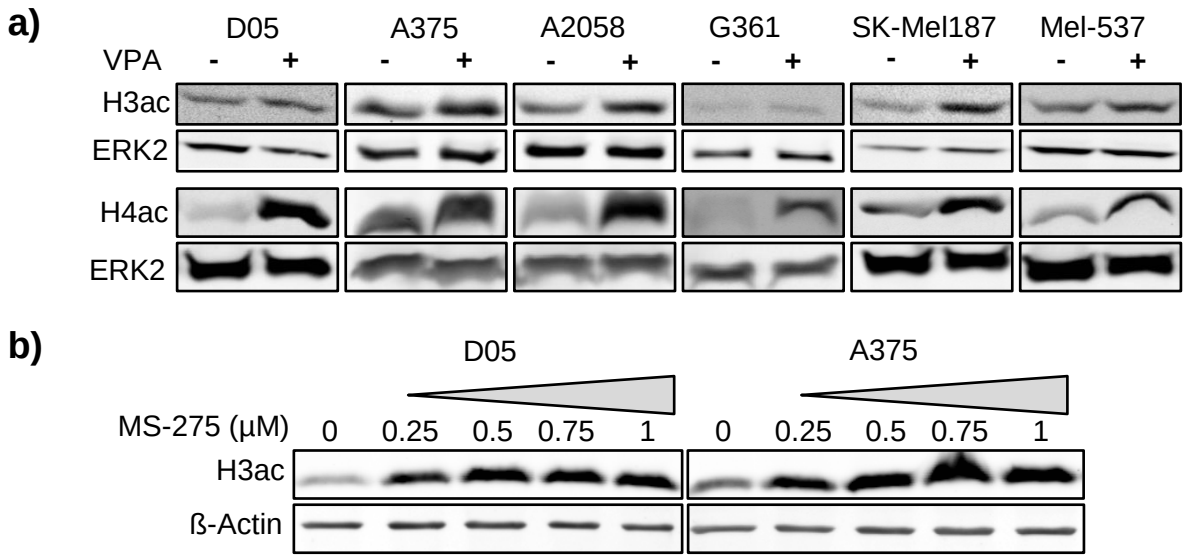

Figure 10 – Histone acetylation in melanoma cells upon HDAC inhibition.
Melanoma cell lines were treated with VPA (168 h, 1 mM) (**a**) or with MS-275 (0-1 µM, 72 h) (**b**) and whole cell protein extracts were subjected to immunoblotting.

HDAC inhibitors have not only been reported to act in combination with radiation, but also to induce cell death in melanoma and lung cancer cells when applied alone (Facchetti *et al.*, 2004; Zhang *et al.*, 2004; Brazelle *et al.*, 2010). Therefore, the question of toxicity of VPA in melanoma cells was addressed by measuring cell death induction by propodium iodide (PI) staining and analysis of the Sub-G1 population. D05 and A375 melanoma cells were treated with VPA and monitored over the period of treatment (168 h). In D05 cells, VPA induced a Sub-G1 fraction of

about 7 % after 168 h, which did not differ significantly from the basal Sub-G1 fraction in cells without treatment. In contrast, VPA had no effect on the Sub-G1 fraction in A375 cells for the period of treatment (Figure 11).

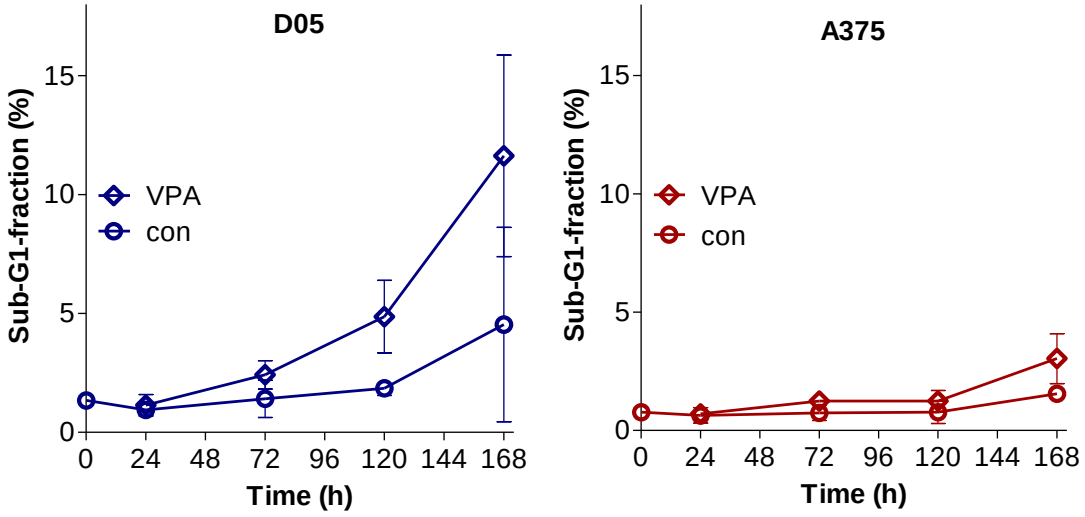

Figure 11 – Toxicity of the HDAC inhibitor VPA on melanoma cell lines.
D05 and A375 melanoma cells were treated with VPA (1 mM), fixed after indicated timepoints and stained with PI for flow cytometry analysis of SubG1 population, which represents apoptotic cells.

HDAC inhibitors have been shown to arrest the progression of cells through the cell cycle (Noh and Lee, 2003; Cha *et al.*, 2009; Roy *et al.*, 2005; Sandor *et al.*, 2000; Newbold *et al.*, 2014). Therefore, cell cycle distribution and cell growth in response to VPA was analyzed. The cell cycle of D05 cells was insignificantly altered by a 168 h VPA treatment as the G1 population increased from 65 % to 69 %. A375 melanoma cell lines were not affected by a 168 h VPA treatment as measured by PI staining (Figure 12 a). Likewise, the proliferation of A375 cells was not impaired in VPA pretreated cells, while D05 cells were slightly delayed 24 h after drug removal, but resumed a growth rate similar to untreated cells after 48 h (Figure 12 b).

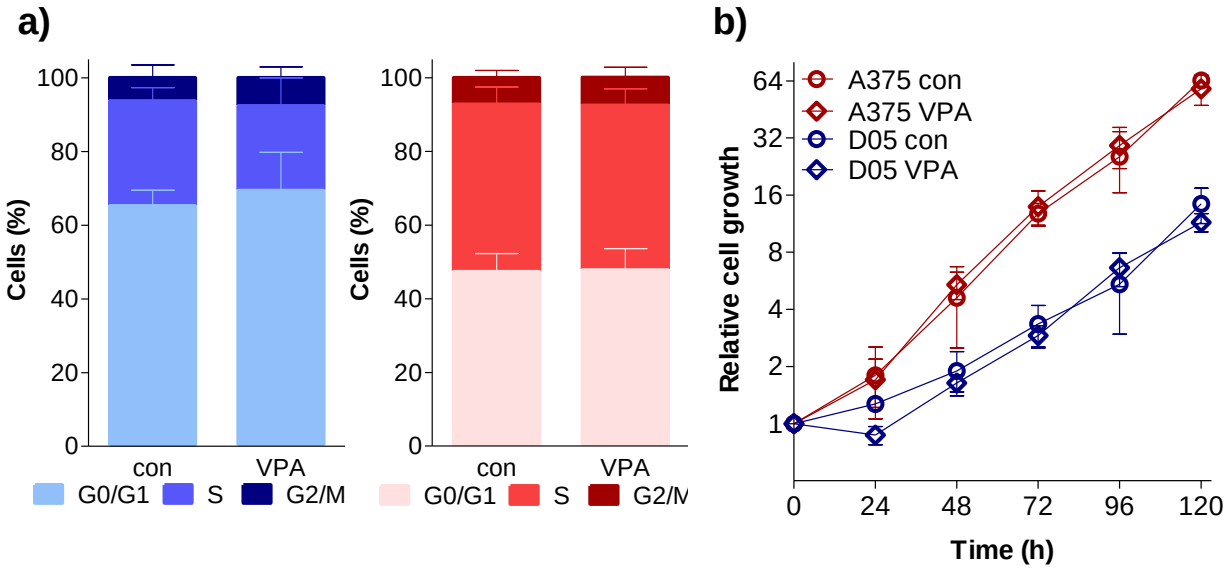

Figure 12 - Effect of the HDAC inhibitor VPA on melanoma cell cycle and proliferation.
D05 (blue) and A375 (red) melanoma cells were treated with VPA (1 mM, 168 h) and cell cycle distribution was measured by PI-staining and flow cytometry analysis (**a**). D05 and A375 control and VPA-pretreated (1 mM, 168 h) cells were seeded at the same density, counted at indicated times and related to the pretreatment number of cells (0 h). Growth analysis was conducted by Dr. C. Barckhausen (**b**).

4.1.3 Influence of HDAC inhibitor pretreatment on the sensitivity of melanoma cells to genotoxic stress

We investigated the role of HDAC1, HDAC2 and HDAC3 in the resistance of melanoma to therapy by HDAC inhibition with VPA or MS-275. Therefore, we applied an HDAC inhibitor pretreatment schedule, which allowed separation of HDAC inhibitor effects from genotoxin effects. To this end, cells were exposed for either 168 h to VPA or 72 h to MS-275 before the HDAC inhibitor was removed and TMZ or FM were added, or before cells were irradiated.

Exposure of melanoma cell lines (D05 and A375) to TMZ, FM or IR alone, induced 5-20 % apoptosis with IR being the least effective, reflecting the radioresistant phenotype of melanoma cells (Figure 13 b). Interestingly, the apoptotic response to TMZ and IR of primary melanocytes (<5 %) was lower than the response of melanoma cell lines, whereas primary melanocytes and melanoma cells respond similar to FM. Pretreatment of the two melanoma cell lines with VPA significantly increased the induction of apoptosis following TMZ, FM and IR exposure. For the alkylating agents TMZ and FM, VPA pretreatment was capable of doubling the cytotoxic effectiveness compared to the drug alone. VPA pretreatment in D05 melanoma cells likewise resulted in a doubling of IR-induced apoptosis, whereas in A375 melanoma cells VPA only slightly increased IR-induced apoptosis. Strikingly, VPA did not sensitize primary melanocytes. In fact, it decreased their sensitivity to TMZ and FM, while having no effect on the IR response.

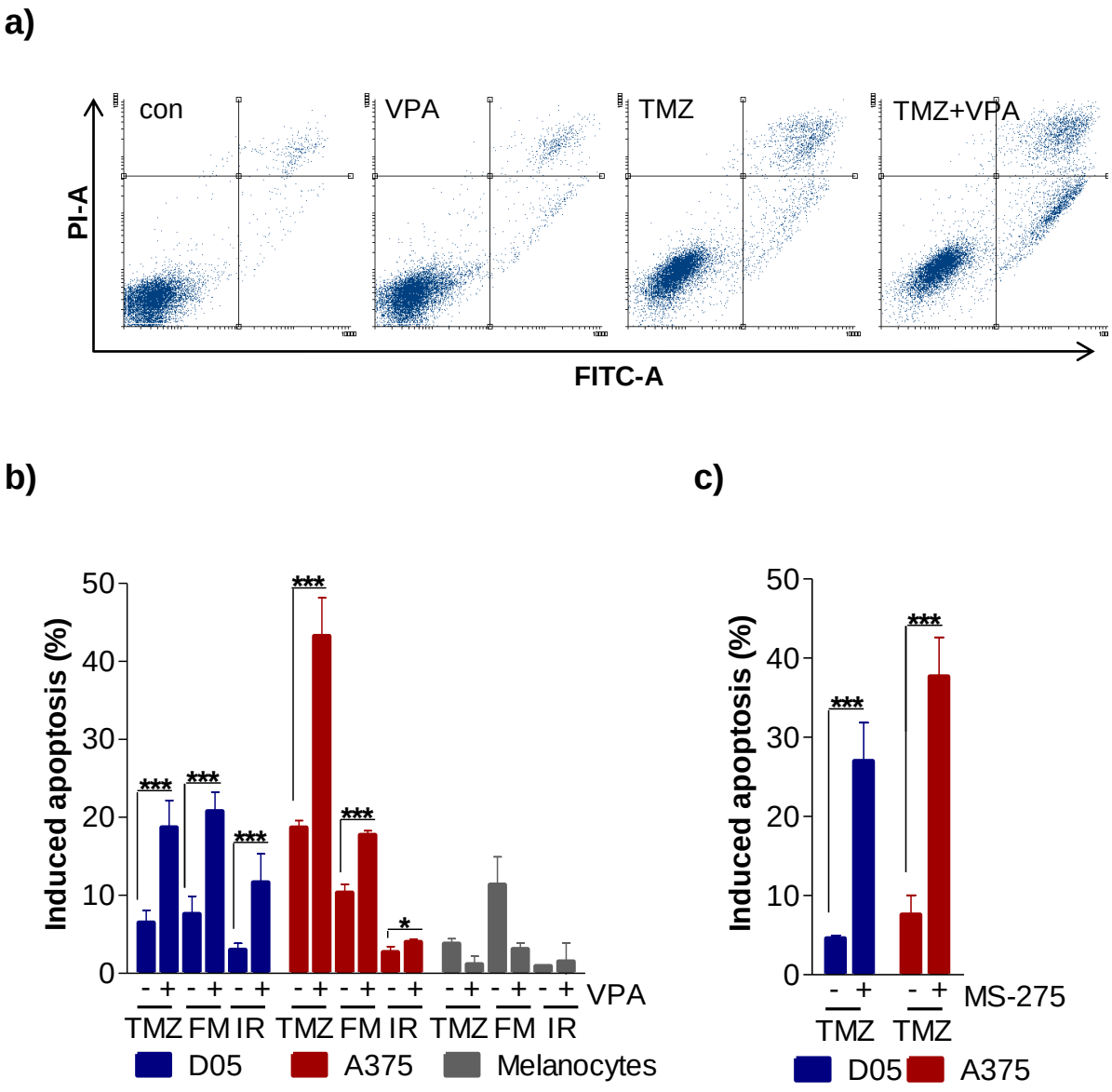

Figure 13 - Effect of HDAC inhibitor pretreatment on the sensitivity of melanoma cells to alkylating agents and ionizing radiation.
Melanoma cells (D05, A375) and primary melanocytes were pretreated with an HDAC inhibitor, which was removed before treatment with TMZ (50 µM, 120 h), FM (32 µM, 120 h) or irradiation (5 Gy, 72 h). In TMZ- or FM-treated samples, MGMT was depleted by addition of O^6BG (10 µM) 1 h before treatment. Apoptosis was detected by AnnexinV-FITC/PI-staining and flow cytometry analysis (FITC-positive, PI-negative population). Representative dot plots of AnnexinV-FITC/PI staining in control and VPA pretreated (1 mM, 168 h) D05 cells with and without TMZ treatment (**a**). Effect of VPA pretreatment (1 mM, 168 h) on apoptosis induction upon various genotoxic stressors. (**b**) Effect of MS-275 pretreatment (1 µM, 72 h) on TMZ-induced apoptosis (**c**)

Similar to VPA, pretreatment with MS-275 increased the sensitivity of melanoma cell lines to TMZ as demonstrated by an approximately threefold higher induction of apoptosis (Figure 13 c).

To examine how general the sensitizing effect of HDAC inhibitors is on melanoma cells, four additional cell lines were selected according to their p53 and B-RAF status, as both determine

therapy response. Whereas p53 confers resistance by mediating DNA repair (Barckhausen *et al.*, 2014; Naumann *et al.*, 2009), mutant B-RAF is linked to a lower response to chemotherapy, although the mechanism has not been identified yet. Though, differential cell death induction was excluded in *in vitro* studies (Long *et al.*, 2011; Roos *et al.*, 2014). In addition to A375 (*BRAF*^{V600E}, *TP53* wt) that was included as control, since sensitization has been shown on the level of apoptosis induction, A2058 (*BRAF*^{V600E}, *TP53* mt), G361 (*BRAF*^{V600E}, *TP53* wt), SK-Mel187 (*TP53* mt, *BRAF* wt) and Mel537 (*BRAF* wt, *TP53* wt) were chosen. For these cell lines the effect of VPA pretreatment on TMZ sensitivity was examined using the colony formation assay. In line with the increased amount of apoptosis induced by TMZ after VPA pretreatment in D05 and A375 cells, fewer colonies formed in this broader panel of cell lines using the combination of VPA pretreatment and TMZ as compared to TMZ alone (Figure 14). Remarkably, sensitization was largely independent of p53 and B-RAF status.

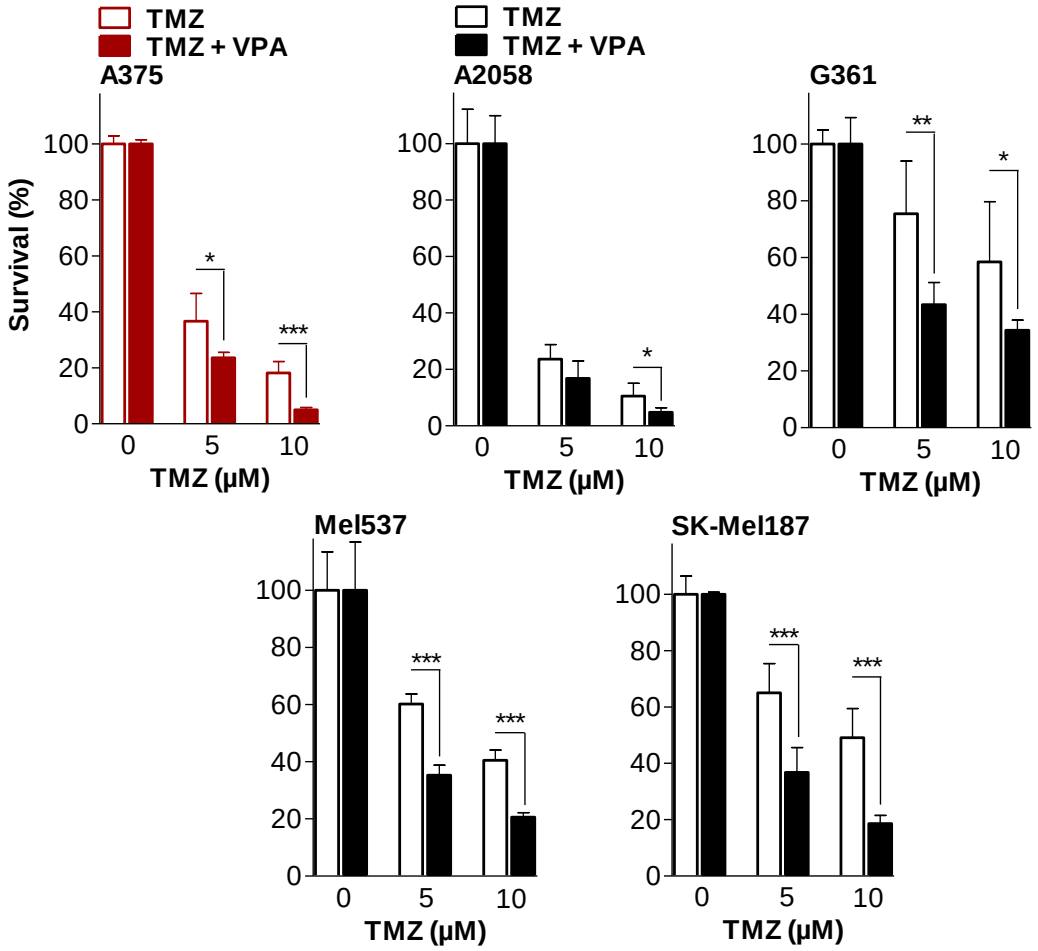

Figure 14 - Clonogenic survival of VPA pretreated and untreated melanoma cells upon TMZ.
Melanoma cell lines (A375, A2058, G361, SK-Mel187 and Mel537) were pretreated with the HDAC inhibitor VPA (1 mM, 168 h). VPA was removed and cells were reseeded for colony formation assay. MGMT was depleted by O^6BG (10 µM, 1 h) before TMZ treatment.

4.1.3.1 Characteristics of HDAC inhibitor-mediated sensitization

Having shown that HDAC inhibition increased the cytotoxic effect of DNA damaging therapy approaches in a panel of melanoma cell lines while not impacting on primary melanocytes, two questions regarding the clinical relevance emerged: At which (clinically) relevant doses for genotoxin and HDAC inhibitor do both interact synergistically? Is it possible to reduce systemically applied drugs to spare effect on healthy tissue while still having an effect on tumor cells? To answer the former question, D05 melanoma cells were pretreated with VPA and exposed to increasing doses of TMZ or IR before measuring the apoptotic response by AnnexinV-FITC/PI-staining. At the highest concentration tested (100 µM), TMZ alone induced approximately 10 % of apoptosis, whereas in combination with VPA pretreatment a four-fold decrease in TMZ concentration (25 µM) resulted in 15 % apoptosis. With increasing TMZ doses apoptosis induction further increased up to 25 % (Figure 15 a). Using IR in combination with VPA pretreatment showed similar effects: irradiating D05 cells with 7 Gy increased the apoptotic fraction by approximately 5 % over basal level compared to an increase by 18% apoptosis induction following VPA pretreatment. In VPA pretreated cells, the effect of IR alone was surpassed at a dose of only 2 Gy (Figure 15 b).

Evaluation of HDAC inhibitor doses that enhance the TMZ response of D05 cells revealed that for VPA and MS-275 pretreatment with low doses of 0.25 mM and 0.25 µM, respectively, were sufficient to slightly sensitize D05 cells to TMZ (3-5 % apoptosis induction over TMZ alone) (Figure 15 c and d). Furthermore, a steady increase in sensitization was observed for both inhibitors with increasing pretreatment concentrations. Comparison of VPA and MS-275 showed a higher sensitizing effect for MS-275, although, at the highest concentration of 1 µM used for MS-275, it was also more toxic when applied alone.

Furthermore, the impact of pretreatment duration was investigated to determine whether longer HDAC inhibitor pretreatments are actually necessary for sensitization. Thus, D05 cells were pretreated for increasing times with VPA and treated with TMZ for 120 h. Apoptosis was measured by AnnexinV-FITC/PI-staining. The experimental results demonstrated that already a 48 h VPA pretreatment was sufficient to act synergistically on TMZ induced apoptosis in melanoma cells (Figure 15 e). Nevertheless, the highest increase in sensitivity to TMZ was observed following 168 h pretreatment time, demonstrating the benefit of prolonged pretreatment. In addition, apoptosis execution after TMZ addition in VPA pretreated and control cells showed that both start to die 72 h after TMZ addition. However, sensitization was most pronounced 120 h after TMZ treatment (Figure 15 f).

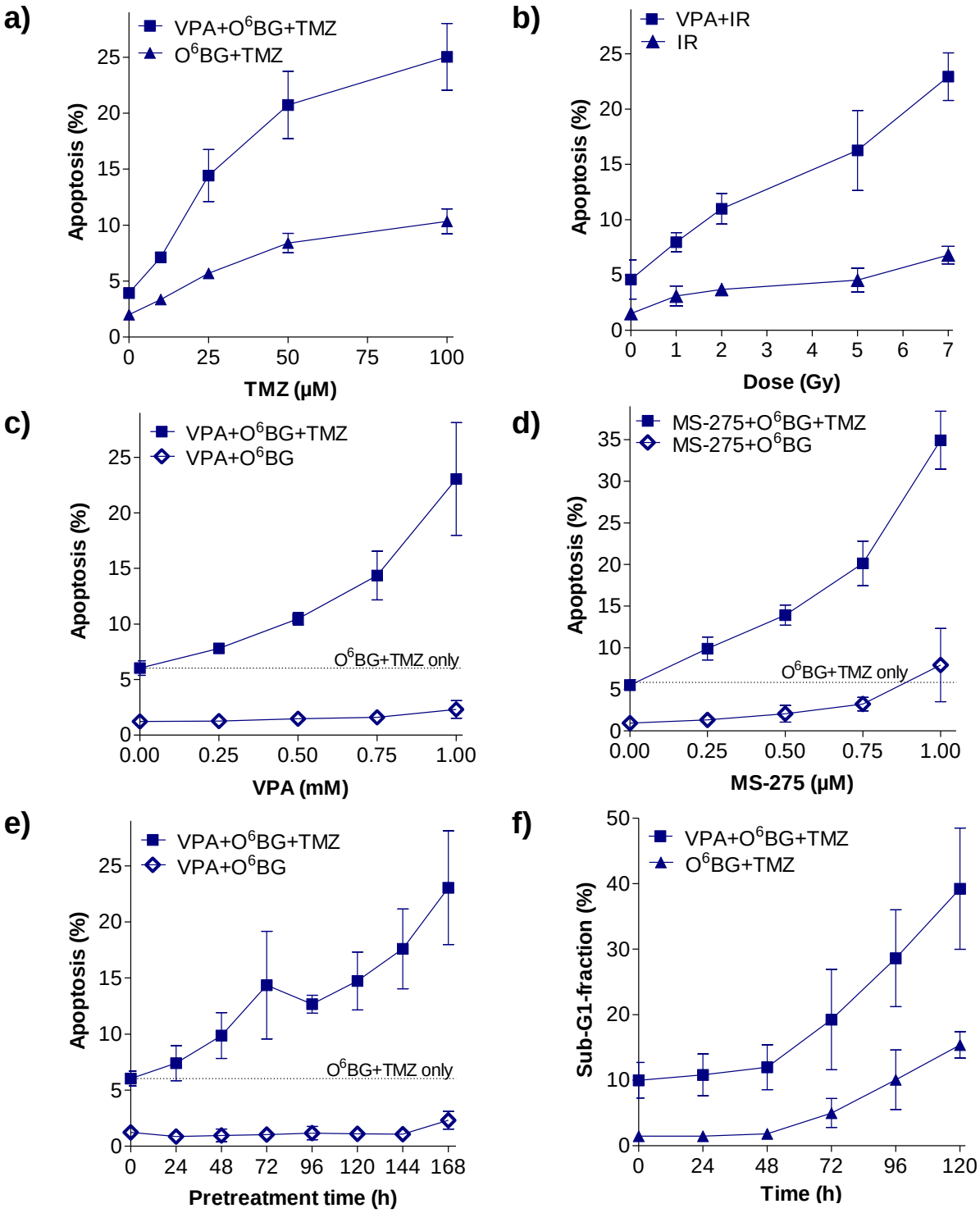

Figure 15 - Apoptosis induction upon genotoxic stress in HDAC-inhibitor pretreated and untreated D05 melanoma cells.

Apoptosis was measured by AnnexinV-FITC/PI-staining (**a**-**e**) or PI-staining for quantification of the Sub-G1 population (**f**) and flow cytometry analysis. In TMZ-treated samples MGMT was depleted by *O*^{6}BG (10 µM) 1 h before TMZ-treatment. Dose-response of TMZ (120 h) (**a**) or IR (72 h) (**b**) in control and VPA pretreated (1 mM, 168 h) cells. Dose-response of pretreatment with VPA (168 h) (**c**) or MS-275 (72 h) (**d**) in TMZ-induced apoptosis 120 h after TMZ addition (50 µM). Kinetics of VPA pretreatment (1 mM) in TMZ-induced apoptosis (50 µM, 120 h) (**e**). Kinetics of TMZ-induced apoptosis (50 µM, 120 h) in control and VPA pretreated cells (**f**).

4.1.3.2 Role of O^6-methylguanine-DNA methyltransferase in HDAC inhibitor-mediated sensitization of melanoma cells to TMZ

The previous characterization of the kinetics underlying sensitization of melanoma cells to alkylating agents by HDAC inhibitors revealed that D05 cells require 72 h incubation with TMZ before they initiate apoptosis, irrespective of VPA pretreatment. This indicates a possible role of the clinically relevant TMZ-induced lesion O^6MeG since the model of its cytotoxic action requires two cell cycles before induction of cell death (Quiros *et al.*, 2010). Therefore, the impact of VPA on the repair protein MGMT was analyzed. MGMT is responsible for removal of the methyl group from O^6MeG which occurs in a suicidal manner by transfer of the methyl-group onto an internal cysteine followed by proteasomal degradation of MGMT (Srivenugopal *et al.*, 1996; Lindahl *et al.*, 1982). We measured MGMT activity in response to VPA pretreatment in an attempt to elucidate whether sensitivity is also conferred in MGMT-proficient cells. We found that VPA pretreatment decreased MGMT activity in D05 and A375 melanoma cells (Figure 16 a). Whereas D05 display a low basal activity (150 fmol/mg) and a non-significant VPA-mediated activity reduction (120 fmol/mg), A375 cells with a higher basal MGMT activity (370 fmol/mg) responded to VPA with a significant decrease in MGMT activity (290 fmol/mg).

The question whether the VPA-mediated MGMT reduction was sufficient to overcome resistance to O^6MeG, was addressed by manipulation of MGMT with its artificial substrate O^6-benzylguanine (O^6BG). It inactivates MGMT, causes MGMT degradation, consequently leading to the persistence of O^6MeG. Allowing MGMT proficient D05 and A375 to repair O^6MeG (no O^6BG) completely abolished TMZ induced apoptosis in both: VPA pretreated cells and untreated control cells. Whereas the addition of O^6BG, and therefore the persistence of O^6MeG, restored the sensitization phenotype. Under these conditions TMZ induced low amounts of apoptosis while following VPA pretreatment TMZ induced twice as much apoptosis (Figure 16 b). Though, reduction of MGMT activity by VPA pretreatment was not sufficient to confer sensitivity to O^6MeG, since apoptosis induction upon TMZ was detected only in the presence of O^6BG, irrespective of pretreatment. In the presence of O^6BG, VPA pretreatment doubled the response to TMZ, indicating a sensitization effect specific to the O^6MeG lesion.

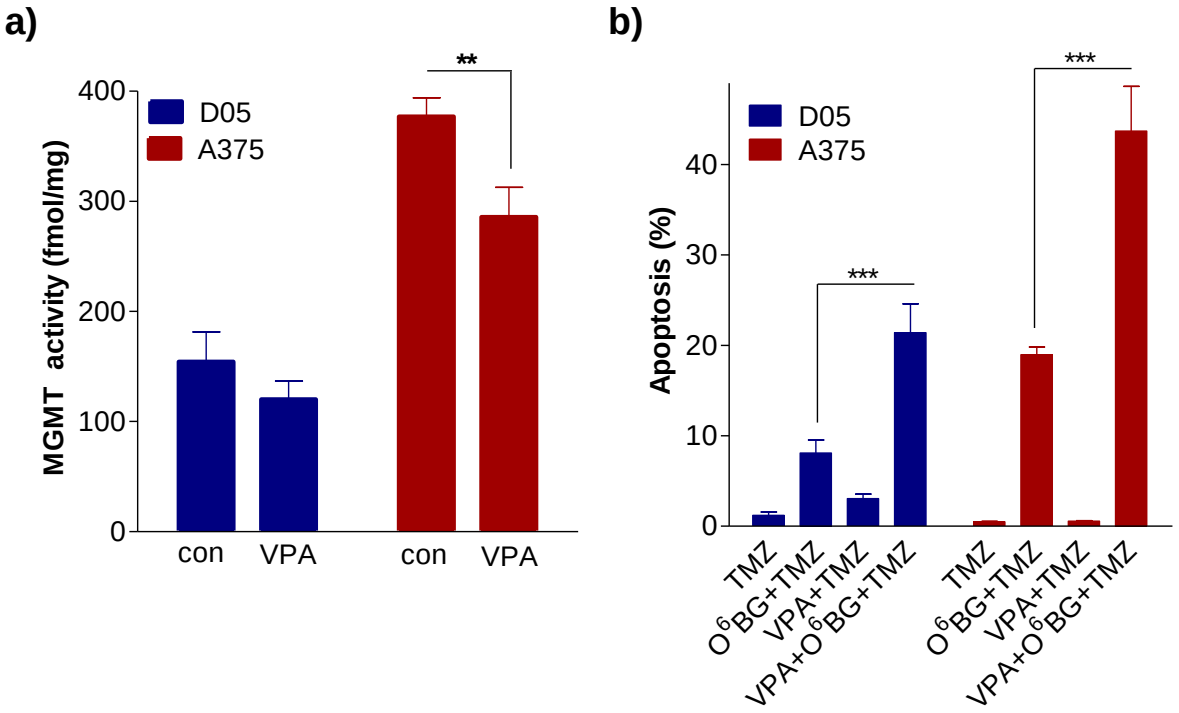

Figure 16 - Role of MGMT in VPA-mediated sensitization to TMZ.
MGMT activity was analyzed in VPA pretreated (1 mM, 168 h) and untreated D05 and A375 melanoma cells by measuring the transfer of a ^{3}H-labelled methyl group from calf-thymus DNA onto MGMT in corresponding cell extracts (**a**). VPA pretreated (1 mM, 168 h) and control D05 and A375 melanoma cells were either left MGMT proficient or MGMT was depleted by addition of O^6BG (10 µM) 1 h before TMZ treatment. Apoptosis was measured 120 h after TMZ exposure (50 µM) by AnnexinV-FITC/PI-staining and flow cytometry analysis (**b**).

4.1.4 HDAC inhibitor regulated genes and proteins that determine TMZ sensitivity

As demonstrated, HDAC inhibitors increase the apoptotic response of melanoma cells to TMZ-induced O^6MeG. Having excluded effects of HDAC inhibitors on MGMT, the mechanistic reasons for the HDAC inhibitor-mediated sensitization effect needed to be elucidated. Sensitivity of melanoma cells to TMZ is defined by their capability of undergoing apoptosis and by their DNA repair capacity, specifically by mismatch repair (MMR) and HR processes (Fu *et al.*, 2012; Roos and Kaina, 2013). As DNA damage signaling and checkpoint activation acts upstream of apoptosis and DNA repair, it likewise determines TMZ-sensitivity. The most abundant proteins affected by HDAC inhibition are histones, which become hyperacetylated resulting in an open chromatin structure and, therefore, have direct effects on transcription and gene expression. Based on this, the impact of HDAC inhibition on the expression of genes involved in apoptosis, DNA repair and DNA damage signaling was analyzed by using a PCR array of 180 genes involved in these processes.

VPA altered the gene expression profile in D05 cells compared to untreated cells by downregulating and upregulating a number of genes (complete list see S 5). Amongst the

upregulated genes, three that code for pro-apoptotic BCL-2-family members were found (*BAX, NOXA, PUMA*) (Table 2). In addition, the *BCL2* gene encoding the corresponding anti-apoptotic protein was downregulated. The DNA repair genes *RAD51*, *RAD51D*, *KU80* and *FANCD2*, as well as the damage signaling kinase *ATR* were all downregulated by VPA.

Table 2 – Regulation of DNA repair, apoptosis and cell cycle genes by the HDAC inhibitor VPA in D05 melanoma cells.
D05 melanoma cells were treated with VPA (1 mM, 168 h) and gene expression was measured by a qPCR-based array. Fold change in gene expression is shown relative to the untreated control. Selected gene expression data are shown, for the complete list see S 5.

Gene	Fold change	Gene	Fold change
MMP3	0.17±0.06	***IL6***	2.07±0.50
TDG	0.30±0.34	***CDKN1A***	2.11±0.68
RAC1	0.35±0.34	***GADD45A***	2.37±0.07
RAD51	0.37±0.24	***NOXA***	2.59±0.26
ATR	0.54±0.41	***PUMA***	2.66±1.26
PARP2	0.57±0.26	***BAX***	2.95±2.05
FAN1	0.58±0.30	***C-IAP1***	3.11±0.75
RAD51D	0.58±0.15	***GADD45G***	3.45±1.21
KU80	0.62±0.12	***CYP1A1***	3.46±0.65
GADD45B	0.66±0.08	***MMP13***	7.30±3.21
BCL2	0.66±0.33	***CCNA1***	18.29±5.33
FANCD2	0.67±0.22		

To validate the transcriptomics data, protein levels of the corresponding VPA-regulated genes were assessed by immunoblotting in untreated and VPA pretreated D05 and A375 cells. For the apoptosis proteins (BCL-2, BAX, PUMA, NOXA), no differential regulation was observed (Figure 17). Neither were differences upon VPA detected for the NHEJ-repair protein KU80 nor for RAD51D. However, the protein level of the key protein in HR processes, RAD51 (Baumann and West, 1998), was reduced to approximately half in VPA pretreated D05 and A375 cells. Likewise, FANCD2 was clearly downregulated at protein level upon VPA. A downregulating effect was also seen on ATR which was reduced by 20-30 % compared to the untreated control.

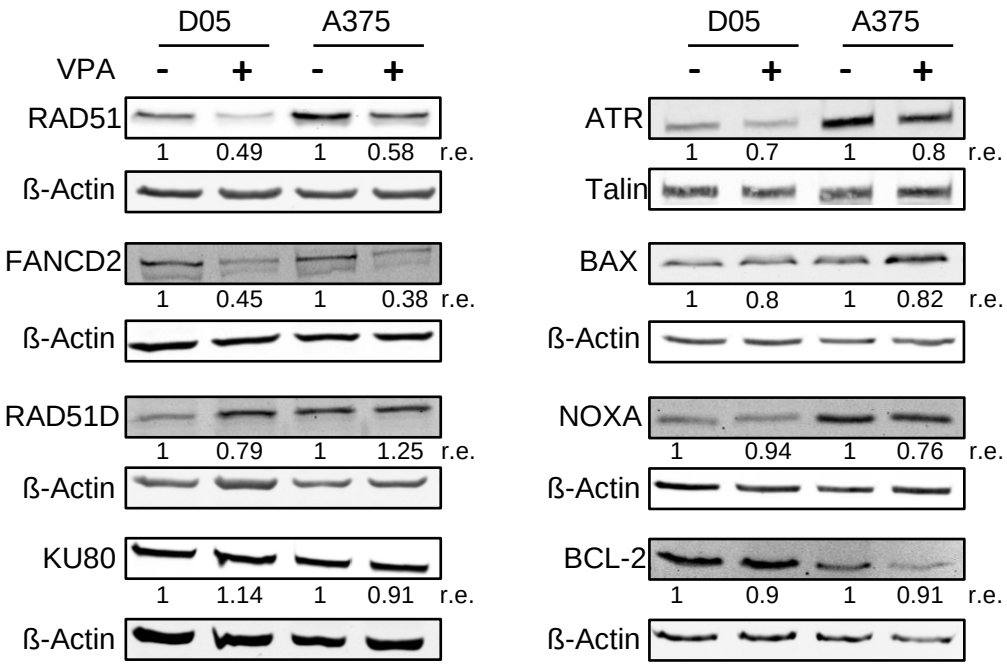

Figure 17 - Regulation of DNA repair, apoptosis and cell cycle proteins by the HDAC inhibitor VPA in melanoma cells.
Whole-cell protein extracts of VPA pretreated (1 mM, 168 h) and untreated D05 and A375 melanoma cells were subjected to immunoblotting. Relative expression (r.e.) was calculated from quantification of protein and loading control (β-Actin or Talin).

4.1.4.1 Role of checkpoint signaling in HDAC inhibitor-mediated sensitization of melanoma cells to TMZ

After identifying the DNA repair proteins RAD51 and FANCD2, as well as the signaling kinase ATR as possible contributors of HDAC inhibitor-mediated sensitization, their role in sensitization was analyzed. Upon TMZ, activated ATR phosphorylates CHK1 (Cimprich and Cortez, 2008). Here, levels of phosphorylated CHK1 were quantified by western blot and used as readout of ATR activity. The basal level of CHK1 phosphorylation was low and did not differ between controls and pretreated cells (Figure 18). TMZ-treatment led to an increase in the activating phosphorylation of CHK1 reaching its maximum after 24 h (A375) or 48 h (D05), irrespective of pretreatment. Although less certain, CHK2 is also phosphorylated by ATR (Wang *et al.*, 2006; Pabla *et al.*, 2008). Therefore, CHK2 phosphorylation was analyzed but no differences in activation were observed upon TMZ between control and VPA pretreated cells (S 2). This indicates that VPA-mediated downregulation of ATR leaves sufficient protein for effective damage signaling. Therefore, it may not contribute to the sensitizing effect of HDAC inhibitors.

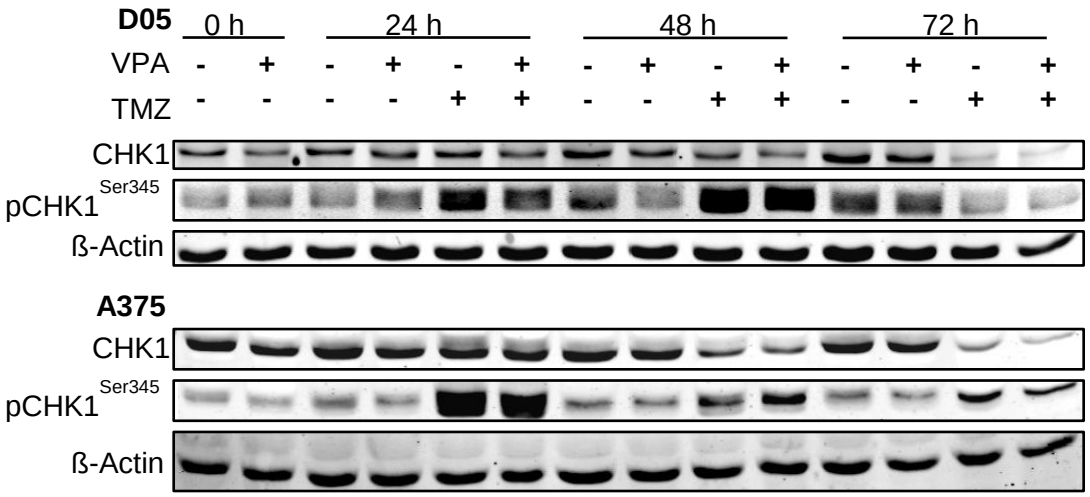

Figure 18 - TMZ-induced CHK1 phosphorylation in VPA pretreated and untreated melanoma cells. VPA pretreated (1 mM, 168 h) and untreated D05 and A375 melanoma cells were exposed to TMZ (50 µM). MGMT was depleted by O^6BG 1 h before TMZ addition. At indicated times after TMZ treatment, whole cells protein extracts were subjected to immunoblotting using phospho-specific and total CHK1 antibodies.

4.1.4.2 Role of DNA repair in HDAC inhibitor-mediated sensitization of melanoma cells to TMZ

We have excluded that neither impaired checkpoint signaling nor deregulation of apoptosis-driving BCL-2 proteins are responsible for the observed HDAC inhibitor mediated sensitization. The role of the DNA repair proteins RAD51 and FANCD2 was therefore examined. RAD51 downregulation confers sensitivity to TMZ in glioma and CHO cells (Roos *et al.*, 2009; Quiros *et al.*, 2011), which is explained by the role of RAD51 during HR-mediated replication fork stabilization/initiation or DSB repair. The role of FANCD2 in the cytotoxicity of TMZ has also been shown, but the reasons are still unclear, ranging from a role in replication fork stabilization to a role in signaling (Chen *et al.*, 2007a; Moldovan and D'Andrea, 2009). However, its role in cytotoxicity of chloroethylating agents like FM is well described, as the chloroethyl group rearranges to a DNA-interstrand crosslink, which is repaired by the Fanconi anemia (FA) pathway in which FANCD2 serves as a damage sensor and repair-protein recruiter (Deans and West, 2011). As they were found to be downregulated by VPA and MS-275, both are interesting suspects for HDAC inhibitor-mediated sensitization of melanoma cells. A further characterization of doses and kinetics of HDAC inhibitor-driven downregulation of these proteins should enable a comparison to sensitization characteristics in section 4.1.3.1 and, therefore, a better estimation of its impact on the sensitization effect.

Firstly, the impact of HDAC inhibition on RAD51 and FANCD2 was analyzed in a panel of melanoma cell lines that was shown to respond to HDAC inhibitor-mediated sensitization (Figure

14). VPA pretreatment led to a decrease in both proteins as compared to the untreated control in all of the tested cell lines (Figure 19).

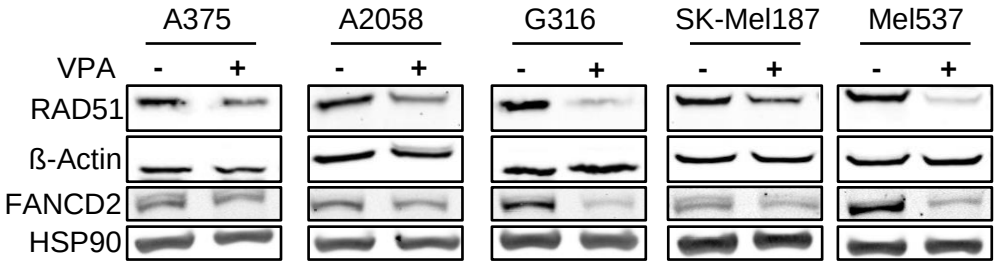

Figure 19 – Influence of VPA on RAD51 and FANCD2 protein in melanoma cells.
Melanoma cell lines (A375, A2058, G361, SK-Mel187 and Mel537) were treated with VPA (1 mM, 168 h) and whole-cell protein extracts were subjected to immunoblotting

VPA decreased the level of RAD51 protein with increasing doses (Figure 20). This is in line with the HDAC inhibitor dose-dependent sensitization of melanoma cells to TMZ. In addition, the duration of VPA pretreatment defined the level of downregulation of RAD51 and FANCD2, which was also in accordance with a time-dependent sensitization.

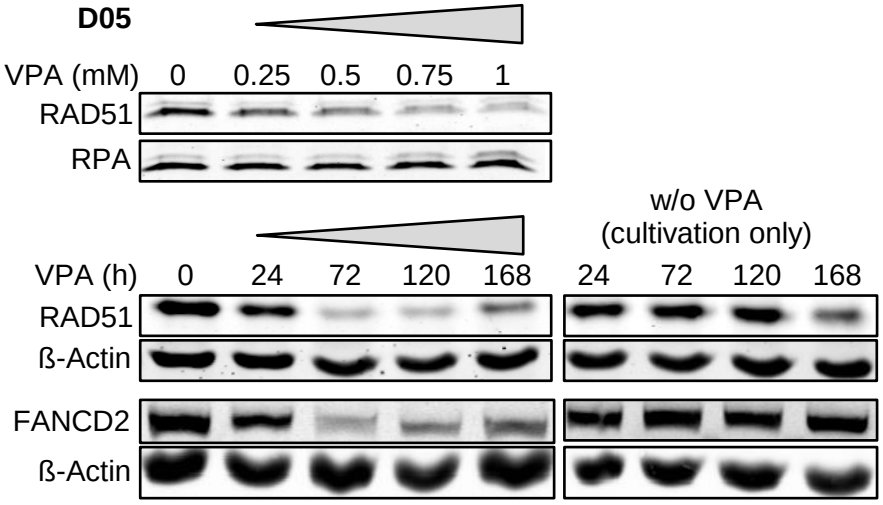

Figure 20 – Time- and VPA concentration-dependent downregulation of DNA repair proteins.
D05 melanoma cells were treated with indicated doses of VPA for 168 h or with 1 mM VPA for indicated periods. Nuclear or whole cell extracts were subjected to immunoblotting.

To clarify whether the downregulation of RAD51 and FANCD2 is due to the HDAC inhibitory function of VPA, gene expression and protein levels in response to a second HDAC inhibitor, MS-275, were analyzed. Real-time PCR revealed a downregulation of *RAD51* and *FANCD2* upon MS-275 treatment to 15 % and 60 % of the basal levels in D05 and A375 cells, respectively (Figure 21 a). Measuring the protein levels of RAD51 and FANCD2 after increasing doses of MS-275 by

immunoblotting in D05 cells revealed a dose-dependent downregulation of both proteins (Figure 21 b).

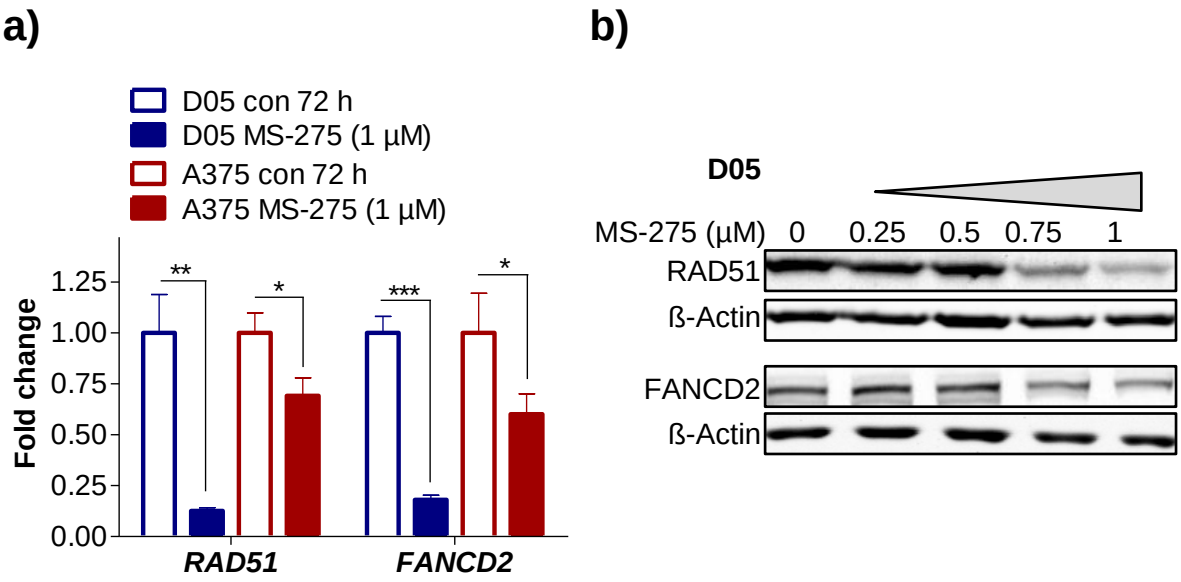

Figure 21 – Regulation of RAD51 and FANCD2 by the HDAC inhibitor MS-275 in melanoma cells. D05 and A375 melanoma cells were pretreated with MS-275 (1 µM, 72 h) and relative gene levels were measured by real time PCR (**a**). Whole cell protein extracts of MS-275 pretreated (0-1 µM, 72 h) D05 cells were subjected to immunoblotting (**b**).

Considering the model of O^6MeG-induced apoptosis, which requires two cell cycles of lesion-processing and the finding that D05 cells take approximately 46 h until they enter the second cell cycle (Figure 12 b), necessitated monitoring of RAD51 levels upon VPA removal. RAD51 protein levels were monitored by western blot analysis until 72 h after VPA removal to investigate if it was downregulated until required for repair of processing intermediates of O^6MeG. Furthermore, the influence of TMZ on RAD51 was assessed in this experiment. After VPA-pretreatment and removal, the downregulation of RAD51 protein was observed as previously described. This was visible up to 48 h after VPA removal (Figure 22). This coincided with when RAD51 is actually needed to repair DSBs occurring during the second S-phase after O^6MeG induction (Quiros *et al.*, 2010). TMZ treatment alone did not influence RAD51 levels compared to the time-matched untreated controls 24 h and 48 h after addition. Although at 72 h, less protein was detected for TMZ-treated samples, irrespective of VPA pretreatment.

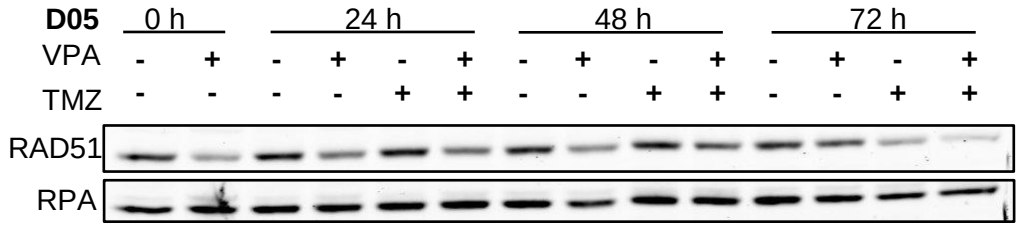

Figure 22 - Influence of VPA pretreatment and TMZ on RAD51 protein.
VPA-pretreated (1 mM, 168 h) and untreated D05 melanoma cells were treated with TMZ (50 µM) or left untreated for controls. MGMT was depleted with O^6BG (10 µM) 1 h before TMZ treatment. Nuclear protein extracts were taken at the indicated timepoints and were subjected to immunoblotting for RAD51 protein.

4.1.4.2.1 The functional consequence of HDAC inhibitor-mediated downregulation of DNA repair proteins

As we have shown, throughout the course of the experiment, RAD51 and FANCD2 levels are reduced by HDAC inhibition. However, residual protein levels were also detected leading to the question, what impact the reduced RAD51 and FANCD2 protein levels have on HR repair of DSBs induced by TMZ. To answer this, cells were generated which carry a pDRGFP plasmid, a construct with two modified non-functional *GFP* genes. One of them with an inserted I-SceI recognition site that can be cleaved by Intron-encoded endonuclease (I-SceI) leaving a 3' four nucleotide overhang. The other is truncated but able to serve as a HR repair template for the cleaved *GFP* gene. Transfection of cells carrying the described plasmid with a second, I-SceI coding, plasmid leads to the expression of the endonuclease, resulting in a DSB that can be repaired in HR proficient cells leading to a wild type GFP detectable by flow cytometry.

VPA pretreated and untreated D05 and A375 cells carrying the pDRGFP plasmid were transfected with the I-SceI-coding plasmid after VPA removal. In both cell lines, VPA pretreatment reduced the number of GFP-positive cells by half compared to the untreated control, which means that VPA pretreated cells repaired only half of the I-SceI-induced DSBs by HR compared to repair in untreated cells (Figure 23).

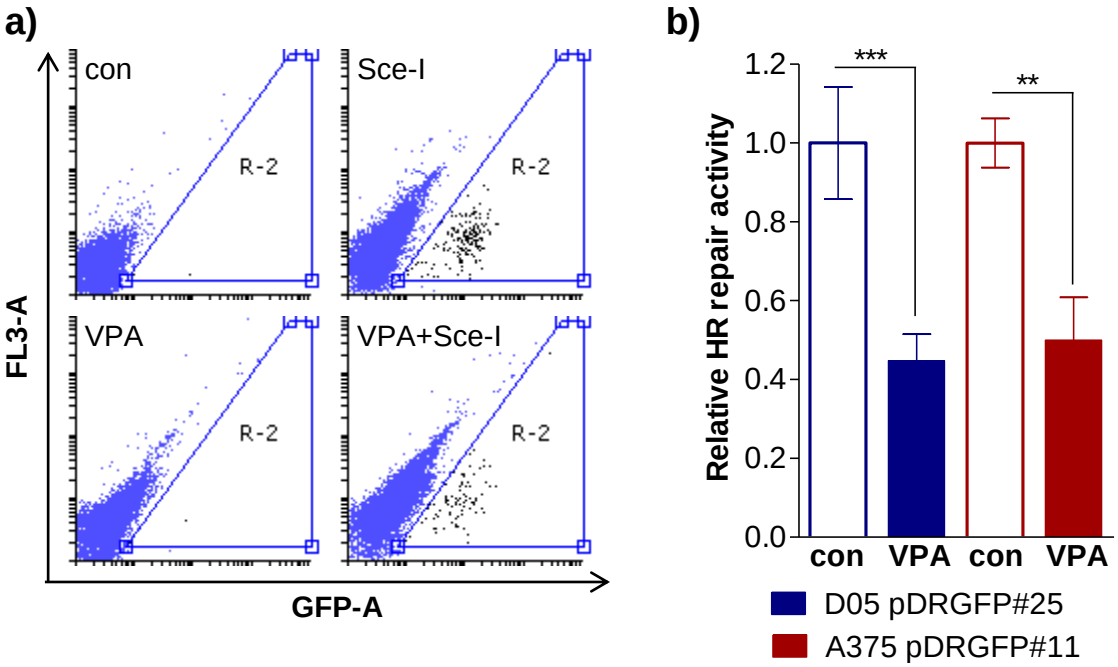

Figure 23 - Influence of VPA pretreatment on DNA double-strand break repair capacity by homologous recombination.
D05 and A375 control and VPA-pretreated (1 mM, 168 h) pDRGFP cells were transiently transfected with I-SceI expressing plasmid. Cells were analyzed by flow cytometry 48 h (A375) or 72 h (D05) after transient transfection. Representative dot-plots (**a**, D05 pDRGFP#25, R-2/black-GFP positives) and quantification of three independent experiments are shown (**b**).

Since HDAC inhibitor-mediated downregulation of RAD51 negatively affects HR capacity, HDAC-inhibitor pretreatment might be the ideal prerequisite for combination with PARP inhibition. PARP1 inhibitors exploit the inability of HR-deficient cells to circumvent DNA lesions which then leads to apoptosis. PARP1 inhibitor-induced lesions are either bulky adducts of PARP1 and its inhibitor stuck to the DNA or unrepaired single-strand breaks which are encountered by a replication fork (Helleday, 2011). Thus, untreated and VPA-pretreated D05 cells were exposed to increasing doses of the PARP1 inhibitor Olaparib and the level of apoptosis was determined. Untreated cells were not affected even at high concentrations of Olaparib (20 µM), whereas in VPA-pretreated cells, the same dose induced 11 % apoptosis (Figure 24).

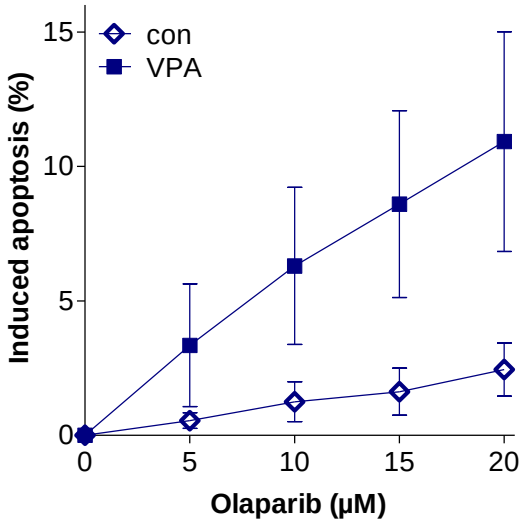

Figure 24 – PARP inhibitor-induced apoptosis in untreated and VPA-pretreated D05 cells.
D05 melanoma cells were pretreated with VPA (1 mM, 168 h) and treated with indicated doses of the PARP1 inhibitor Olaparib. Apoptosis was measured 72 h after Olaparib addition by Annexin-V/PI-staining and flow cytometry analysis.

This showed that the residual RAD51 and FANCD2 protein after HDAC inhibition is not sufficient to execute HR processes. In the absence or exhaustion of HR capacity, TMZ-induced O^6MeG might lead to persistent DSBs. Therefore, the induction of DSBs after TMZ in control and VPA pretreated D05 cells was analyzed by γH2AX foci formation, a classical DSB marker. VPA pretreated cells display the same basal number of foci per cell as untreated cells. TMZ induced the highest amount of γH2AX foci after 48 h of treatment (3.7/cell) and the amount of TMZ-induced γH2AX foci was doubled in VPA pretreated cells (8/cell) (Figure 25 a, b). The higher amount of γH2AX foci remained until 72 h after TMZ treatment, but was no longer visible 96 h later. The analysis of γH2AX foci did not allow inclusion of cells that detached from the plate due to either apoptosis or mitosis, therefore, immunoblotting was carried out (Figure 25 c). This revealed that VPA pretreatment alone led to a phosphorylation of H2AX over the whole period of analysis (0-120 h after VPA-removal), most likely due to cell death, as it was shown in Figure 11 in D05 cells. Addition of TMZ to untreated D05 cells increased the γH2AX signal to a maximum at 120 h after addition. In VPA pretreated cells however, led to a much higher γH2AX signal from 48 h-120 h after TMZ addition.

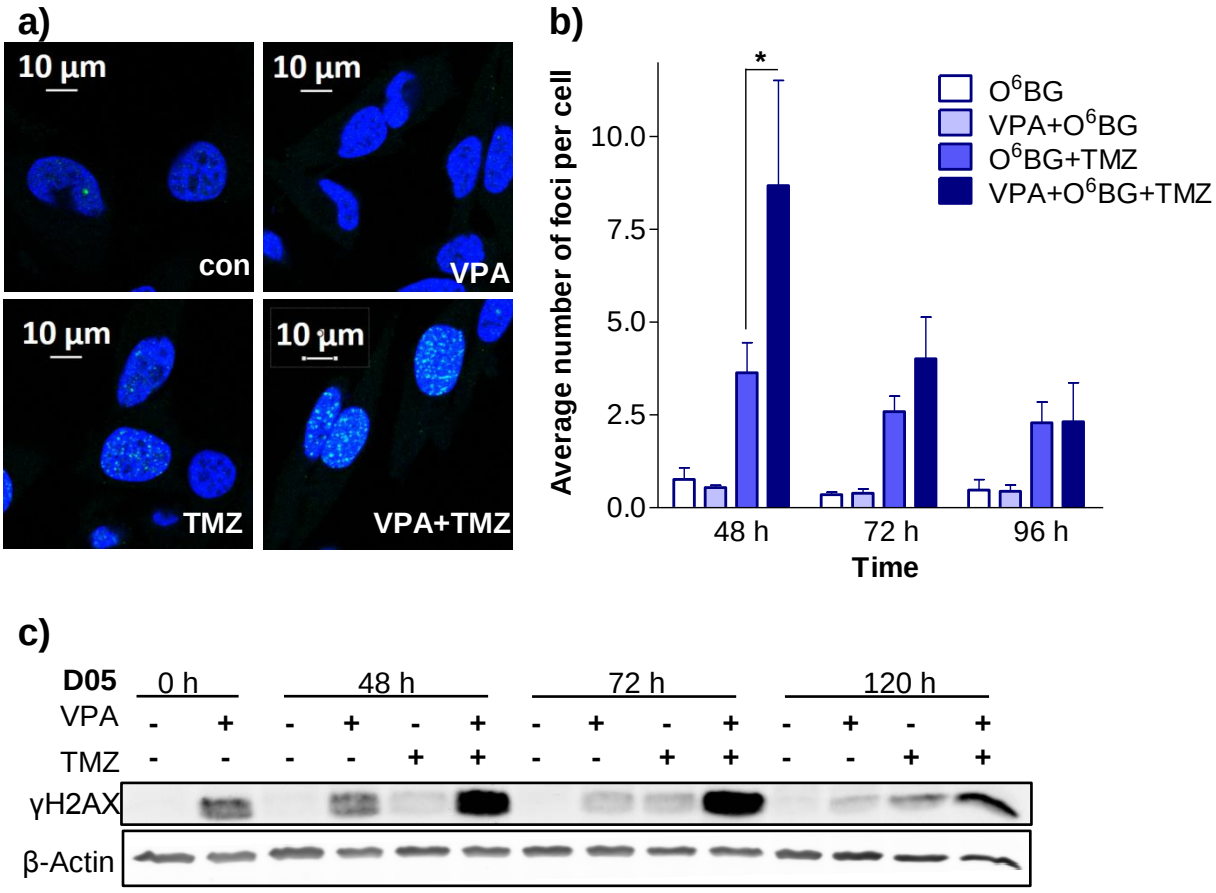

Figure 25 - Influence of VPA pretreatment on TMZ-induced H2AX phosphorylation.
VPA-pretreated (1 mM, 168 h) and untreated D05 melanoma cells were treated with TMZ (10 µM) and stained for immunofluorescence. MGMT was depleted by O^6BG (10 µM) 1 h before TMZ treatment. Representative image sections (48 h) (**a**) and quantification of foci (**b**) are shown. VPA-pretreated (1 mM, 168 h) and control D05 cells were treated with TMZ (50 µM, depletion of MGMT – 10 µM O^6BG) and whole-cell protein extracts were taken at the indicated timepoints and were subjected to immunoblotting (**c**).

4.1.4.2.2 Role of RAD51 in sensitivity of melanoma cells to TMZ

This study identified that HDAC inhibition increases the sensitivity of melanoma cells to TMZ, coinciding with a downregulation of RAD51 and an elevation of potentially cytotoxic DSBs. Still, the role of RAD51 in the sensitivity of melanoma cells to TMZ has not been addressed. Therefore, stable clones of A375 melanoma cells were generated that carry a plasmid coding for shRNA targeting RAD51 mRNA and clones with the empty vector-backbone as a control. Knockdown was verified on protein level in nuclear protein extracts (Figure 26 a). Treatment of RAD51-knockdown cells with TMZ increased the apoptosis induction up to 40-50 % as compared to wild type and empty-vector control cells with only 20 % apoptosis induction after 50 µM of TMZ (Figure 26 b).

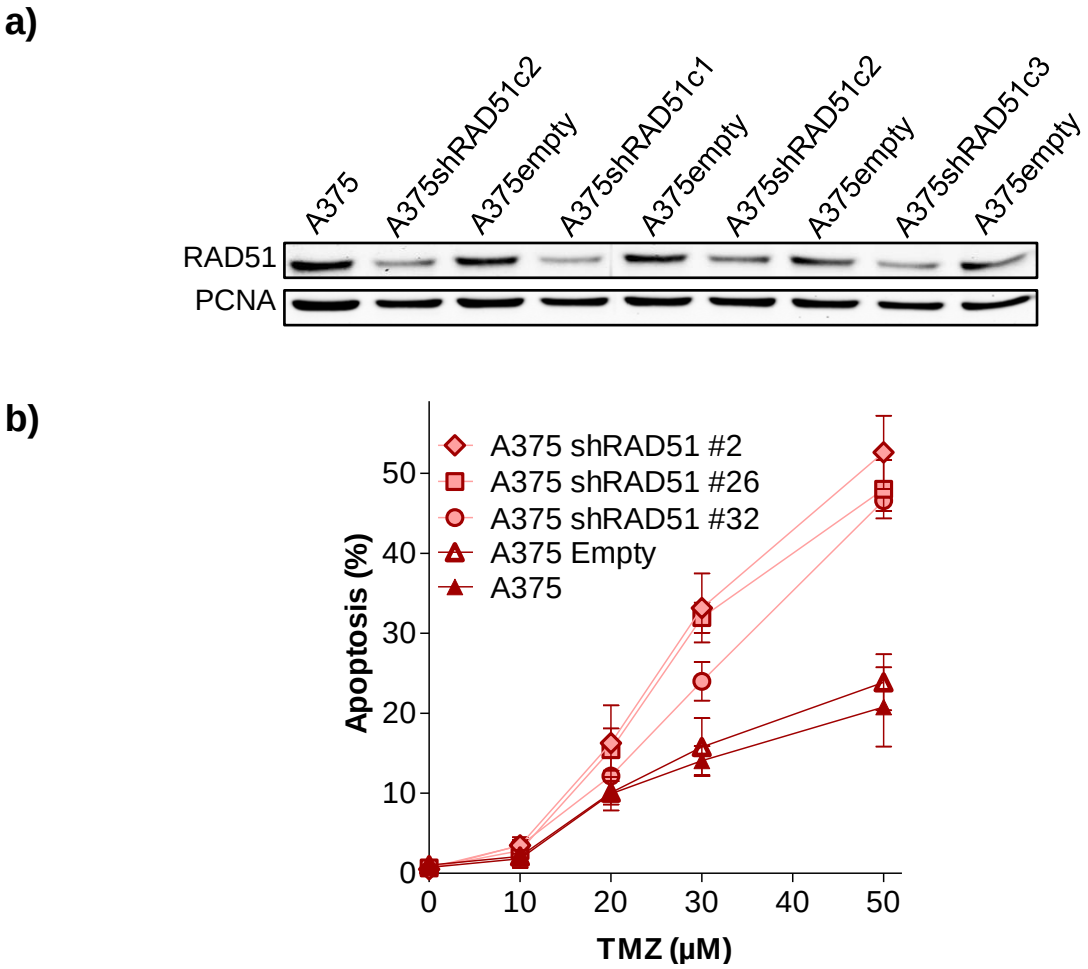

Figure 26 - Sensitivity of RAD51 knockdown cells to TMZ.
RAD51 nuclear protein level in RAD51 knockdown cells (shRAD51) and empty-vector transfected cells (a). A375 wild type, A375 empty and A375 shRAD51 knockdown cells were treated with indicated doses of TMZ and 120 h after TMZ addition apoptosis was measured by Annexin-V/PI staining and flow cytometry analysis (b). MGMT was depleted by O^6BG (10 µM) 1 h before TMZ treatment. Experiment conducted in collaboration with Dr. W. P. Roos.

4.1.5 Influence of the HDAC inhibitor VPA on RAD51 and melanoma tumor growth *in vivo*

To test whether the HDAC inhibitor-mediated RAD51 downregulation also applies to *in vivo* settings, Mel537 cells were injected subcutaneously into BALB/c immunodeficient nude mice and after tumor development, mice received intraperitoneal injections of PBS or VPA (200-500 mg/kg bwt) twice a day for five days. Mouse experiment was conducted by Dr. K. H. Tomaszowski until experiment termination. One out of three control mice was excluded from the analysis since it did not develop tumors. Tumor size was acquired throughout the treatment time and 2 h after the last injection mice were sacrificed and tumors were surgically harvested for immunoblotting analysis. Monitoring of tumor growth revealed a growth inhibitory effect of VPA alone when mice received at least 2 x 350 mg/kg body weight (bwt) (Figure 27 a). The highest dose

of 2 x 500 mg/kg bwt showed the biggest but insignificant tumor inhibitory effect and RAD51 protein levels at this dose were only slightly decreased in these tumors (Figure 27 b).

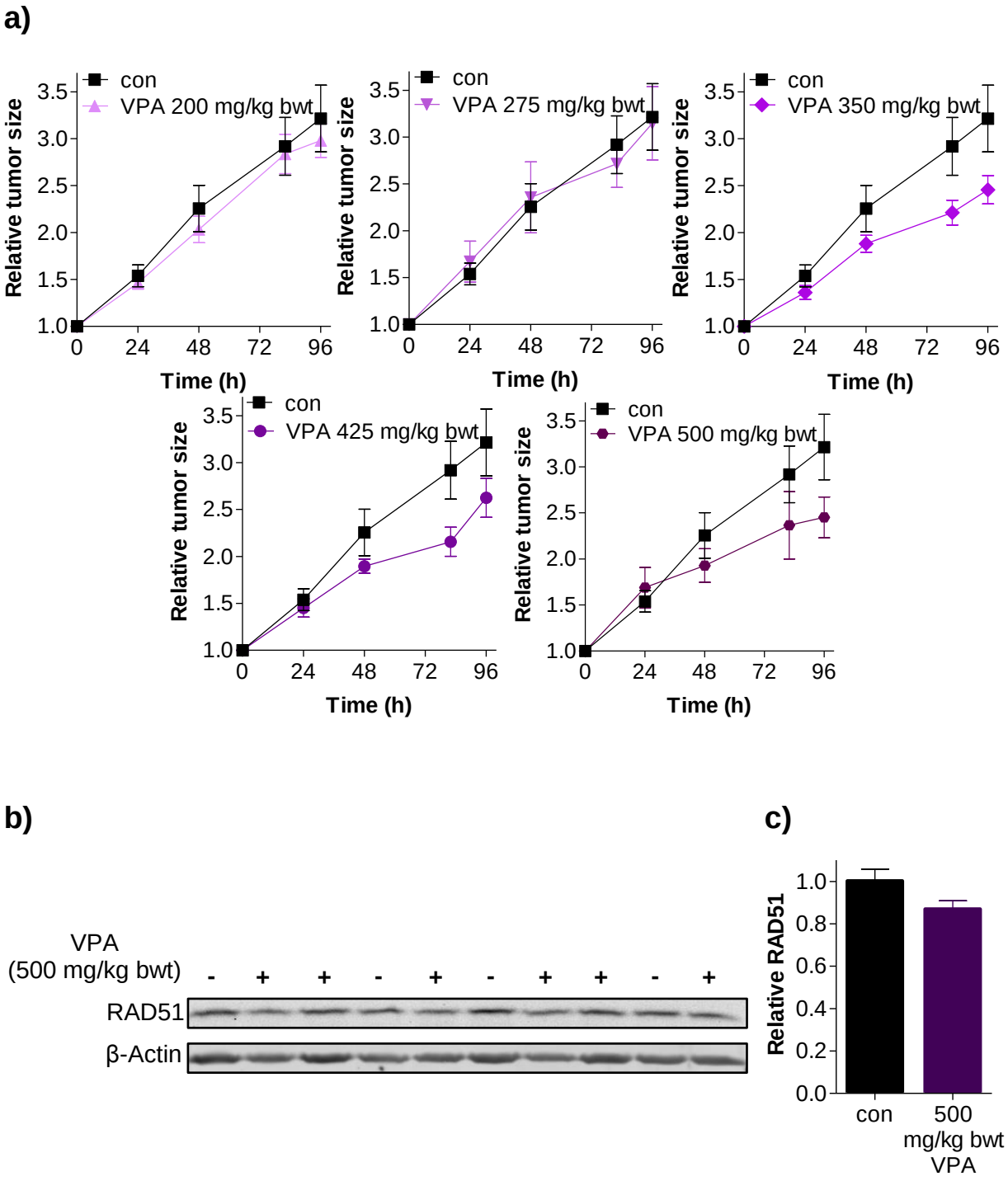

Figure 27 - Influence of HDAC inhibitor VPA on RAD51 and tumor growth *in vivo*.
Growth of Mel537 xenograft tumors in BALB/c nude mice treated with increasing doses of VPA (dose indicated was administered twice daily) (**a**). RAD51 protein levels of Mel537 xenografts in VPA treated (96 h, 500 mg/kg bwt) and untreated BALB/c nude mice (**b**) and quantification of immunoblots (**c**). Means of four tumors in two individuals (control) or six tumors in three mice (VPA) are shown. Error bars depict SEM.

4.2 Effect of histone deacetylase inhibition on the sensitivity of glioblastoma cells to TMZ

In the preceding sections it was shown that inhibition of class I HDACs by either VPA or MS-275 impairs HR, thereby sensitizes melanoma cells to the methylating agent TMZ, the chloroethylating agent FM and to IR. Since GBM is a tumor type that also exhibits low response rates to therapy and is treated with a comparable spectrum of DNA damaging therapies (TMZ and IR), the second part will focus on a combinational approach of HDAC inhibitors with TMZ in glioblastoma cells.

4.2.1 Effect of HDAC inhibitor pretreatment on the sensitivity of glioblastoma cells to TMZ

Initially, the effect of HDAC inhibitor pretreatment on TMZ sensitivity of a panel of GBM cell lines was tested. All of the cell lines displayed MGMT promoter methylation and were therefore MGMT deficient, this is important because TMZ rarely impacts on tumors without MGMT promoter methylation (Stupp *et al.*, 2009). It is important to note that the cells differed in p53 and PTEN status. The tumor suppressor p53 is mutated in 25-30 % of primary glioblastomas and determines the cell's DNA damage response and sensitivity (LN229-proficient, LN308-deficient, LN428-mt, U87MG-wt). PTEN is impaired in 60 % of glioblastoma by either loss of heterozygosity, mutation or promoter methylation and also accounts for sensitivity to DNA damaging agents (LN229-wt, LN308-null, LN428-mt, U87MG-wt) (Roos and Kaina, 2013). The cell lines were pretreated with VPA, which was removed before TMZ addition. Apoptosis measurement by AnnexinV-FITC/PI-staining and flow cytometry analysis 120 h after TMZ revealed that all cell lines were resistant to VPA alone and in three of the cell lines (LN229, U87MG and LN308) VPA pretreatment had no effect on TMZ-induced apoptosis (Figure 28 a). The only exception was LN428, which showed a slight, but not significant increase in TMZ-induced apoptosis in VPA pretreated cells as compared to cells that received TMZ only. This is in line with the regulation of RAD51 by VPA, which was examined 168 h after VPA pretreatment by western blot. VPA did not impact RAD51 levels in any of the cell lines (Figure 28 b).

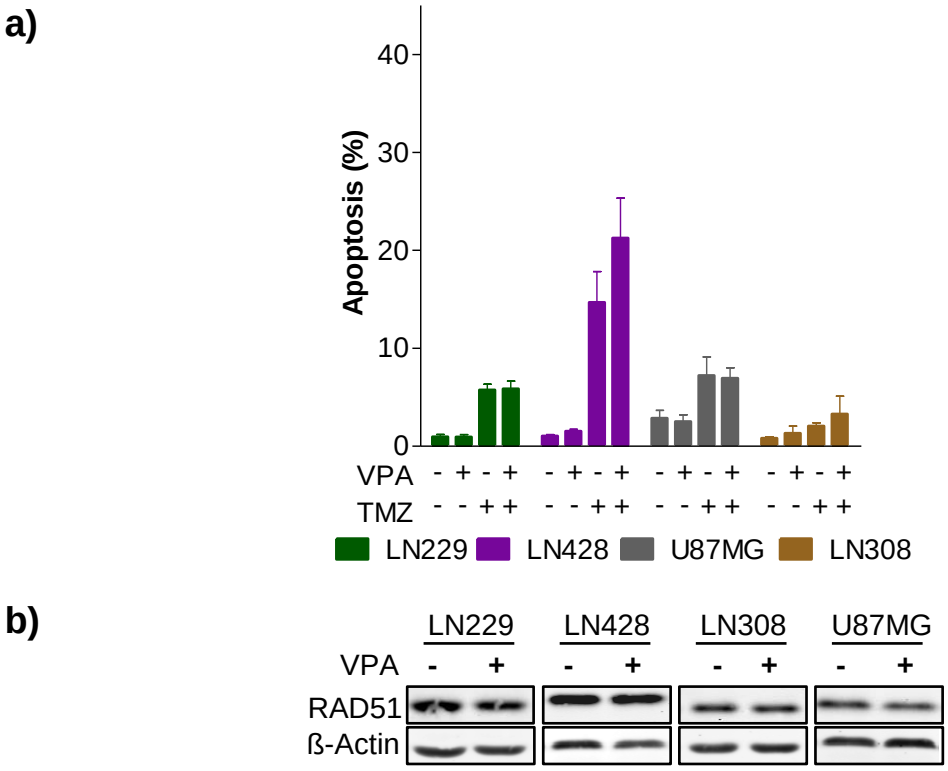

Figure 28 – Influence of the HDAC inhibitor VPA on sensitivity to TMZ and RAD51 protein levels of glioblastoma cells.
TMZ-induced (50 µM) apoptosis in VPA-pretreated (1 mM, 168 h) and control cells measured 120 h after TMZ treatment by AnnexinV-FITC/PI staining and flow cytometry analysis (**a**). RAD51 levels in VPA pretreated (1 mM, 168 h) and untreated control cells were determined by immunoblotting of whole-cell protein extracts (**b**).

Furthermore, pretreatment with the HDAC inhibitor MS-275 was analyzed in regard to glioma TMZ sensitivity. Therefore, the cells were pretreated with different doses of MS-275 for 72 h, which was then replaced by TMZ. In two of the cell lines (U87MG and LN308), no effect was observed for MS-275 in TMZ-induced apoptosis (Figure 29). In contrast, in LN229 and LN428 MS-275 pretreatment increased apoptosis induction upon TMZ by approximately 10 % as compared to TMZ alone.

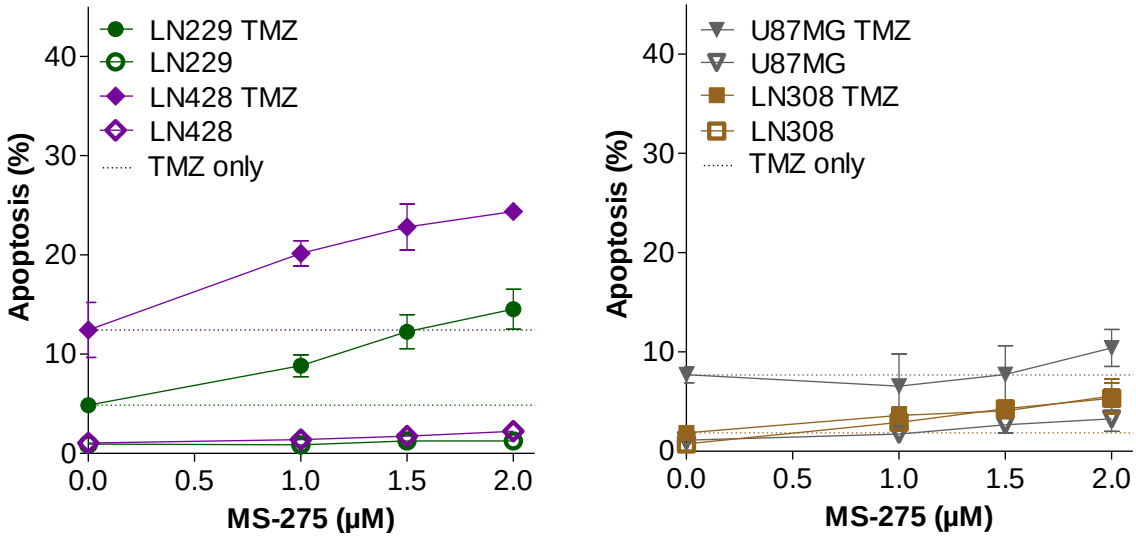

Figure 29 - Influence of pretreatment with the HDAC inhibitor MS-275 on TMZ sensitivity of glioblastoma cells.
TMZ-induced (50 µM) apoptosis in MS-275, VPA pretreated (72 h) cells was measured 120 h after TMZ treatment by AnnexinV-FITC/PI-staining and flow cytometry analysis.

4.2.2 Effect of HDAC inhibitor and TMZ co-treatment on glioblastoma cells

Having shown that pretreatment of GBM cells with HDAC inhibitors had, at most, marginal effects on TMZ-induced apoptosis, the simultaneous treatment of MS-275 and TMZ was tested so that also short-term effects of HDAC inhibition were included. Thus, the same panel of cell lines was again treated with different doses of MS-275, but 1 h later TMZ was added, without MS-275 removal. Apoptosis was measured at 120 h by AnnexinV/PI-staining and flow cytometry analysis. Again LN308 and U87MG were resistant, as neither TMZ nor the combination of MS-275 and TMZ induced more than 10 % apoptosis (Figure 30). LN229 and LN428 cells, however, were greatly sensitized in the combination treatment. At the highest concentration of MS-275 (1.5 µM), 35 % of LN229 cells and 20 % of LN428 cells underwent apoptosis compared to single treatment with TMZ, after compensating for background apoptosis levels. At this concentration, the toxicity of MS-275 alone was very low as apoptosis induction was below 4 % (Figure 30).

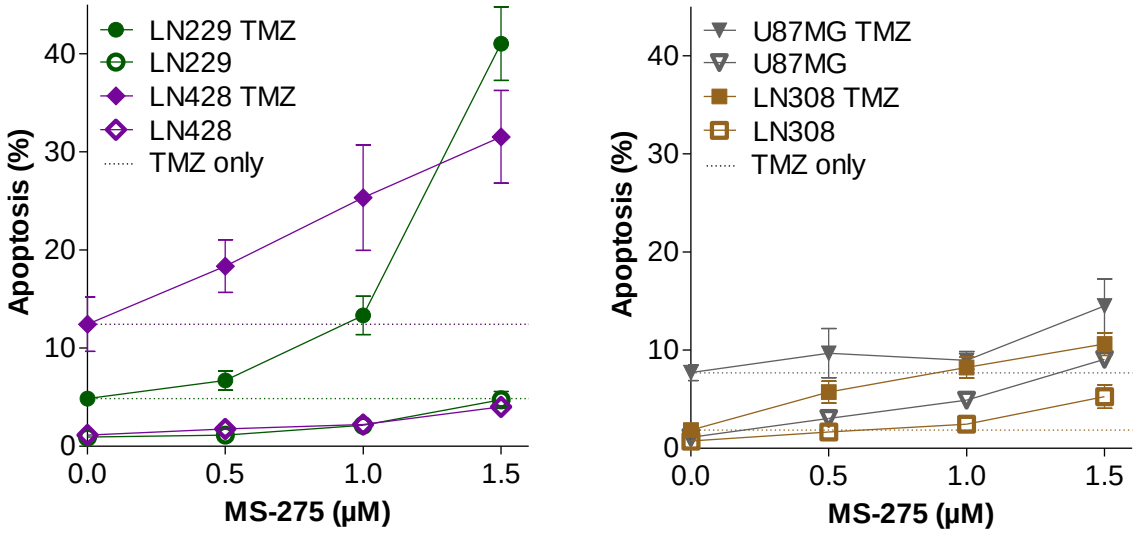

Figure 30 - Influence of concomitant MS-275 treatment on TMZ-induced apoptosis in glioblastoma cells.
TMZ-induced (50 µM) apoptosis in MS-275-pretreated (72 h) cells was measured 120 h after TMZ treatment by AnnexinV-FITC/PI-staining and flow cytometry analysis.

Based on the finding that MS-275 ameliorated the response of some GBM cell lines to TMZ the question of the underlying mechanism arose. To answer which timeframe after drug exposure is relevant for the observed sensitizing effect, the kinetics of apoptosis induction were acquired for LN229 by Sub-G1 measurement. Whereas for TMZ alone and MS-275 alone, only a negligible amount of apoptosis was induced 96 h and 120 h after treatment, combination of both resulted in an increase in apoptosis induction from 72 h onwards (Figure 31). Together with the observation that the addition of MS-275 24 h after TMZ had a similar sensitizing effect (S 3), we speculated that TMZ-induced O^6MeG is the lesion that LN229 cells are sensitized to upon treatment with MS-275.

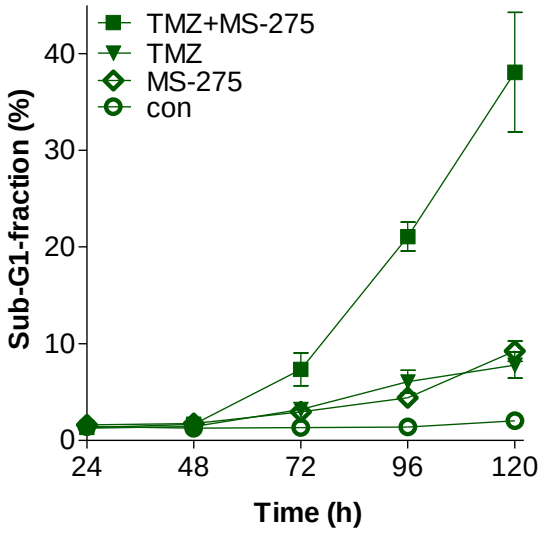

Figure 31 – Kinetics of apoptosis induction upon TMZ and MS-275 treatment in LN229 glioblastoma cells.
LN229 cells were treated with TMZ (50 µM), MS-275 (1.5 µM), a combination of the two drugs or were left untreated for control and fixed at indicated times after exposure. Sub-G1 fraction was measured in PI stained cells by flow cytometry.

4.2.2.1 Regulation of RAD51 by MS-275 in glioblastoma cells

Immunoblots of whole-cell extracts of LN229 treated with MS-275, TMZ or both demonstrated that MS-275 single treatments downregulated the protein from 60 h post-treatment (Figure 32 a). The combination of both decreased protein levels even stronger, which was detected 24 h after treatment. To test whether the MS-275-mediated RAD51 downregulation has a functional impact, a possible synergistic effect with the PARP1 inhibitor Olaparib was tested. LN229 cells treated with Olaparib showed a marginal increase in apoptosis induction following increasing doses (up to 20 µM). Combination of Olaparib with MS-275 did not alter the response to Olaparib, indicating that RAD51 downregulation upon MS-275 did not have functional implications (Figure 32 b).

As RAD51 is regulated cell cycle-dependently and expressed in S and G2 phase, cell growth and cell cycle distribution was determined in response to MS-275. Untreated LN229 cells exhibit an exponential growth with a doubling time of approximately 24 h. MS-275-treated LN229 cells slowed down proliferation, so that between 96 h and 120 h of MS-275 almost no increase in cell number was observed (Figure 32 c). The average doubling time was elongated to 53 h. Analysis of cell cycle distribution provided a possible explanation for the anti-proliferative effect of MS-275. Two days after MS-275 addition, LN229 displayed reduced number of cells in S and G2 phase, which further decreased over time, so that 120 h after treatment only 8 % of cells were in S- and G2-phase compared to untreated cells out of which 27 % were in S- and G2-phase (Figure 32 d). MS-275 treated cells accumulated in G1. Consequently, the observed MS-275-mediated downregulation of RAD51 can likely to be attributed to the inhibitory effect of the HDAC inhibitor on proliferation and cell cycle progression.

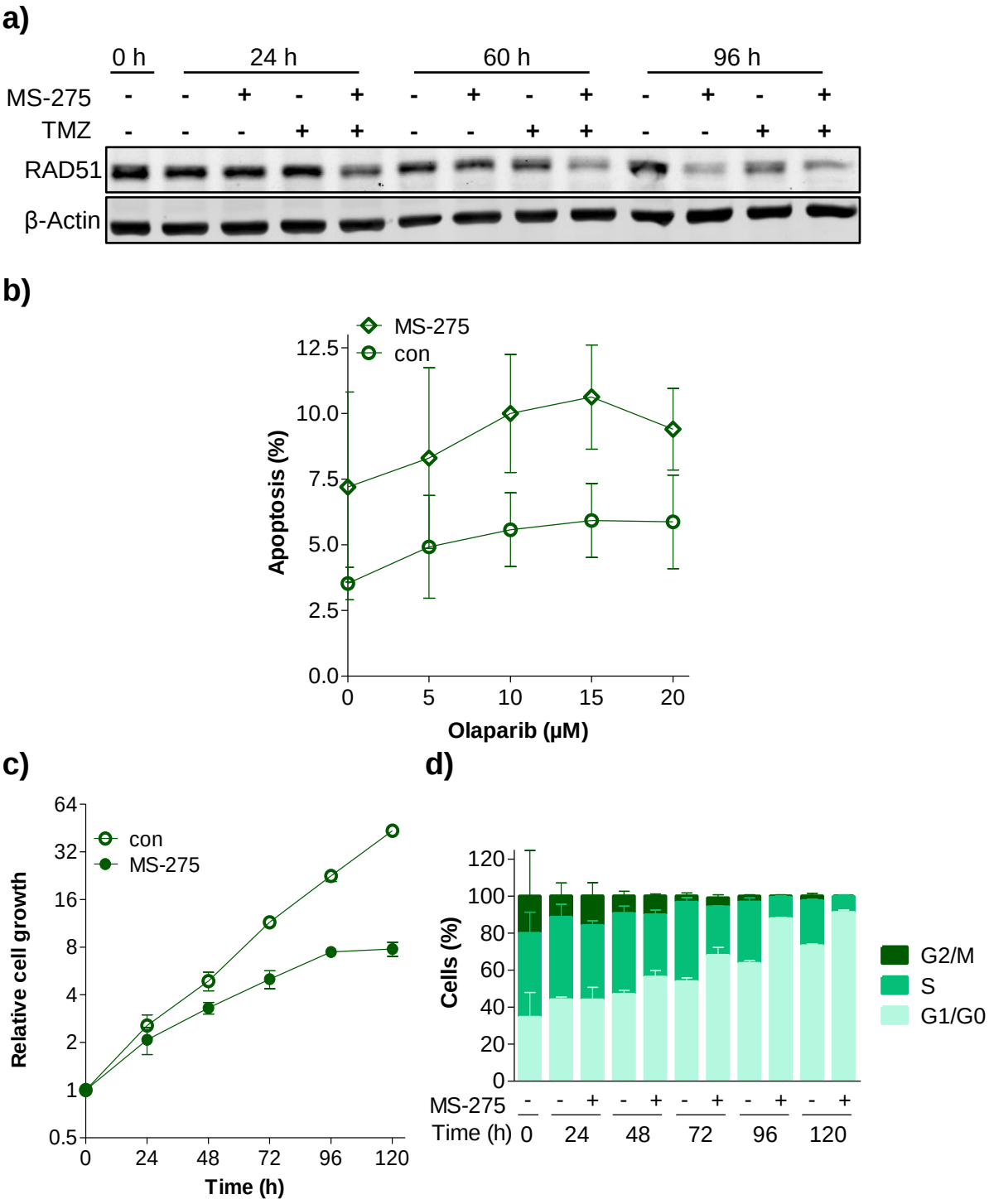

Figure 32 - MS-275-mediated downregulation of RAD51 in glioblastoma cells is due to the inhibition of proliferation and cell cycle progression.
RAD51 protein levels were analyzed in untreated and MS-275 (1.5 µM, 72 h) treated LN229 cells that were either additionally exposed to TMZ (50 µM) or left untreated for controls. Whole cell protein extracts of indicated timepoints were subjected to immunoblotting (**a**). Apoptosis induction by PARP1 inhibitor Olaparib and concomitant MS-275 (1.5 µM) treatment was assessed by AnnexinV-FITC/PI staining 72 h after treatment (**b**). Cell growth of LN229 cells in absence or presence of MS-275 (1.5 µM) was measured by counting cells at indicated timepoints and relating to the pretreatment cell numbers (**c**). Cell cycle distribution was analyzed in MS-275 (1.5 µM) treated or untreated LN229 cells by PI staining and flow cytometry analysis (**d**).

4.2.2.2 Cell cycle regulation upon MS-275 and TMZ co-treatment in glioblastoma cells

Since the classical model of cytotoxicity of O^6MeG strictly depends on proliferation and S-phase progression and is characterized by the induction of a G2/M-arrest, the question arose, whether TMZ combined with MS-275 followed this cell cycle profile. Therefore, the cell cycle of TMZ treated and TMZ/MS-275 treated cells was acquired over 120 h by PI staining and flow cytometry analysis. TMZ treatment led to a G2/M arrest 48 h after treatment. At this time, the combination treatment also showed a high G2/M peak, though in addition many cells were detected with a DNA content characteristic for late S-phase (Figure 33). This cell cycle distribution was also observed 72 h after treatment. This indicates that even though proliferation is impaired after MS-275, it was still possible to undergo two cell cycles before accumulation of cells in G2/M. Interestingly, 96 h after TMZ treatment in the single-treated cells, a population with a DNA content of approximately 8n appeared that did not appear in the combined treatment with MS-275. This divergence was even more pronounced 120 h after treatment. Furthermore, 120 h after treatment approximately 40 % of cells treated with TMZ alone cells had a DNA content >4n whereas in a combination of MS-275 and TMZ the >4n population was almost completely lost (10 %). The process resulting from DNA replication without cytokinesis is referred to as endoreplication.

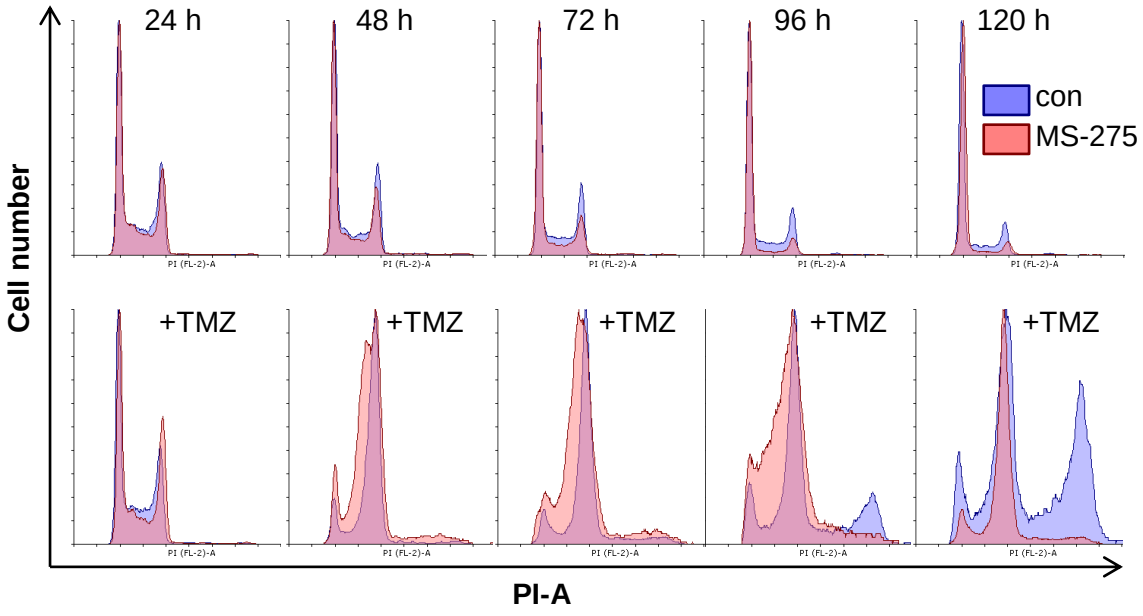

Figure 33 - Cell cycle distribution in LN229 cells exposed to MS-275 and TMZ and combination of both drugs.
LN229 cells were treated with MS-275 (1.5 µM), TMZ (50 µM), both or left untreated for control and fixed at indicated timepoints. Cells were stained with PI and analyzed by flow cytometry.

4.2.2.3 DNA damage response of glioblastoma cells exposed to TMZ in combination with MS-275

Based on fundamentally different cell cycle profiles of TMZ treated and TMZ/MS-275 co-treated cells, we suspected an aberrant DNA damage response was causing this differential cell cycle control. Therefore, the TMZ-induced phosphorylation of ATR/ATM and their downstream targets, checkpoint kinases CHK1/CHK2, was assessed in LN229 cells by immunoblots. Whereas TMZ activated ATM as early as 24 h after treatment and stably until 96 h post-treatment, phosphorylation was absent following treatment with TMZ and MS-275 (Figure 34). Although ATR is activated 96 h after TMZ, phosphorylation is absent following combination treatment. CHK1 and CHK2 kinases are slightly activated 24-60 h after TMZ or TMZ/MS-275 combination, but highly phosphorylated 96 h after TMZ, but not after combined treatment. A decline in activation of ATR/ATM and CHK1/2 was likewise observed when the HDAC inhibitor MS-275 was applied 24 h after TMZ treatment (S 4).

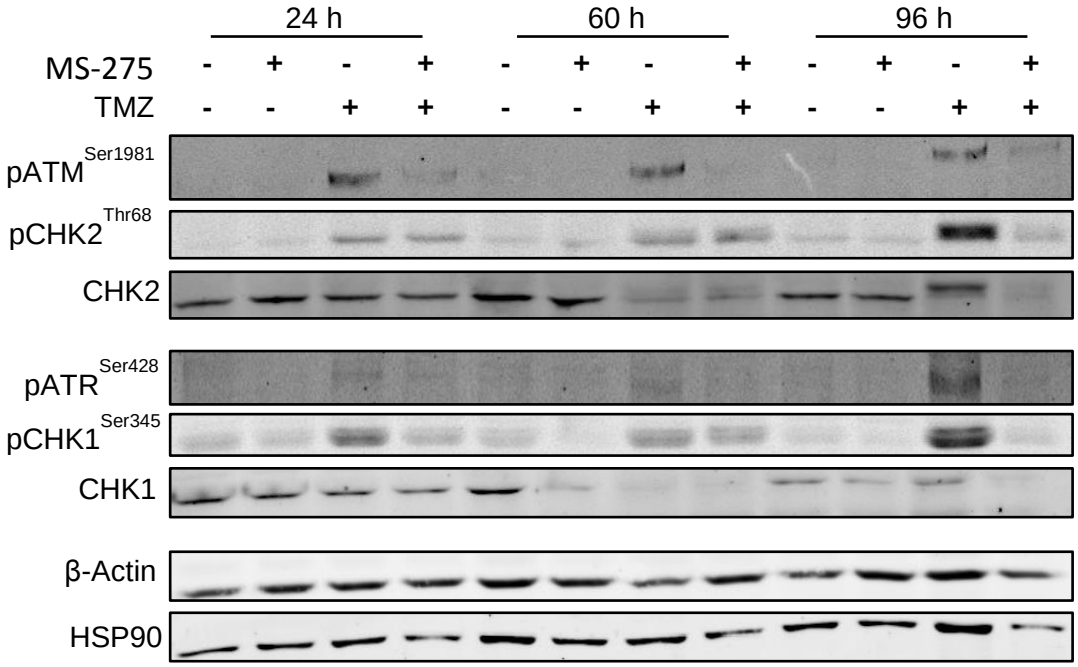

Figure 34 - Influence of the HDAC inhibitor MS-275 on TMZ-induced phosphorylation of DNA damage response proteins and checkpoint kinases.
Whole cell extracts of LN229 cells treated with MS-275 (1.5 µM), TMZ (50 µM), in combination or left untreated were subjected to immunoblotting to analyze DNA damage signaling.

Collectively, these observations pointed to a MS-275-mediated disruption of DNA damage signaling which potentially results in aberrant p53 stabilization and $p21^{Cip1/Waf1}$ transactivation. Testing this hypothesis by immunoblotting revealed increasing p53 levels upon TMZ accompanied with $p21^{Cip1/Waf1}$ induction, both of which was abolished by MS-275 (Figure 35).

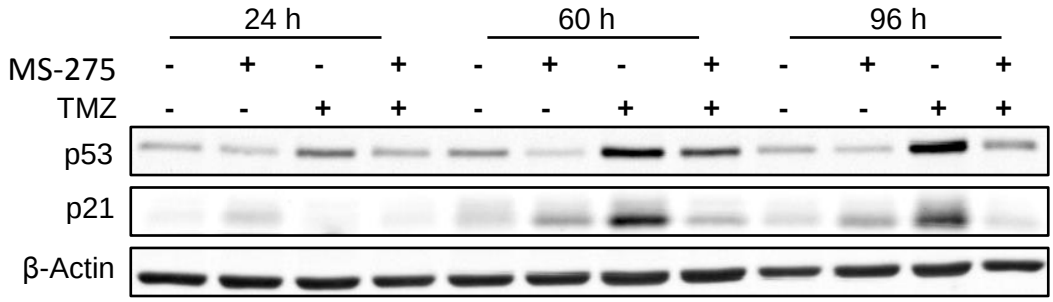

Figure 35 – Influence of HDAC inhibitor MS-275 on TMZ-induced p53 stabilization and p21 induction in LN229 glioblastoma cells.
Whole cell protein extracts of LN229 cells treated with MS-275 (1.5-µM), TMZ (50 µM), in combination or left untreated for controls were subjected to immunoblotting.

5 Discussion

Cancer, as a life-threatening disease, is becoming one of the best-studied pathologies in medicine and biology. Scientific breakthroughs in the last century enabled the identification of cancer risk factors, biological features of cancer and better cancer diagnostics. For some cancer entities, research efforts resulted in improved therapy. However, for most malignancies, the translation of research into effective therapies is still lagging behind. This especially applies to exceptionally aggressive tumors like metastatic melanomas and glioblastomas. Patients suffering from these cancers display low median overall survival ranging between one and two years even with the most advanced therapies currently available (Chinot *et al.*, 2014; Westphal *et al.*, 2015; Stupp *et al.*, 2014b; Robert *et al.*, 2015).

Still, recent insights into mechanisms of resistance established new targets and avenues for therapeutic intervention. In the case of methylating agents, used to treat glioblastoma and malignant melanoma, the mechanism of cytotoxicity and opposing resistance mechanisms like HR proficiency and MGMT expression are widely understood (Tuominen *et al.*, 2015; Stupp *et al.*, 2009; Quiros *et al.*, 2011). Further, resistance to apoptosis initiation limits sensitivity of these cancers to methylating agents (Roos *et al.*, 2011). Given the prognostic role of the overexpression of HDACs and the anti-neoplastic effect of HDAC inhibitors that target the aforementioned resistance factors (West and Johnstone, 2014), warranted further investigation of the anti-neoplastic effects of combining HDAC inhibitors and methylating agents.

5.1 Inhibition of histone deacetylases sensitizes melanoma cells to methylating agents by impairing homologous recombination

To validate the use of cell lines as an appropriate model for examining a combinational therapy, class I HDAC levels were examined in a panel of melanoma cell lines. All of them expressed all class I HDACs, though comparison to non-cancerous cells revealed a significant overexpression of HDAC2 and HDAC3, a three-fold higher but non-significant elevation of HDAC1 and a negligible upregulation of HDAC8 (Figure 9). Thus, we demonstrated an HDAC upregulation in melanoma cells which justified the use of the class I HDAC inhibitors VPA and MS-275. Both were further shown to exhibit HDAC inhibitory action on melanoma cells as seen by increases in histone 3 and 4 acetylation (Figure 10). For further studies, two melanoma cell lines (D05 and A375) were used to measure the lethality in an HDAC inhibitor pretreatment scheme. After 168 h of VPA treatment, a 7 % higher (over control) but non-significant apoptosis induction was observed in D05 cells. In A375 cells, VPA did not significantly affect apoptosis induction (Figure 11). Thus, D05 cells display a weak HDAC inhibitor response whereas A375 were non-responsive

when the inhibitor was applied on its own, which is in line with the reported differential response of melanoma cell lines to HDAC inhibitors (Chang *et al.*, 2012). The low response is further explained by the low concentrations of VPA (1 mM) used here in comparison to similar *in vitro* studies that achieved a higher toxicity with higher drug concentrations (Valentini *et al.*, 2007). Since this work used HDAC inhibitors as an adjuvant to classical chemotherapy, a low response of HDAC inhibitor-single treatment was favored. It should further be noted, that due to the pretreatment approach, detached apoptotic cells induced by HDAC inhibition were removed before addition of the chemotherapeutic drug and therefore reduced basal apoptosis was measured for combination treatment experiments (e.g. VPA Figure 15 a) compared to that observed for VPA alone (Figure 11).

A prerequisite for combination of alkylating agents with HDAC inhibitors is the absence of cell cycle arrest and proliferation rate after pretreatment, as replication is required for alkylating agent-mediated toxicity (Quiros *et al.*, 2010; Roos *et al.*, 2004). However, in our test-system, no significant change in cell cycle distribution was observed in D05 and A375 cells (Figure 12). Though, VPA increased the amount of G1 cells from 65 % to 69 % in D05 cells and decelerated proliferation up to 24 h after HDAC inhibitor removal in this cell line, while not impacting on A375 cells (Figure 12). This again underlined that D05 slightly responds to VPA and A375 does not. Based on the mild effects of VPA observed in these cell lines, interference of VPA with DNA-damaging therapies was not expected.

Indeed, this study revealed that a combination of VPA pretreatment with genotoxic intervention acts synergistically in melanoma cells. Importantly, no synergy was observed in non-transformed primary melanocytes (Figure 13 b). A detailed comparison of the response to genotoxic stress in melanocytes to the response in malignant melanoma cells showed that melanocytes were less sensitive to TMZ and ionizing radiation than both melanoma cell lines and that FM induced approximately the same amount of apoptosis (8-11 %) in malignant and primary cells (Figure 13 b). The aforementioned treatment modalities exploit the proliferative phenotype of cancerous cells while sparing quiescent and differentiated cells (Helleday *et al.*, 2008). This may explain why the slower cycling melanocytes were less affected by TMZ and IR. This may be even more pronounced *in vivo*, as the experimental system stimulated melanocyte proliferation whereas physiologically, melanocytes rarely divide (Cichorek *et al.*, 2013). In addition to a replication block, FM induces transcription blocking-interstrand crosslinks that are thought to induce apoptosis (Ljungman and Zhang, 1996) independent of proliferation and, therefore, hit both: fast proliferating melanoma cells and slow dividing melanocytes and explains the similar response of both cell types to FM.

In combination of VPA with the alkylating agents TMZ and FM, pronounced differences between melanoma cells and melanocytes were observed. Both alkylating agents induced less apoptosis (reduction of ~30 %) in VPA pretreated melanocytes, while increasing apoptosis by 1.8-2.8 fold in

VPA pretreated melanoma cells (Figure 13 b). This supports the finding that HDAC inhibitors act selectively on transformed cells if applied alone (Bolden *et al.*, 2013; Insinga *et al.*, 2005). Our data extends the tumor selectivity of HDAC inhibitors by targeting melanomas and not their cells of origin (melanocytes) as well as to a sensitization effect to alkylating agents even in the absence of a (clear) response to the HDAC inhibitor alone. Consequently, combination of alkylating agents with HDAC inhibitors in melanoma cells confers selectivity in a dual way: by targeting highly proliferative cells (also applies to non-transformed cells) and by selectively targeting tumor cells. Although repeatedly reported, the underlying mechanism of cancer cell selectivity of HDAC inhibitors is still elusive. The concept of oncogene addiction (Weinstein, 2002) that assumes redundant pathways in non-transformed cells opposing one efficient and, therefore, targetable pathway in tumor cells might explain tumor selectivity (Dawson and Kouzarides, 2012). A second explanation assumes that epigenetic reprogramming during carcinogenesis leads to different outcomes in response to HDAC inhibitors, e.g. different expression of pro-apoptotic *BCL2*-genes (Bolden *et al.*, 2013; Falkenberg and Johnstone, 2014).

Moreover, sensitization to TMZ was observed in a panel of melanoma cell lines differing in p53 and B-RAF status (Figure 14). Therefore, it can be regarded as independent from both resistance factors: p53 as a DNA repair-mediating resistance factor (Barckhausen *et al.*, 2014; Naumann *et al.*, 2009) and oncogenic B-RAF that was shown to be a negative prognostic marker in melanoma for therapy different than B-RAF inhibition (Long *et al.*, 2011).

Based on the observation that apoptosis induction started 72 h after TMZ addition in combination treatments, (Figure 15 f) we speculated that O^6MeG is the lesion responsible for cell death. Therefore, we repeated the experiments in the absence of the synthetic substrate for MGMT (O^6BG) and, consequently, in the presence of MGMT activity. HDAC inhibitor pretreated cells that were exposed to TMZ in the presence of MGMT (without O^6BG) did not show an apoptotic response, which was also absent in cells treated only with TMZ (Figure 16). Thereby, we show that MGMT confers resistance to TMZ in control and HDAC inhibitor-pretreated cells. Secondly, our data reveal that HDAC inhibitor mediated sensitivity to TMZ can be attributed to the specific lesion O^6MeG since, only if MGMT is inactive (treatment with O^6BG), apoptosis is induced. This further shows that the MGMT downregulating effect of VPA is not sufficient to sensitize melanoma cells to TMZ. Regarding the translation into the clinic, this means that sensitization would be limited to MGMT promoter methylated tumors, which comprise 38 % of malignant melanomas (Hassel *et al.*, 2010). Recent efforts tried to target MGMT tumor-selectively by conjugating MGMT inhibitors to folate (Javanmard *et al.*, 2007) or by generation of a MGMT inhibitor analog, that, under hypoxic conditions reduces to functional O^6BG (Penketh *et al.*, 2012). Both have proven to inactivate MGMT in *in vitro* studies. A promising effort to overcome the resistance factor MGMT is by transfer of autologous hematopoietic stem cells that express an O^6BG resistant MGMT. This attenuated myelosuppression in a combination of alkylating agents

with O^6BG and increased the number of TMZ-treatment cycles tolerated by patients as shown in a phase I clinical trial (Adair *et al.*, 2014). These attempts might overcome MGMT-mediated resistance that could also expand the effectiveness of HDAC inhibitor-mediated sensitization.

In the absence of MGMT, resistance to O^6MeG-induced apoptosis has been attributed to pathways of DNA repair, apoptosis suppression and DNA damage signaling (Quiros *et al.*, 2011; Eich *et al.*, 2013; Roos *et al.*, 2007; Roos *et al.*, 2011). In our test system, VPA neither regulated pro-apoptotic *BCL2* family members (*BAX*, *NOXA*, *PUMA*) on protein level, nor the anti-apoptotic BCL-2 protein (Figure 17). This is contradictory to publications that relate apoptosis induction and sensitization effects of HDAC inhibitors to the induction of BAX and/or the downregulation of BCL-2 (Vrana *et al.*, 1999; Sonnemann *et al.*, 2014; Jones *et al.*, 2009). However, a direct comparison between the data obtained in this study with the data obtained in the published studies is difficult due to the use of different inhibitors and cell systems. However, the study by Papi and colleagues (Papi *et al.*, 2010) analyzed both proteins in response to VPA in melanoma cells. The authors observed, in the mildly VPA sensitive G361 cell line (5 % apoptosis at 1 mM, 24 h), an upregulation of BAX (20 %) and a downregulation of BCL-2 (-20 %) at a concentration of 1 mM VPA.

Another suspect we found to be downregulated upon VPA is the damage signaling kinase ATR. In response to TMZ, phosphorylation of the ATR substrate CHK1 in D05 cells was delayed in VPA pretreated cells, though reaching the phosphorylation level of TMZ single treatment 48 h after TMZ addition (Figure 18). Most likely, this delay results from the observed retardation in growth, that was detected in VPA pretreated D05 cells 24 h after VPA removal (Figure 12 b), but not 48 h after HDAC inhibitor removal. Interestingly, TMZ induced phosphorylation of CHK1 by 3-6.6-fold increase over control after 24 h, which, in regard to the processing model of O^6MeG, is an early event. Early activation might arise directly from the recognition of adducted guanine:thymine by MMR (Yoshioka *et al.*, 2006) or may reflect the heterogeneity of cell cycle progression in non-synchronized cells. This early activation however, is unlikely to be involved in apoptosis induction, as this occurs at later timepoints (72 h after TMZ).

With the VPA-mediated downregulation of the DNA repair proteins RAD51 and FANCD2 by 40-60 % in melanoma cells (Figure 17), we revealed a further prospective mechanism of HDAC inhibitor mediated sensitization to TMZ. This hypothesis is strengthened by a row of observations presented in this study. The panel of VPA-sensitizable melanoma cell lines showed a downregulation of RAD51 upon VPA pretreatment (Figure 14 and Figure 19). Further, VPA reduced RAD51 dose dependently, which is in line with a dose dependent sensitization of VPA pretreated cells (Figure 20 and Figure 15 c). Similarly, VPA pretreatment time determined the degree of sensitization as well as of RAD51 and FANCD2 reduction (Figure 20 and Figure 15 e). Experiments conducted with MS-275, that show sensitization to TMZ and RAD51/FANCD2

downregulation underline that both effects are likely attributed to the HDAC inhibitory function and that HDAC1, HDAC2 and HDAC3 are the relevant targets, as these are impeded by MS-275.

Early studies of HDAC inhibition in melanoma cells reported a reduction of KU proteins and DNA-PKcs, parts of NHEJ DSB repair pathway, to confer radiosensitivity (Munshi *et al.*, 2005; Munshi *et al.*, 2006). These findings were not reproduced in this work, since VPA did not impact on KU80 (Figure 17). On the other hand, research in prostate, colon and bone cancer cells confirmed the effect of HDAC inhibition on RAD51 expression, which coincided with an enhanced sensitivity to irradiation (Chinnaiyan *et al.*, 2005; Adimoolam *et al.*, 2007; Kachhap *et al.*, 2010; Blattmann *et al.*, 2010). This study confirms the aforementioned studies, as VPA pretreatment sensitized melanoma cells to irradiation. However, the effect of HDAC inhibition on alkylating agent-induced apoptosis was more pronounced than on IR-induced apoptosis in the cell lines tested (Figure 13). This supports the role of RAD51 and HR in HDAC inhibitor-mediated sensitization. DSBs induced by IR are primarily repaired via NHEJ, whereas TMZ or FM induce DSBs replication-dependently or block replication and therefore require HR for recovery. This makes alkylating agents a better choice in combination with HDAC inhibition. Further, if HDAC inhibitor-mediated impairment of HR also applies to other solid tumors a combination of HDAC inhibition with agents that replication-dependently introduce DNA-strand breaks might be a reasonable therapy approach. These agents are for instance topoisomerase inhibitors that are used for colon or lung cancer therapy.

In addition to RAD51, we identified FANCD2 as a novel mediator of HDAC inhibitor-induced sensitization. FANCD2 interacts with BRCA2 to mediate RAD51 filament formation during HR repair, although it is not essential for the repair event (Hussain *et al.*, 2004; Wang *et al.*, 2004; Ohashi *et al.*, 2005). Further, FANCD2 stabilizes stalled replication forks, which, in the absence of FANCD2, is taken over by RAD51 (Schlacher *et al.*, 2012). As both are diminished upon HDAC inhibitor treatment, combination of HDAC inhibition with agents that stall replication like Hydroxyurea, Gemcitatbin or 5-Fluorouracil might be a promising approach for fighting tumors treated with these agents. Apart from that, the damage-signaling and repair protein-recruiting function of FANCD2 in ICL repair indicates a possible sensitization to other crosslinking agents like cisplatin.

A recent treatment approach in BRCA1/2 deficient cancers exploits the absence of functional HR by introducing replication-dependent lesions with a PARP1 inhibitor. The inhibitor either traps PARP1 on the DNA which blocks replication, or it prevents the sealing of BER intermediate SSBs that result in stalled replication or one-ended DSBs (Helleday, 2011). In a HR proficient background, these lesions can be stabilized and repaired, whereas in cancer cells lacking HR, unrepaired lesions lead to cell death. Here, we showed that in accordance with the VPA-mediated reduction of RAD51/FANCD2 protein and reduced repair of DSBs by HR, PARP1 inhibition by Olaparib induced apoptosis (11 %) in VPA pretreated cells but not in control cells (2 %) (Figure

24). This underlines the functional impairment of HR brought about by VPA-mediated RAD51/FANCD2 suppression. Remarkably, the HDAC inhibitor-mediated sensitization to PARP1 inhibition is independent of MGMT and therefore most likely applicable to all melanomas.

HR was shown, in glioblastoma cells, to repair DSBs induced by O^6MeG; thereby protecting against methylating agent-induced cell death (Quiros *et al.*, 2011). Accordingly, we showed in VPA pretreated melanoma cells, and therefore, HR impaired cells, a higher number of TMZ-induced γH2AX foci 48 h after TMZ. However, the number of γH2AX foci decreased in VPA pretreated cells 72 h after TMZ addition despite the impairment of HR (Figure 25 a and b). This contradicts the findings in glioblastomas, where TMZ induced the same number of γH2AX foci in RAD51 knockdown and parental cells, but repair was impaired in knockdown cells. The findings in VPA pretreated cells rather point to a higher induction of DSBs by TMZ, which is followed by a reduction at later timepoints (72-96 h post-treatment). Though, the decrease in DSBs does not necessarily result from repair. We speculated that the reduction of γH2AX foci 72 h and 96 h after TMZ treatment resulted from severely damaged cells that underwent apoptosis, detached from the growth surface and were not included in immunofluorescent analysis. Western blot analysis of γH2AX performed on protein extracts, including detached cells, showed high H2AX phosphorylation 48 h after TMZ addition in VPA pretreated cells and only slight phosphorylation in cells only treated with TMZ (Figure 25 c). In contrast to foci analysis, this remarkable difference remained for up to 120 h post-treatment with TMZ. Importantly, H2AX is also phosphorylated during apoptotic DNA fragmentation (Rogakou *et al.*, 2000), thus impeding distinction of TMZ- and apoptosis-induced γH2AX. Still, the initial difference in H2AX phosphorylation, which was detected by immunofluorescence and by western blot, suggests a higher induction of DSBs by TMZ in VPA pretreated cells. As divergence of foci number and overall H2AX appears at the timepoint of apoptosis induction (72 h), the reduction of foci number in VPA pretreated cells could be linked to the detachment of severely damaged apoptotic cells.

Apoptotic H2AX phosphorylation further explains the high basal γH2AX in VPA pretreated cells and is in accordance with the slight responsiveness of D05 cells to VPA alone (Figure 11 and Figure 15 a, b and f).

To clarify whether RAD51 and HR actually confer resistance to TMZ in melanoma cells, apoptosis induction was examined in A375 RAD51 knockdown cells. The higher apoptosis induction in RAD51 knockdown cells, compared to the untransfected and empty transfected cells, clearly links HR to TMZ resistance (Figure 26). Therefore, HDAC inhibitor-mediated suppression of RAD51, FANCD2 and HR represents a plausible explanation for the sensitization effect to TMZ in melanoma. Furthermore, the influence of RAD51 on TMZ sensitivity is in accordance with findings in glioma and CHO cells (Quiros *et al.*, 2011; Roos *et al.*, 2009), strengthening HR as a general resistance mechanism for S_N1 methylating agents.

Furthermore, we analyzed RAD51 downregulation *in vivo* using a Mel537 xenograft mouse model. The RAD51 levels in tumors of mice receiving 2 x 500 mg/kg bwt were slightly decreased by 13 %. For mice receiving at least 350 mg/kg bwt twice daily, an inhibitory effect was observed on tumor growth, though it was not significant (Figure 27). This contrasts with a study conducted with colon cancer xenografts that achieved a reduction of RAD51 in the tumor tissue with the pan-HDAC inhibitor abexinostat (Adimoolam *et al.*, 2007). It should be noted that, in our work, animal groups were small (three mice for VPA treatments, two mice in control group since a third did not develop tumors) and may not be representative. Therefore, further experiments with a higher number of animals are required to clarify the *in vivo* potential of a combinational therapy with HDAC inhibitors and TMZ. Furthermore, MS-275 as a more specific HDAC inhibitor should be tested.

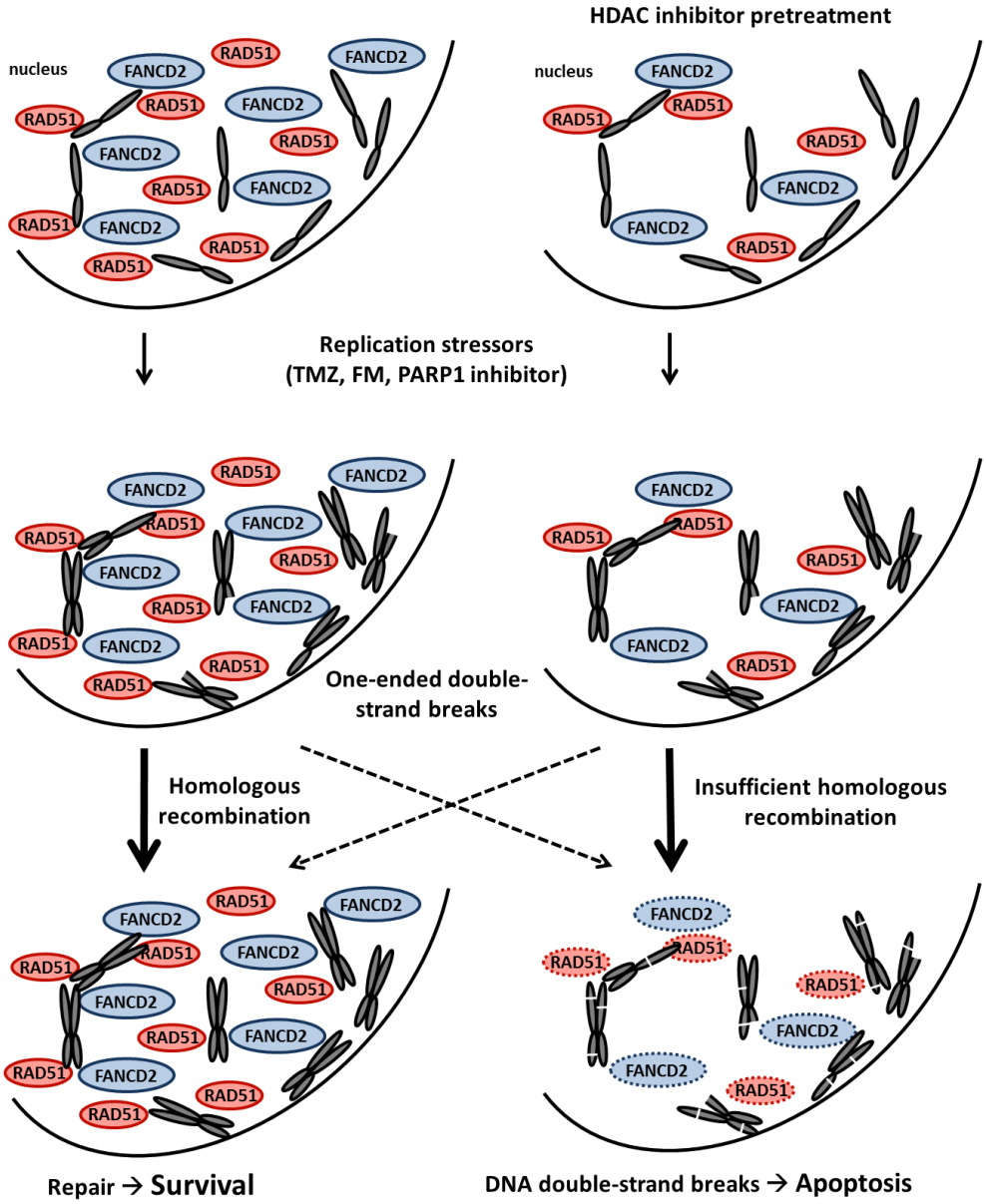

Figure 36 – Mechanism of HDAC inhibitor mediated sensitization to genotoxic stress.
HDAC inhibition reduces RAD51 and FANCD2 protein levels; thereby leading to an accumulation of one-ended double-strand breaks and the induction of apoptosis (right). Whereas in the absence of an HDAC inhibitor, DSBs are repaired via HR, leading to survival (left).

In conclusion, this study demonstrates a sensitization of melanoma cells by HDAC inhibition to DNA damage, in particular to replication-associated damage. This results from a transcriptional downregulation of the DNA repair proteins RAD51 and FANCD2, which attenuates HR processes and lowers the apoptosis threshold of lesions needed to initiate cell death (Figure 36).

5.2 Combination of histone deacetylase inhibition and TMZ partially sensitizes glioblastoma cells by disruption of DNA damage signaling

Even though drivers of GBM like EGF-receptor, VEGF or specific integrin expression (Verhaak *et al.*, 2010; Plate *et al.*, 1992; Schnell *et al.*, 2008) were recently discovered and can be targeted therapeutically, corresponding clinical trials failed to improve overall survival of patients (Westphal *et al.*, 2015; Chinot *et al.*, 2014; Stupp *et al.*, 2014b). On the other hand, the use of VPA as an antiepileptic drug against seizures in GBM patients allowed retrospective analyses of its influence on survival. These studies revealed an improvement of overall survival in patients receiving IR, TMZ and VPA compared to chemo/radiotherapy alone (Weller *et al.*, 2011; Barker *et al.*, 2013). *In vitro* studies confirmed a sensitization effect of HDAC inhibitors on DNA damage-induced apoptosis in GBM cells (Das *et al.*, 2007; Pont *et al.*, 2015), though its mechanism remains widely unclear. Therefore, we hypothesized a similar mechanism of HDAC inhibitors as found in melanoma cells that could sensitize GMB cells to DNA damaging agents. More precisely, this would include the downregulation of the HR proteins RAD51 and FANCD2, leading to reduced repair and increased apoptosis induction.

The response of GBM cell lines (LN229, LN428, U87MG and LN308) to TMZ was tested with and without HDAC inhibitor pretreatment. VPA did not significantly modify the response to TMZ in any of the four tested cell lines, which was in line with constant RAD51 protein levels after VPA pretreatment. The same panel of cell lines was tested with MS-275 pretreatment in combination with TMZ. Two of the cell lines (LN229 and LN428) responded to the pretreatment with an approximately 10 % higher apoptosis induction than TMZ alone (Figure 28 and Figure 29). Two other cell lines (U87MG, LN308) did not respond. This agrees with preclinical studies in glioblastoma cells that show only mild and non-significant effects of pretreatment with an HDAC inhibitor on TMZ sensitivity at clinically relevant doses (Bangert *et al.*, 2011; Van Nifterik *et al.*, 2012).

To imitate the treatment, which was shown to be beneficial in GBM patients receiving chemoradiation and an HDAC inhibitor, the influence of MS-275 on TMZ-induced apoptosis was analyzed when given concomitantly. In U87MG and LN308 glioblastoma cells, no effect of the double treatment was observed. However, the two PTEN-proficient cell lines that were already slightly sensitized by MS-275 pretreatment (LN229 and LN428) were highly sensitized by simultaneous treatment with MS-275 and TMZ showing a 2.5-8.5 fold increase in apoptosis. The response was dependent on MS-275 dose, though LN428 cells displayed a linear response, while LN229 cells did not (Figure 30). This might indicate different mechanisms of sensitization.

We showed in a time-dependent analysis of apoptosis induction in LN229 cells that cells start to undergo apoptosis 72 h after TMZ addition following combined treatment (Figure 31), again supporting a sensitization to O^6MeG based on the late induction of apoptosis as per the findings in melanoma. The observed MS-275-mediated downregulation of RAD51 in LN229 cells further affirms this assumption (Figure 32 a). Surprisingly, reduced RAD51 levels did not lead to increased sensitivity to PARP1 inhibition as expected due to synthetic lethal interaction of HR impairment and PARP1 inhibition (Figure 32 b). This means, that the protein reduction may not have a functional consequence in LN229 cells. This could be explained by the cell-cycle dependent regulation of RAD51 as G1/G0 cells do not express the protein (Chen *et al.*, 1997; Flygare *et al.*, 1996). In this situation, cells are not susceptible to replication-dependent toxins like PARP1-inhibitors. Indeed, we showed that MS-275 treatment accumulated cells in G1/G0 from 72 h (Figure 32 c) and was accompanied by proliferation attenuation (Figure 32 d), which provides evidence for a late cell cycle-dependent downregulation of RAD51 with no functional implication in replication-dependent stressors like PARP inhibitors or O^6MeG. Of importance, MS-275 treated cells still divided at least two more times, meaning that O^6MeG may still be responsible for induced apoptosis, though (lack of) repair of processing intermediates is not.

An HR-independent mechanism for MS-275-mediated sensitization to TMZ in LN229 cells may be explained by varying cell cycle distributions in combination treatment compared to single treatment. Here it was shown that combination of TMZ with MS-275 increased cells with a DNA content representative for late S-phase cells (48 h, 72 h, 96 h). In contrast, TMZ single treatment firstly induced an arrest at G2/M (>48 h) and later an increase in cells with a DNA content >4n (Figure 33), indicative of cells that underwent reduplication. Since the increase in reduplicated cells in TMZ single treatment correlates with the increase in Sub-G1 cells in combination treatment, we speculated that preventing reduplication and/or G2/M arrest might drive cells receiving combined treatment into apoptosis instead of reduplication.

As ATM and ATR kinases are principle regulators of cell cycle arrest in response to DNA damage, both were analyzed upon TMZ treatment alone and in combination with MS-275. This study demonstrates that DNA damage induced signaling is lost in combination of TMZ with HDAC inhibition, although it is present following TMZ alone (Figure 34). This means that TMZ single treated cells activate ATM and ATR, as well as downstream targets to initiate cell cycle arrest, specifically at G2/M, which are well-known events upon S_N1 methylating agents (Quiros *et al.*, 2010; Eich *et al.*, 2013; Stojic *et al.*, 2004; Caporali *et al.*, 2004). An elongation of G2-phase is a prerequisite for re-replication. A G2/M-arrest is shown in our data by an increase of 4n cells during TMZ treatment (Figure 33). It is known that a subsequent mitosis can be prevented by sustained ATM/ATR activation and its downstream factors CHK1/CHK2, which inactivate cdc25 so that CDK1/Cyclin B is not activated and mitosis not initiated. This was shown to occur in response to the radiomimetic drugs Bleomycin and Zeocin, as well as upon telomeric ATR/ATM activation

(Nakayama 2009, Davoli 2010). Despite a sustained G2/M arrest, cells can degrade Geminin, a protein which blocks replication by inactivating the origin licenser Cdt1 and that is degraded in late mitosis during the normal cell cycle. Therefore, cells that are arrested in G2 long enough for Geminin degradation to occur, replicate DNA in the absence of mitosis; leading to polyploid cells (Nakayama *et al.*, 2009; Davoli *et al.*, 2010). Our observation of increasing numbers of polyploid cells upon TMZ treatment supports a similar mechanism in this test system, although this was not tested. Notably, geminin depletion-induced over-replication is independent of p53 status (Zhu *et al.*, 2004) and could apply to the responder cell lines LN229 (p53 proficient) and LN428 (*TP53* mt).

In contrast, during combination treatment, neither ATM/ATR nor their downstream targets CHK1/CHK2 are activated, which might result in an impaired G2/M block. Cells would then enter mitosis bearing DNA damage, which could drive them into mitotic catastrophe. In fact, DNA damage was shown to induce mitotic catastrophe in the absence of CHK activation. Mitotic catastrophe is a type of cell death which displays features of apoptosis like phosphatidylserine exposure and DNA fragmentation (Kimura *et al.*, 2013; Castedo *et al.*, 2004), which would be detected in our apoptosis assays. Another observation substantiates the hypothesis of mitotic catastrophe cell death in co-treated cells: from 48 h post-treatment, co-treated cells show an increase of cells with a DNA content between 2n and 4n. These are not necessarily S-phase cells, since death related DNA degradation likewise generates intermediates with a comparable DNA content.

A reduction of CHK1 and/or CHK2 on protein level by HDAC inhibition has already been published, though their activation upon DNA damage and HDAC inhibition has not been analyzed (Brazelle *et al.*, 2010; Cornago *et al.*, 2014). In the case of CHK1, we found a low protein level but a high phosphorylation status 96 h after TMZ, whereas the combination treatment resulted in low protein and low activation (Figure 34). Therefore, HDAC inhibition may target the phosphorylation of checkpoint proteins. This is further supported by the finding that the upstream ATM kinase is also activated in TMZ single treatment but not in combination with MS-275.

A further question remains: what is the fate of endoreplicated cells in TMZ single treatment? Polyploidy is linked to senescence (Wagner *et al.*, 2001; Yang *et al.*, 2007), a state of cellular quiescence that can be induced by sustained damage signaling leading to expression of CDK inhibitors $p21^{Cip1/Waf1}$ or $p16^{INK4a}$. It is likely that polyploid cells, resulting from TMZ treatment alone enter a state of senescence as $p21^{Cip1/Waf1}$ was shown to be induced following activation of ATM, CHK and consequently p53 stabilization (Figure 35). Additionally, senescence is a well described consequence of TMZ in glioblasatoma cells (Knizhnik *et al.*, 2013; Hirose *et al.*, 2001b). Senescence as an end point of therapy is rather disadvantageous, because cells with a senescent phenotype were shown to re-enter the cell cycle in absence of damage signaling instead of being arrested permanently (Wang *et al.*, 2013; d'Adda di Fagagna *et al.*, 2003; Davoli *et al.*, 2010).

These cells could potentially contribute to relapse (Elmore *et al.*, 2005; Roberson *et al.*, 2005). Secondly, cells that enter senescence upon DNA damage secrete cytokines like interleukin 6 which increase invasion and resistance to chemotherapeutics (Rodier *et al.*, 2009; Campisi, 2013). Since induction of senescence and mitotic catastrophe are mutually exclusive, elimination of cancer cells by mitotic catastrophe is more desirable.

In summary, we present a sensitization approach in a subset of glioblastoma cell lines that is based on HDAC inhibitor-mediated disruption of TMZ-induced ATM/ATR and subsequent CHK activation. This leads to a loss of G2/M arrest and entry into mitosis is unperturbed despite the presence of DNA damage, resulting in mitotic catastrophe and apoptosis (Figure 37).

Even though the presented data are in accordance with the proposed model, further analyses are required for confirmation. On the one hand, the presence/absence of G2/M blockage needs to be confirmed by molecular markers like CHK downstream targets and their phosphorylation status like cdc25C and Wee1. Both modulate CDK1, which is required for entry into mitosis. Phosphorylation by cdc25 activates CDK1 whereas dephosphorylation by Wee1 inactivates it (Reinhardt and Yaffe, 2009). Accordingly, analysis of the CDK1 activation status would likewise confirm G2/M arrest. On the other hand, initiation of mitotic catastrophe needs to be shown with indicators like cleavage of caspase-2. Furthermore, abolishment of TMZ induced ATM/ATR/CHK activation in the presence of MS-275 needs to be verified in further cell lines to exclude that this resistance mechanism is limited to LN229 and LN428 glioblastoma cell lines.

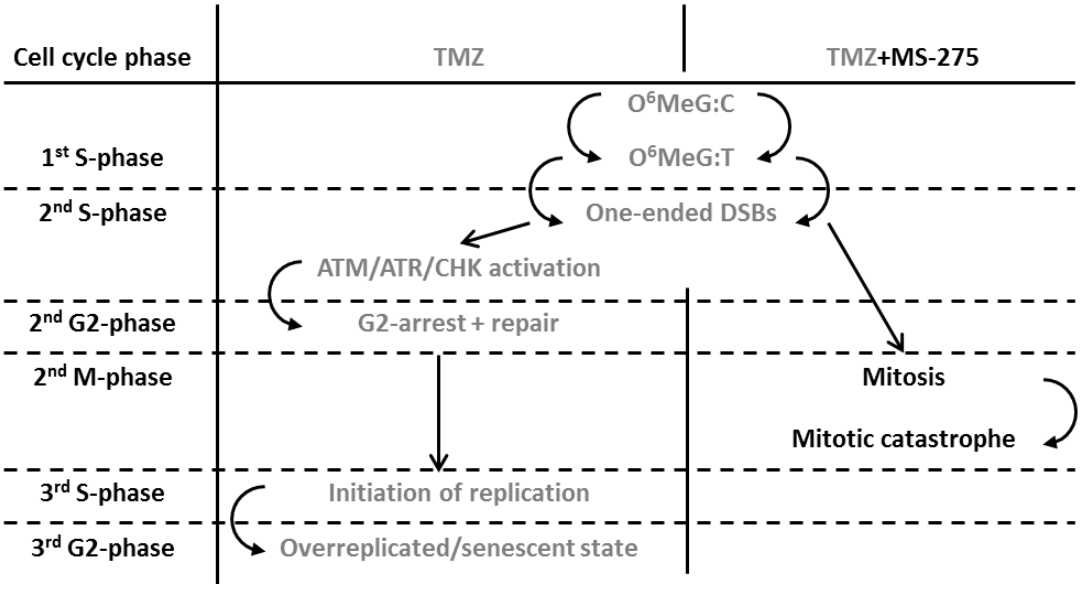

Figure 37 – Proposed mechanism of HDAC inhibitor-mediated sensitization to TMZ in glioblastoma cells.
TMZ-induced single-ended double strand breaks activate ATM/ATR and lead to a CHK-induced G2 arrest followed by endoreplication and senescence (left). CHK is not activated in the presence of MS-275 and cells bearing DNA damage proceed to mitosis where they undergo mitotic catastrophe (right).

5.3 Outlook

We have shown that HDAC inhibitors increase the apoptotic response to TMZ in melanoma cells by impairing HR, and in glioblastoma cells, by disrupting the DNA damage response. In fact, we further excluded that modification of damage signaling is involved in HDAC mediated sensitization in melanomas as well as RAD51 being involved in sensitization of GBM cells. This illustrates once again, that therapy resistance relies on a variety of mechanisms that not only differ between tumor entities but also between tumors of one entity as not all GBM cell lines responded to the treatment. Nevertheless, we found two resistance mechanisms that are targetable by HDAC inhibitors that provide a basis for further research, which could reveal insights into the underlying mechanisms of resistance. One such point is the observed downregulation of RAD51 and FANCD2, which was observed to occur at transcriptional level after HDAC inhibition in melanomas. Investigating how this is regulated for instance by modulation of transcription factors, promotor methylation or miRNAs might also reveal the difference why other tumor entities like glioblastoma do not respond to this pathway. Similarly, an investigation of the loss of ATM/ATR phosphorylation by HDAC inhibition could offer a prediction of the molecular requirements of responding and non-responding cells. The reduced ATM/ATR phosphorylation might arise from lower protein levels, impairment of autophosphorylation or increased dephosphorylation. Another question remaining is the impact of each HDAC (HDAC1, HDAC2, HDAC3) in the respective sensitization modes since effects seen with MS-275 only display the sum of inhibiting all three.

This work expands on the numerous therapy-improving features of HDAC inhibitors and transferred it to two remarkably therapy resistant tumor types, namely malignant melanoma and glioblastoma. Based on this and on the characteristic of HDAC inhibitors as being well tolerated, a therapy of alkylating agents with adjuvant HDAC inhibitor is a promising approach for improving the poor prognoses of patients suffering from GBM or metastatic melanoma.

6 References

Abbott, P. J. and Saffhill, R. (1979) DNA synthesis with methylated poly(dC-dG) templates. Evidence for a competitive nature to miscoding by O(6)-methylguanine. Biochim Biophys Acta, 562, 51-61.

Adair, J. E., Johnston, S. K., Mrugala, M. M., Beard, B. C., Guyman, L. A., Baldock, A. L., Bridge, C. A., Hawkins-Daarud, A., Gori, J. L., Born, D. E., Gonzalez-Cuyar, L. F., Silbergeld, D. L., Rockne, R. C., Storer, B. E., Rockhill, J. K., Swanson, K. R. and Kiem, H. P. (2014) Gene therapy enhances chemotherapy tolerance and efficacy in glioblastoma patients. J Clin Invest, 124, 4082-4092.

Adimoolam, S., Sirisawad, M., Chen, J., Thiemann, P., Ford, J. M. and Buggy, J. J. (2007) HDAC inhibitor PCI-24781 decreases RAD51 expression and inhibits homologous recombination. Proc Natl Acad Sci U S A, 104, 19482-19487.

Alao, J. P., Stavropoulou, A. V., Lam, E. W., Coombes, R. C. and Vigushin, D. M. (2006) Histone deacetylase inhibitor, trichostatin A induces ubiquitin-dependent cyclin D1 degradation in MCF-7 breast cancer cells. Mol Cancer, 5, 8.

Arnaudeau, C., Lundin, C. and Helleday, T. (2001) DNA double-strand breaks associated with replication forks are predominantly repaired by homologous recombination involving an exchange mechanism in mammalian cells. J Mol Biol, 307, 1235-1245.

Bakkenist, C. J. and Kastan, M. B. (2003) DNA damage activates ATM through intermolecular autophosphorylation and dimer dissociation. Nature, 421, 499-506.

Balch, C. M., Gershenwald, J. E., Soong, S. J., Thompson, J. F., Atkins, M. B., Byrd, D. R., Buzaid, A. C., Cochran, A. J., Coit, D. G., Ding, S., Eggermont, A. M., Flaherty, K. T., Gimotty, P. A., Kirkwood, J. M., McMasters, K. M., Mihm, M. C., Jr., Morton, D. L., Ross, M. I., Sober, A. J. and Sondak, V. K. (2009) Final version of 2009 AJCC melanoma staging and classification. J Clin Oncol, 27, 6199-6206.

Ball, H. L., Myers, J. S. and Cortez, D. (2005) ATRIP binding to replication protein A-single-stranded DNA promotes ATR-ATRIP localization but is dispensable for Chk1 phosphorylation. Mol Biol Cell, 16, 2372-2381.

Bangert, A., Hacker, S., Cristofanon, S., Debatin, K. M. and Fulda, S. (2011) Chemosensitization of glioblastoma cells by the histone deacetylase inhibitor MS275. Anticancer Drugs, 22, 494-499.

Banuelos, C. A., Banath, J. P., MacPhail, S. H., Zhao, J., Reitsema, T. and Olive, P. L. (2007) Radiosensitization by the histone deacetylase inhibitor PCI-24781. Clin Cancer Res, 13, 6816-6826.

Barckhausen, C. (2012) Mechanismen der Resistenz und Sensitivierung von menschlichen malignen Melanomzellen gegenüber DNA-alkylierenden Zytostatika. In Institute of Toxicology, Vol. PhD Johannes-Gutenberg University, Mainz.

Barckhausen, C., Roos, W. P., Naumann, S. C. and Kaina, B. (2014) Malignant melanoma cells acquire resistance to DNA interstrand cross-linking chemotherapeutics by p53-triggered upregulation of DDB2/XPC-mediated DNA repair. Oncogene, 33, 1964-1974.

Barker, C. A., Bishop, A. J., Chang, M., Beal, K. and Chan, T. A. (2013) Valproic acid use during radiation therapy for glioblastoma associated with improved survival. Int J Radiat Oncol Biol Phys, 86, 504-509.

Batista, L. F., Roos, W. P., Christmann, M., Menck, C. F. and Kaina, B. (2007) Differential sensitivity of malignant glioma cells to methylating and chloroethylating anticancer drugs: p53 determines the switch by regulating xpc, ddb2, and DNA double-strand breaks. Cancer Res, 67, 11886-11895.

Baumann, P. and West, S. C. (1998) Role of the human RAD51 protein in homologous recombination and double-stranded-break repair. Trends Biochem Sci, 23, 247-251.

Beck, B. D., Lee, S. S., Williamson, E., Hromas, R. A. and Lee, S. H. (2011) Biochemical characterization of metnase's endonuclease activity and its role in NHEJ repair. Biochemistry, 50, 4360-4370.

Beranek, D. T. (1990) Distribution of methyl and ethyl adducts following alkylation with monofunctional alkylating agents. Mutat Res, 231, 11-30.

Beucher, A., Birraux, J., Tchouandong, L., Barton, O., Shibata, A., Conrad, S., Goodarzi, A. A., Krempler, A., Jeggo, P. A. and Lobrich, M. (2009) ATM and Artemis promote homologous recombination of radiation-induced DNA double-strand breaks in G2. Embo J, 28, 3413-3427.

Bhaskara, S., Knutson, S. K., Jiang, G., Chandrasekharan, M. B., Wilson, A. J., Zheng, S., Yenamandra, A., Locke, K., Yuan, J. L., Bonine-Summers, A. R., Wells, C. E., Kaiser, J. F., Washington, M. K., Zhao, Z., Wagner, F. F., Sun, Z. W., Xia, F., Holson, E. B., Khabele, D. and Hiebert, S. W. (2010) Hdac3 is essential for the maintenance of chromatin structure and genome stability. Cancer Cell, 18, 436-447.

Bieliauskas, A. V. and Pflum, M. K. (2008) Isoform-selective histone deacetylase inhibitors. Chem Soc Rev, 37, 1402-1413.

Blattmann, C., Oertel, S., Ehemann, V., Thiemann, M., Huber, P. E., Bischof, M., Witt, O., Deubzer, H. E., Kulozik, A. E., Debus, J. and Weber, K. J. (2010) Enhancement of radiation response in osteosarcoma and rhabdomyosarcoma cell lines by histone deacetylase inhibition. Int J Radiat Oncol Biol Phys, 78, 237-245.

Bodell, W. J. (2009) DNA alkylation products formed by 1-(2-chloroethyl)-1-nitrosourea as molecular dosimeters of therapeutic response. J Neurooncol, 91, 257-264.

Bodell, W. J., Aida, T., Berger, M. S. and Rosenblum, M. L. (1986) Increased repair of O6-alkylguanine DNA adducts in glioma-derived human cells resistant to the cytotoxic and cytogenetic effects of 1,3-bis(2-chloroethyl)-1-nitrosourea. Carcinogenesis, 7, 879-883.

Bolden, J. E., Shi, W., Jankowski, K., Kan, C. Y., Cluse, L., Martin, B. P., MacKenzie, K. L., Smyth, G. K. and Johnstone, R. W. (2013) HDAC inhibitors induce tumor-cell-selective pro-apoptotic transcriptional responses. Cell Death Dis, 4, e519.

Bonner, W. M., Redon, C. E., Dickey, J. S., Nakamura, A. J., Sedelnikova, O. A., Solier, S. and Pommier, Y. (2008) GammaH2AX and cancer. Nat Rev Cancer, 8, 957-967.

Bradford, M. M. (1976) A rapid and sensitive method for the quantitation of microgram quantities of protein utilizing the principle of protein-dye binding. Anal Biochem, 72, 248-254.

Bradner, J. E., Mak, R., Tanguturi, S. K., Mazitschek, R., Haggarty, S. J., Ross, K., Chang, C. Y., Bosco, J., West, N., Morse, E., Lin, K., Shen, J. P., Kwiatkowski, N. P., Gheldof, N., Dekker, J., DeAngelo, D. J., Carr, S. A., Schreiber, S. L., Golub, T. R. and Ebert, B. L. (2010) Chemical genetic strategy identifies histone deacetylase 1 (HDAC1) and HDAC2 as therapeutic targets in sickle cell disease. Proc Natl Acad Sci U S A, 107, 12617-12622.

Branch, P., Aquilina, G., Bignami, M. and Karran, P. (1993) Defective mismatch binding and a mutator phenotype in cells tolerant to DNA damage. Nature, 362, 652-654.

Brazelle, W., Kreahling, J. M., Gemmer, J., Ma, Y., Cress, W. D., Haura, E. and Altiok, S. (2010) Histone deacetylase inhibitors downregulate checkpoint kinase 1 expression to induce cell death in non-small cell lung cancer cells. PLoS One, 5, e14335.

Brennan, C. W., Verhaak, R. G., McKenna, A., Campos, B., Noushmehr, H., Salama, S. R., Zheng, S., Chakravarty, D., Sanborn, J. Z., Berman, S. H., Beroukhim, R., Bernard, B., Wu, C. J., Genovese, G., Shmulevich, I., Barnholtz-Sloan, J., Zou, L., Vegesna, R., Shukla, S. A., Ciriello, G., Yung, W. K., Zhang, W., Sougnez, C., Mikkelsen, T., Aldape, K., Bigner, D. D., Van Meir, E. G., Prados, M., Sloan, A., Black, K. L., Eschbacher, J., Finocchiaro, G., Friedman, W., Andrews, D. W., Guha, A., Iacocca, M., O'Neill, B. P., Foltz, G., Myers, J., Weisenberger, D. J., Penny, R., Kucherlapati, R., Perou, C. M., Hayes, D. N., Gibbs, R., Marra, M., Mills, G. B., Lander, E., Spellman, P., Wilson, R., Sander, C., Weinstein, J., Meyerson, M., Gabriel, S., Laird, P. W., Haussler, D., Getz, G. and Chin, L. (2013) The somatic genomic landscape of glioblastoma. Cell, 155, 462-477.

Brenner, M. and Hearing, V. J. (2008) The protective role of melanin against UV damage in human skin. Photochem Photobiol, 84, 539-549.

Bressi, J. C., Jennings, A. J., Skene, R., Wu, Y., Melkus, R., De Jong, R., O'Connell, S., Grimshaw, C. E., Navre, M. and Gangloff, A. R. (2010) Exploration of the HDAC2 foot pocket: Synthesis and SAR of substituted N-(2-aminophenyl)benzamides. Bioorg Med Chem Lett, 20, 3142-3145.

Bronstein, S. M., Skopek, T. R. and Swenberg, J. A. (1992) Efficient repair of O6-ethylguanine, but not O4-ethylthymine or O2-ethylthymine, is dependent upon O6-alkylguanine-DNA alkyltransferase and nucleotide excision repair activities in human cells. Cancer Res, 52, 2008-2011.

Bug, G., Ritter, M., Wassmann, B., Schoch, C., Heinzel, T., Schwarz, K., Romanski, A., Kramer, O. H., Kampfmann, M., Hoelzer, D., Neubauer, A., Ruthardt, M. and Ottmann, O. G. (2005) Clinical trial of valproic acid and all-trans retinoic acid in patients with poor-risk acute myeloid leukemia. Cancer, 104, 2717-2725.

Caldecott, K. W. (2007) Mammalian single-strand break repair: mechanisms and links with chromatin. DNA Repair (Amst), 6, 443-453.

Campisi, J. (2013) Aging, cellular senescence, and cancer. Annu Rev Physiol, 75, 685-705.

Campisi, J. and d'Adda di Fagagna, F. (2007) Cellular senescence: when bad things happen to good cells. Nat Rev Mol Cell Biol, 8, 729-740.

Caporali, S., Falcinelli, S., Starace, G., Russo, M. T., Bonmassar, E., Jiricny, J. and D'Atri, S. (2004) DNA damage induced by temozolomide signals to both ATM and ATR: role of the mismatch repair system. Mol Pharmacol, 66, 478-491.

Castedo, M., Perfettini, J. L., Roumier, T., Valent, A., Raslova, H., Yakushijin, K., Horne, D., Feunteun, J., Lenoir, G., Medema, R., Vainchenker, W. and Kroemer, G. (2004) Mitotic catastrophe constitutes a special case of apoptosis whose suppression entails aneuploidy. Oncogene, 23, 4362-4370.

Cazzalini, O., Sommatis, S., Tillhon, M., Dutto, I., Bachi, A., Rapp, A., Nardo, T., Scovassi, A. I., Necchi, D., Cardoso, M. C., Stivala, L. A. and Prosperi, E. (2014) CBP and p300 acetylate PCNA to link its degradation with nucleotide excision repair synthesis. Nucleic Acids Res, 42, 8433-8448.

Cha, T. L., Chuang, M. J., Wu, S. T., Sun, G. H., Chang, S. Y., Yu, D. S., Huang, S. M., Huan, S. K., Cheng, T. C., Chen, T. T., Fan, P. L. and Hsiao, P. W. (2009) Dual degradation of aurora A and B kinases by the histone deacetylase inhibitor LBH589 induces G2-M arrest and apoptosis of renal cancer cells. Clin Cancer Res, 15, 840-850.

Chang, J., Varghese, D. S., Gillam, M. C., Peyton, M., Modi, B., Schiltz, R. L., Girard, L. and Martinez, E. D. (2012) Differential response of cancer cells to HDAC inhibitors trichostatin A and depsipeptide. Br J Cancer, 106, 116-125.

Chapman, P. B., Hauschild, A., Robert, C., Haanen, J. B., Ascierto, P., Larkin, J., Dummer, R., Garbe, C., Testori, A., Maio, M., Hogg, D., Lorigan, P., Lebbe, C., Jouary, T., Schadendorf, D., Ribas, A., O'Day, S. J., Sosman, J. A., Kirkwood, J. M., Eggermont, A. M., Dreno, B., Nolop, K., Li, J., Nelson, B., Hou, J., Lee, R. J., Flaherty, K. T. and McArthur, G. A. (2011) Improved survival with vemurafenib in melanoma with BRAF V600E mutation. N Engl J Med, 364, 2507-2516.

Chen, C. C., Carson, J. J., Feser, J., Tamburini, B., Zabaronick, S., Linger, J. and Tyler, J. K. (2008) Acetylated lysine 56 on histone H3 drives chromatin assembly after repair and signals for the completion of repair. Cell, 134, 231-243.

Chen, C. C., Taniguchi, T. and D'Andrea, A. (2007a) The Fanconi anemia (FA) pathway confers glioma resistance to DNA alkylating agents. J Mol Med (Berl), 85, 497-509.

Chen, C. S., Wang, Y. C., Yang, H. C., Huang, P. H., Kulp, S. K., Yang, C. C., Lu, Y. S., Matsuyama, S., Chen, C. Y. and Chen, C. S. (2007b) Histone deacetylase inhibitors sensitize prostate cancer cells to agents that produce DNA double-strand breaks by targeting Ku70 acetylation. Cancer Res, 67, 5318-5327.

Chen, F., Nastasi, A., Shen, Z., Brenneman, M., Crissman, H. and Chen, D. J. (1997) Cell cycle-dependent protein expression of mammalian homologs of yeast DNA double-strand break repair genes Rad51 and Rad52. Mutat Res, 384, 205-211.

Chinnaiyan, P., Vallabhaneni, G., Armstrong, E., Huang, S. M. and Harari, P. M. (2005) Modulation of radiation response by histone deacetylase inhibition. Int J Radiat Oncol Biol Phys, 62, 223-229.

Chinot, O. L., Wick, W., Mason, W., Henriksson, R., Saran, F., Nishikawa, R., Carpentier, A. F., Hoang-Xuan, K., Kavan, P., Cernea, D., Brandes, A. A., Hilton, M., Abrey, L. and Cloughesy, T. (2014) Bevacizumab plus radiotherapy-temozolomide for newly diagnosed glioblastoma. N Engl J Med, 370, 709-722.

Choi, J. Y., Chowdhury, G., Zang, H., Angel, K. C., Vu, C. C., Peterson, L. A. and Guengerich, F. P. (2006) Translesion synthesis across O6-alkylguanine DNA adducts by recombinant human DNA polymerases. J Biol Chem, 281, 38244-38256.

Choudhary, C., Kumar, C., Gnad, F., Nielsen, M. L., Rehman, M., Walther, T. C., Olsen, J. V. and Mann, M. (2009) Lysine acetylation targets protein complexes and co-regulates major cellular functions. Science, 325, 834-840.

Christmann, M., Verbeek, B., Roos, W. P. and Kaina, B. (2011) O(6)-Methylguanine-DNA methyltransferase (MGMT) in normal tissues and tumors: enzyme activity, promoter methylation and immunohistochemistry. Biochim Biophys Acta, 1816, 179-190.

Ciccia, A. and Elledge, S. J. (2010) The DNA damage response: making it safe to play with knives. Mol Cell, 40, 179-204.

Cichorek, M., Wachulska, M., Stasiewicz, A. and Tyminska, A. (2013) Skin melanocytes: biology and development. Postepy Dermatol Alergol, 30, 30-41.

Cimprich, K. A. and Cortez, D. (2008) ATR: an essential regulator of genome integrity. Nat Rev Mol Cell Biol, 9, 616-627.

Clauson, C., Scharer, O. D. and Niedernhofer, L. (2013) Advances in understanding the complex mechanisms of DNA interstrand cross-link repair. Cold Spring Harb Perspect Biol, 5, a012732.

Clement, F. C., Camenisch, U., Fei, J., Kaczmarek, N., Mathieu, N. and Naegeli, H. (2010) Dynamic two-stage mechanism of versatile DNA damage recognition by xeroderma pigmentosum group C protein. Mutat Res, 685, 21-28.

Codogno, P. and Meijer, A. J. (2005) Autophagy and signaling: their role in cell survival and cell death. Cell Death Differ, 12 Suppl 2, 1509-1518.

Cohen, H. Y., Lavu, S., Bitterman, K. J., Hekking, B., Imahiyerobo, T. A., Miller, C., Frye, R., Ploegh, H., Kessler, B. M. and Sinclair, D. A. (2004) Acetylation of the C terminus of Ku70 by CBP and PCAF controls Bax-mediated apoptosis. Mol Cell, 13, 627-638.

Cornago, M., Garcia-Alberich, C., Blasco-Angulo, N., Vall-Llaura, N., Nager, M., Herreros, J., Comella, J. X., Sanchis, D. and Llovera, M. (2014) Histone deacetylase inhibitors promote glioma cell death by G2 checkpoint abrogation leading to mitotic catastrophe. Cell Death Dis, 5, e1435.

Crespo, I., Vital, A. L., Gonzalez-Tablas, M., Patino Mdel, C., Otero, A., Lopes, M. C., de Oliveira, C., Domingues, P., Orfao, A. and Tabernero, M. D. (2015) Molecular and Genomic Alterations in Glioblastoma Multiforme. Am J Pathol, 185, 1820-1833.

d'Adda di Fagagna, F. (2008) Living on a break: cellular senescence as a DNA-damage response. Nat Rev Cancer, 8, 512-522.

d'Adda di Fagagna, F., Reaper, P. M., Clay-Farrace, L., Fiegler, H., Carr, P., Von Zglinicki, T., Saretzki, G., Carter, N. P. and Jackson, S. P. (2003) A DNA damage checkpoint response in telomere-initiated senescence. Nature, 426, 194-198.

Das, C., Lucia, M. S., Hansen, K. C. and Tyler, J. K. (2009) CBP/p300-mediated acetylation of histone H3 on lysine 56. Nature, 459, 113-117.

Das, C. M., Aguilera, D., Vasquez, H., Prasad, P., Zhang, M., Wolff, J. E. and Gopalakrishnan, V. (2007) Valproic acid induces p21 and topoisomerase-II (alpha/beta) expression and synergistically enhances etoposide cytotoxicity in human glioblastoma cell lines. J Neurooncol, 85, 159-170.

Davis, A. J., Chen, B. P. and Chen, D. J. (2014) DNA-PK: a dynamic enzyme in a versatile DSB repair pathway. DNA Repair (Amst), 17, 21-29.

Davoli, T., Denchi, E. L. and de Lange, T. (2010) Persistent telomere damage induces bypass of mitosis and tetraploidy. Cell, 141, 81-93.

Dawson, M. A. and Kouzarides, T. (2012) Cancer epigenetics: from mechanism to therapy. Cell, 150, 12-27.

De Bont, R. and van Larebeke, N. (2004) Endogenous DNA damage in humans: a review of quantitative data. Mutagenesis, 19, 169-185.

Deans, A. J. and West, S. C. (2011) DNA interstrand crosslink repair and cancer. Nat Rev Cancer, 11, 467-480.

Dovey, O. M., Foster, C. T., Conte, N., Edwards, S. A., Edwards, J. M., Singh, R., Vassiliou, G., Bradley, A. and Cowley, S. M. (2013) Histone deacetylase 1 and 2 are essential for normal T-cell development and genomic stability in mice. Blood, 121, 1335-1344.

Downs, J. A. and Jackson, S. P. (2004) A means to a DNA end: the many roles of Ku. Nat Rev Mol Cell Biol, 5, 367-378.

Drablos, F., Feyzi, E., Aas, P. A., Vaagbo, C. B., Kavli, B., Bratlie, M. S., Pena-Diaz, J., Otterlei, M., Slupphaug, G. and Krokan, H. E. (2004) Alkylation damage in DNA and RNA--repair mechanisms and medical significance. DNA Repair (Amst), 3, 1389-1407.

Duckett, D. R., Drummond, J. T., Murchie, A. I., Reardon, J. T., Sancar, A., Lilley, D. M. and Modrich, P. (1996) Human MutSalpha recognizes damaged DNA base pairs containing O6-methylguanine, O4-methylthymine, or the cisplatin-d(GpG) adduct. Proc Natl Acad Sci U S A, 93, 6443-6447.

Dummer, R., Hauschild, A., Guggenheim, M., Keilholz, U. and Pentheroudakis, G. (2012) Cutaneous melanoma: ESMO Clinical Practice Guidelines for diagnosis, treatment and follow-up. Ann Oncol, 23 Suppl 7, vii86-91.

Eich, M., Roos, W. P., Nikolova, T. and Kaina, B. (2013) Contribution of ATM and ATR to the resistance of glioblastoma and malignant melanoma cells to the methylating anticancer drug temozolomide. Mol Cancer Ther, 12, 2529-2540.

Elmore, L. W., Di, X., Dumur, C., Holt, S. E. and Gewirtz, D. A. (2005) Evasion of a single-step, chemotherapy-induced senescence in breast cancer cells: implications for treatment response. Clin Cancer Res, 11, 2637-2643.

Elmore, S. (2007) Apoptosis: a review of programmed cell death. Toxicol Pathol, 35, 495-516.

Enari, M., Sakahira, H., Yokoyama, H., Okawa, K., Iwamatsu, A. and Nagata, S. (1998) A caspase-activated DNase that degrades DNA during apoptosis, and its inhibitor ICAD. Nature, 391, 43-50.

Engelward, B. P., Allan, J. M., Dreslin, A. J., Kelly, J. D., Wu, M. M., Gold, B. and Samson, L. D. (1998) A chemical and genetic approach together define the biological consequences of 3-methyladenine lesions in the mammalian genome. J Biol Chem, 273, 5412-5418.

Enoiu, M., Jiricny, J. and Scharer, O. D. (2012) Repair of cisplatin-induced DNA interstrand crosslinks by a replication-independent pathway involving transcription-coupled repair and translesion synthesis. Nucleic Acids Res, 40, 8953-8964.

Facchetti, F., Previdi, S., Ballarini, M., Minucci, S., Perego, P. and La Porta, C. A. (2004) Modulation of pro- and anti-apoptotic factors in human melanoma cells exposed to histone deacetylase inhibitors. Apoptosis, 9, 573-582.

Falkenberg, K. J. and Johnstone, R. W. (2014) Histone deacetylases and their inhibitors in cancer, neurological diseases and immune disorders. Nat Rev Drug Discov, 13, 673-691.

Fantin, V. R. and Richon, V. M. (2007) Mechanisms of resistance to histone deacetylase inhibitors and their therapeutic implications. Clin Cancer Res, 13, 7237-7242.

Finnin, M. S., Donigian, J. R., Cohen, A., Richon, V. M., Rifkind, R. A., Marks, P. A., Breslow, R. and Pavletich, N. P. (1999) Structures of a histone deacetylase homologue bound to the TSA and SAHA inhibitors. Nature, 401, 188-193.

Finzer, P., Kuntzen, C., Soto, U., zur Hausen, H. and Rosl, F. (2001) Inhibitors of histone deacetylase arrest cell cycle and induce apoptosis in cervical carcinoma cells circumventing human papillomavirus oncogene expression. Oncogene, 20, 4768-4776.

Fishel, R., Ewel, A. and Lescoe, M. K. (1994) Purified human MSH2 protein binds to DNA containing mismatched nucleotides. Cancer Res, 54, 5539-5542.

Flaherty, K. T., Infante, J. R., Daud, A., Gonzalez, R., Kefford, R. F., Sosman, J., Hamid, O., Schuchter, L., Cebon, J., Ibrahim, N., Kudchadkar, R., Burris, H. A., 3rd, Falchook, G., Algazi, A., Lewis, K., Long, G. V., Puzanov, I., Lebowitz, P., Singh, A., Little, S., Sun, P., Allred, A., Ouellet, D., Kim, K. B., Patel, K. and Weber, J. (2012) Combined BRAF and MEK inhibition in melanoma with BRAF V600 mutations. N Engl J Med, 367, 1694-1703.

Flygare, J., Benson, F. and Hellgren, D. (1996) Expression of the human RAD51 gene during the cell cycle in primary human peripheral blood lymphocytes. Biochim Biophys Acta, 1312, 231-236.

Fortini, P. and Dogliotti, E. (2007) Base damage and single-strand break repair: mechanisms and functional significance of short- and long-patch repair subpathways. DNA Repair (Amst), 6, 398-409.

Fu, D., Calvo, J. A. and Samson, L. D. (2012) Balancing repair and tolerance of DNA damage caused by alkylating agents. Nat Rev Cancer, 12, 104-120.

Fuchs, Y. and Steller, H. (2015) Live to die another way: modes of programmed cell death and the signals emanating from dying cells. Nat Rev Mol Cell Biol, 16, 329-344.

Gaddameedhi, S., Kemp, M. G., Reardon, J. T., Shields, J. M., Smith-Roe, S. L., Kaufmann, W. K. and Sancar, A. (2010) Similar nucleotide excision repair capacity in melanocytes and melanoma cells. Cancer Res, 70, 4922-4930.

Galloway, S. M., Greenwood, S. K., Hill, R. B., Bradt, C. I. and Bean, C. L. (1995) A role for mismatch repair in production of chromosome aberrations by methylating agents in human cells. Mutat Res, 346, 231-245.

Galluzzi, L. and Kroemer, G. (2008) Necroptosis: a specialized pathway of programmed necrosis. Cell, 135, 1161-1163.

Geng, L., Cuneo, K. C., Fu, A., Tu, T., Atadja, P. W. and Hallahan, D. E. (2006) Histone deacetylase (HDAC) inhibitor LBH589 increases duration of gamma-H2AX foci and confines HDAC4 to the cytoplasm in irradiated non-small cell lung cancer. Cancer Res, 66, 11298-11304.

Genschel, J., Littman, S. J., Drummond, J. T. and Modrich, P. (1998) Isolation of MutSbeta from human cells and comparison of the mismatch repair specificities of MutSbeta and MutSalpha. J Biol Chem, 273, 19895-19901.

Gillespie, S., Borrow, J., Zhang, X. D. and Hersey, P. (2006) Bim plays a crucial role in synergistic induction of apoptosis by the histone deacetylase inhibitor SBHA and TRAIL in melanoma cells. Apoptosis, 11, 2251-2265.

Goode, E. L., Ulrich, C. M. and Potter, J. D. (2002) Polymorphisms in DNA repair genes and associations with cancer risk. Cancer Epidemiol Biomarkers Prev, 11, 1513-1530.

Göttlicher, M., Minucci, S., Zhu, P., Kramer, O. H., Schimpf, A., Giavara, S., Sleeman, J. P., Lo Coco, F., Nervi, C., Pelicci, P. G. and Heinzel, T. (2001) Valproic acid defines a novel class of HDAC inhibitors inducing differentiation of transformed cells. Embo J, 20, 6969-6978.

Gregoretti, I. V., Lee, Y. M. and Goodson, H. V. (2004) Molecular evolution of the histone deacetylase family: functional implications of phylogenetic analysis. J Mol Biol, 338, 17-31.

Halkidou, K., Gaughan, L., Cook, S., Leung, H. Y., Neal, D. E. and Robson, C. N. (2004) Upregulation and nuclear recruitment of HDAC1 in hormone refractory prostate cancer. Prostate, 59, 177-189.

Hanada, K., Budzowska, M., Davies, S. L., van Drunen, E., Onizawa, H., Beverloo, H. B., Maas, A., Essers, J., Hickson, I. D. and Kanaar, R. (2007) The structure-specific endonuclease Mus81 contributes to replication restart by generating double-strand DNA breaks. Nat Struct Mol Biol, 14, 1096-1104.

Hanahan, D. and Weinberg, R. A. (2011) Hallmarks of cancer: the next generation. Cell, 144, 646-674.

Hasan, S., El-Andaloussi, N., Hardeland, U., Hassa, P. O., Burki, C., Imhof, R., Schar, P. and Hottiger, M. O. (2002) Acetylation regulates the DNA end-trimming activity of DNA polymerase beta. Mol Cell, 10, 1213-1222.

Hasan, S., Hassa, P. O., Imhof, R. and Hottiger, M. O. (2001) Transcription coactivator p300 binds PCNA and may have a role in DNA repair synthesis. Nature, 410, 387-391.

Hassel, J. C., Sucker, A., Edler, L., Kurzen, H., Moll, I., Stresemann, C., Spieth, K., Mauch, C., Rass, K., Dummer, R. and Schadendorf, D. (2010) MGMT gene promoter methylation correlates with tolerance of temozolomide treatment in melanoma but not with clinical outcome. Br J Cancer, 103, 820-826.

Hauschild, A., Grob, J. J., Demidov, L. V., Jouary, T., Gutzmer, R., Millward, M., Rutkowski, P., Blank, C. U., Miller, W. H., Jr., Kaempgen, E., Martin-Algarra, S., Karaszewska, B., Mauch, C., Chiarion-Sileni, V., Martin, A. M., Swann, S., Haney, P., Mirakhur, B., Guckert, M. E., Goodman, V. and Chapman, P. B. (2012) Dabrafenib in BRAF-mutated

metastatic melanoma: a multicentre, open-label, phase 3 randomised controlled trial. Lancet, 380, 358-365.

Hauschild, A., Trefzer, U., Garbe, C., Kaehler, K. C., Ugurel, S., Kiecker, F., Eigentler, T., Krissel, H., Schott, A. and Schadendorf, D. (2008) Multicenter phase II trial of the histone deacetylase inhibitor pyridylmethyl-N-{4-[(2-aminophenyl)-carbamoyl]-benzyl}-carbamate in pretreated metastatic melanoma. Melanoma Res, 18, 274-278.

Hayakawa, T. and Nakayama, J. (2011) Physiological roles of class I HDAC complex and histone demethylase. J Biomed Biotechnol, 2011, 129383.

He, C. and Klionsky, D. J. (2009) Regulation mechanisms and signaling pathways of autophagy. Annu Rev Genet, 43, 67-93.

Heideman, M. R., Wilting, R. H., Yanover, E., Velds, A., de Jong, J., Kerkhoven, R. M., Jacobs, H., Wessels, L. F. and Dannenberg, J. H. (2013) Dosage-dependent tumor suppression by histone deacetylases 1 and 2 through regulation of c-Myc collaborating genes and p53 function. Blood, 121, 2038-2050.

Helleday, T. (2011) The underlying mechanism for the PARP and BRCA synthetic lethality: clearing up the misunderstandings. Mol Oncol, 5, 387-393.

Helleday, T., Petermann, E., Lundin, C., Hodgson, B. and Sharma, R. A. (2008) DNA repair pathways as targets for cancer therapy. Nat Rev Cancer, 8, 193-204.

Hickman, M. J. and Samson, L. D. (1999) Role of DNA mismatch repair and p53 in signaling induction of apoptosis by alkylating agents. Proc Natl Acad Sci U S A, 96, 10764-10769.

Hirose, Y., Berger, M. S. and Pieper, R. O. (2001a) Abrogation of the Chk1-mediated G(2) checkpoint pathway potentiates temozolomide-induced toxicity in a p53-independent manner in human glioblastoma cells. Cancer Res, 61, 5843-5849.

Hirose, Y., Berger, M. S. and Pieper, R. O. (2001b) p53 effects both the duration of G2/M arrest and the fate of temozolomide-treated human glioblastoma cells. Cancer Res, 61, 1957-1963.

Hodi, F. S., O'Day, S. J., McDermott, D. F., Weber, R. W., Sosman, J. A., Haanen, J. B., Gonzalez, R., Robert, C., Schadendorf, D., Hassel, J. C., Akerley, W., van den Eertwegh, A. J., Lutzky, J., Lorigan, P., Vaubel, J. M., Linette, G. P., Hogg, D., Ottensmeier, C. H., Lebbe, C., Peschel, C., Quirt, I., Clark, J. I., Wolchok, J. D., Weber, J. S., Tian, J., Yellin, M. J., Nichol, G. M., Hoos, A. and Urba, W. J. (2010) Improved survival with ipilimumab in patients with metastatic melanoma. N Engl J Med, 363, 711-723.

Hodis, E., Watson, I. R., Kryukov, G. V., Arold, S. T., Imielinski, M., Theurillat, J. P., Nickerson, E., Auclair, D., Li, L., Place, C., Dicara, D., Ramos, A. H., Lawrence, M. S., Cibulskis, K., Sivachenko, A., Voet, D., Saksena, G., Stransky, N., Onofrio, R. C., Winckler, W., Ardlie, K., Wagle, N., Wargo, J., Chong, K., Morton, D. L., Stemke-Hale, K., Chen, G., Noble, M., Meyerson, M., Ladbury, J. E., Davies, M. A., Gershenwald, J. E., Wagner, S. N., Hoon, D. S., Schadendorf, D., Lander, E. S., Gabriel, S. B., Getz, G., Garraway, L. A. and Chin, L. (2012) A landscape of driver mutations in melanoma. Cell, 150, 251-263.

Hong, L., Schroth, G. P., Matthews, H. R., Yau, P. and Bradbury, E. M. (1993) Studies of the DNA binding properties of histone H4 amino terminus. Thermal denaturation studies reveal that acetylation markedly reduces the binding constant of the H4 "tail" to DNA. J Biol Chem, 268, 305-314.

http://clinicaltrials.gov/ (2015) National Library of Medicine (US).

Hu, J. and Colburn, N. H. (2005) Histone deacetylase inhibition down-regulates cyclin D1 transcription by inhibiting nuclear factor-kappaB/p65 DNA binding. Mol Cancer Res, 3, 100-109.

Huang, B. H., Laban, M., Leung, C. H., Lee, L., Lee, C. K., Salto-Tellez, M., Raju, G. C. and Hooi, S. C. (2005) Inhibition of histone deacetylase 2 increases apoptosis and p21Cip1/WAF1 expression, independent of histone deacetylase 1. Cell Death Differ, 12, 395-404.

Huang, L., Sowa, Y., Sakai, T. and Pardee, A. B. (2000) Activation of the p21WAF1/CIP1 promoter independent of p53 by the histone deacetylase inhibitor suberoylanilide hydroxamic acid (SAHA) through the Sp1 sites. Oncogene, 19, 5712-5719.

Hussain, S., Wilson, J. B., Medhurst, A. L., Hejna, J., Witt, E., Ananth, S., Davies, A., Masson, J. Y., Moses, R., West, S. C., de Winter, J. P., Ashworth, A., Jones, N. J. and Mathew, C. G.

(2004) Direct interaction of FANCD2 with BRCA2 in DNA damage response pathways. Hum Mol Genet, 13, 1241-1248.

Huynh, M. L., Fadok, V. A. and Henson, P. M. (2002) Phosphatidylserine-dependent ingestion of apoptotic cells promotes TGF-beta1 secretion and the resolution of inflammation. J Clin Invest, 109, 41-50.

Insinga, A., Monestiroli, S., Ronzoni, S., Gelmetti, V., Marchesi, F., Viale, A., Altucci, L., Nervi, C., Minucci, S. and Pelicci, P. G. (2005) Inhibitors of histone deacetylases induce tumor-selective apoptosis through activation of the death receptor pathway. Nat Med, 11, 71-76.

Ishii, N., Maier, D., Merlo, A., Tada, M., Sawamura, Y., Diserens, A. C. and Van Meir, E. G. (1999) Frequent co-alterations of TP53, p16/CDKN2A, p14ARF, PTEN tumor suppressor genes in human glioma cell lines. Brain Pathol, 9, 469-479.

Jasin, M. and Rothstein, R. (2013) Repair of strand breaks by homologous recombination. Cold Spring Harb Perspect Biol, 5, a012740.

Javanmard, S., Loktionova, N. A., Fang, Q., Pauly, G. T., Pegg, A. E. and Moschel, R. C. (2007) Inactivation of O(6)-alkylguanine-DNA alkyltransferase by folate esters of O(6)-benzyl-2'-deoxyguanosine and of O(6)-[4-(hydroxymethyl)benzyl]guanine. J Med Chem, 50, 5193-5201.

Ji, Z., Njauw, C. N., Taylor, M., Neel, V., Flaherty, K. T. and Tsao, H. (2012) p53 rescue through HDM2 antagonism suppresses melanoma growth and potentiates MEK inhibition. J Invest Dermatol, 132, 356-364.

Jiricny, J. (2013) Postreplicative mismatch repair. Cold Spring Harb Perspect Biol, 5, a012633.

Jones, J., Juengel, E., Mickuckyte, A., Hudak, L., Wedel, S., Jonas, D. and Blaheta, R. A. (2009) The histone deacetylase inhibitor valproic acid alters growth properties of renal cell carcinoma in vitro and in vivo. J Cell Mol Med, 13, 2376-2385.

Juan, L. J., Shia, W. J., Chen, M. H., Yang, W. M., Seto, E., Lin, Y. S. and Wu, C. W. (2000) Histone deacetylases specifically down-regulate p53-dependent gene activation. J Biol Chem, 275, 20436-20443.

Kaatsch, P., Spix, C., Hentschel, S., Katalinic, A., Luttmann, S. and C., S. (2009/2010) Krebs in Deutschland. Vol. 9. (Ed, Koch-Institut, R.) Robert Koch-Institut.

Kachhap, S. K., Rosmus, N., Collis, S. J., Kortenhorst, M. S., Wissing, M. D., Hedayati, M., Shabbeer, S., Mendonca, J., Deangelis, J., Marchionni, L., Lin, J., Hoti, N., Nortier, J. W., DeWeese, T. L., Hammers, H. and Carducci, M. A. (2010) Downregulation of homologous recombination DNA repair genes by HDAC inhibition in prostate cancer is mediated through the E2F1 transcription factor. PLoS One, 5, e11208.

Kaidi, A., Weinert, B. T., Choudhary, C. and Jackson, S. P. (2010) Human SIRT6 promotes DNA end resection through CtIP deacetylation. Science, 329, 1348-1353.

Kaina, B. (1985) The interrelationship between SCE induction, cell survival, mutagenesis, aberration formation and DNA synthesis inhibition in V79 cells treated with N-methyl-N-nitrosourea or N-methyl-N'-nitro-N-nitrosoguanidine. Mutat Res, 142, 49-54.

Kaina, B. and Aurich, O. (1985) Dependency of the yield of sister-chromatid exchanges induced by alkylating agents on fixation time. Possible involvement of secondary lesions in sister-chromatid exchange induction. Mutat Res, 149, 451-461.

Kaina, B., Christmann, M., Naumann, S. and Roos, W. P. (2007) MGMT: key node in the battle against genotoxicity, carcinogenicity and apoptosis induced by alkylating agents. DNA Repair (Amst), 6, 1079-1099.

Kaina, B., Ziouta, A., Ochs, K. and Coquerelle, T. (1997) Chromosomal instability, reproductive cell death and apoptosis induced by O6-methylguanine in Mex-, Mex+ and methylation-tolerant mismatch repair compromised cells: facts and models. Mutat Res, 381, 227-241.

Kanzawa, T., Germano, I. M., Komata, T., Ito, H., Kondo, Y. and Kondo, S. (2004) Role of autophagy in temozolomide-induced cytotoxicity for malignant glioma cells. Cell Death Differ, 11, 448-457.

Kerr, E., Holohan, C., McLaughlin, K. M., Majkut, J., Dolan, S., Redmond, K., Riley, J., McLaughlin, K., Stasik, I., Crudden, M., Van Schaeybroeck, S., Fenning, C., O'Connor, R., Kiely, P., Sgobba, M., Haigh, D., Johnston, P. G. and Longley, D. B. (2012) Identification of an acetylation-dependant Ku70/FLIP complex that regulates FLIP expression and HDAC inhibitor-induced apoptosis. Cell Death Differ, 19, 1317-1327.

Kerr, J. F., Wyllie, A. H. and Currie, A. R. (1972) Apoptosis: a basic biological phenomenon with wide-ranging implications in tissue kinetics. Br J Cancer, 26, 239-257.

Kimura, M., Yoshioka, T., Saio, M., Banno, Y., Nagaoka, H. and Okano, Y. (2013) Mitotic catastrophe and cell death induced by depletion of centrosomal proteins. Cell Death Dis, 4, e603.

Knizhnik, A. V., Roos, W. P., Nikolova, T., Quiros, S., Tomaszowski, K. H., Christmann, M. and Kaina, B. (2013) Survival and death strategies in glioma cells: autophagy, senescence and apoptosis triggered by a single type of temozolomide-induced DNA damage. PLoS One, 8, e55665.

Krishan, A. (1975) Rapid flow cytofluorometric analysis of mammalian cell cycle by propidium iodide staining. J Cell Biol, 66, 188-193.

Krokan, H. E. and Bjoras, M. (2013) Base excision repair. Cold Spring Harb Perspect Biol, 5, a012583.

Krusche, C. A., Wulfing, P., Kersting, C., Vloet, A., Bocker, W., Kiesel, L., Beier, H. M. and Alfer, J. (2005) Histone deacetylase-1 and -3 protein expression in human breast cancer: a tissue microarray analysis. Breast Cancer Res Treat, 90, 15-23.

Kummar, S., Gutierrez, M., Gardner, E. R., Donovan, E., Hwang, K., Chung, E. J., Lee, M. J., Maynard, K., Kalnitskiy, M., Chen, A., Melillo, G., Ryan, Q. C., Conley, B., Figg, W. D., Trepel, J. B., Zwiebel, J., Doroshow, J. H. and Murgo, A. J. (2007) Phase I trial of MS-275, a histone deacetylase inhibitor, administered weekly in refractory solid tumors and lymphoid malignancies. Clin Cancer Res, 13, 5411-5417.

Kunz, C., Saito, Y. and Schar, P. (2009) DNA Repair in mammalian cells: Mismatched repair: variations on a theme. Cell Mol Life Sci, 66, 1021-1038.

Lacroix, M., Abi-Said, D., Fourney, D. R., Gokaslan, Z. L., Shi, W., DeMonte, F., Lang, F. F., McCutcheon, I. E., Hassenbusch, S. J., Holland, E., Hess, K., Michael, C., Miller, D. and Sawaya, R. (2001) A multivariate analysis of 416 patients with glioblastoma multiforme: prognosis, extent of resection, and survival. J Neurosurg, 95, 190-198.

Larkin, J., Ascierto, P. A., Dreno, B., Atkinson, V., Liszkay, G., Maio, M., Mandala, M., Demidov, L., Stroyakovskiy, D., Thomas, L., de la Cruz-Merino, L., Dutriaux, C., Garbe, C., Sovak, M. A., Chang, I., Choong, N., Hack, S. P., McArthur, G. A. and Ribas, A. (2014) Combined vemurafenib and cobimetinib in BRAF-mutated melanoma. N Engl J Med, 371, 1867-1876.

Larkin, J., Chiarion-Sileni, V., Gonzalez, R., Grob, J. J., Cowey, C. L., Lao, C. D., Schadendorf, D., Dummer, R., Smylie, M., Rutkowski, P., Ferrucci, P. F., Hill, A., Wagstaff, J., Carlino, M. S., Haanen, J. B., Maio, M., Marquez-Rodas, I., McArthur, G. A., Ascierto, P. A., Long, G. V., Callahan, M. K., Postow, M. A., Grossmann, K., Sznol, M., Dreno, B., Bastholt, L., Yang, A., Rollin, L. M., Horak, C., Hodi, F. S. and Wolchok, J. D. (2015) Combined Nivolumab and Ipilimumab or Monotherapy in Untreated Melanoma. N Engl J Med, 373, 23-34.

Lee, J. H. and Paull, T. T. (2005) ATM activation by DNA double-strand breaks through the Mre11-Rad50-Nbs1 complex. Science, 308, 551-554.

Li, G. M. (2008) Mechanisms and functions of DNA mismatch repair. Cell Res, 18, 85-98.

Li, Q., Zhou, H., Wurtele, H., Davies, B., Horazdovsky, B., Verreault, A. and Zhang, Z. (2008) Acetylation of histone H3 lysine 56 regulates replication-coupled nucleosome assembly. Cell, 134, 244-255.

Li, X. and Heyer, W. D. (2008) Homologous recombination in DNA repair and DNA damage tolerance. Cell Res, 18, 99-113.

Li, X., Stith, C. M., Burgers, P. M. and Heyer, W. D. (2009) PCNA is required for initiation of recombination-associated DNA synthesis by DNA polymerase delta. Mol Cell, 36, 704-713.

Li, Y., Kao, G. D., Garcia, B. A., Shabanowitz, J., Hunt, D. F., Qin, J., Phelan, C. and Lazar, M. A. (2006) A novel histone deacetylase pathway regulates mitosis by modulating Aurora B kinase activity. Genes Dev, 20, 2566-2579.

Lian, C. G., Xu, Y., Ceol, C., Wu, F., Larson, A., Dresser, K., Xu, W., Tan, L., Hu, Y., Zhan, Q., Lee, C. W., Hu, D., Lian, B. Q., Kleffel, S., Yang, Y., Neiswender, J., Khorasani, A. J., Fang, R., Lezcano, C., Duncan, L. M., Scolyer, R. A., Thompson, J. F., Kakavand, H.,

Houvras, Y., Zon, L. I., Mihm, M. C., Jr., Kaiser, U. B., Schatton, T., Woda, B. A., Murphy, G. F. and Shi, Y. G. (2012) Loss of 5-hydroxymethylcytosine is an epigenetic hallmark of melanoma. Cell, 150, 1135-1146.

Lieber, M. R. (2010) The mechanism of double-strand DNA break repair by the nonhomologous DNA end-joining pathway. Annu Rev Biochem, 79, 181-211.

Lin, C. J., Lee, C. C., Shih, Y. L., Lin, T. Y., Wang, S. H., Lin, Y. F. and Shih, C. M. (2012) Resveratrol enhances the therapeutic effect of temozolomide against malignant glioma in vitro and in vivo by inhibiting autophagy. Free Radic Biol Med, 52, 377-391.

Lindahl, T., Demple, B. and Robins, P. (1982) Suicide inactivation of the E. coli O6-methylguanine-DNA methyltransferase. In Embo J, Vol. 1, pp. 1359-1363.

Liu, J., Doty, T., Gibson, B. and Heyer, W. D. (2010) Human BRCA2 protein promotes RAD51 filament formation on RPA-covered single-stranded DNA. Nat Struct Mol Biol, 17, 1260-1262.

Ljungman, M. and Zhang, F. (1996) Blockage of RNA polymerase as a possible trigger for u.v. light-induced apoptosis. Oncogene, 13, 823-831.

Llorente, B., Smith, C. E. and Symington, L. S. (2008) Break-induced replication: what is it and what is it for? Cell Cycle, 7, 859-864.

Long, G. V., Menzies, A. M., Nagrial, A. M., Haydu, L. E., Hamilton, A. L., Mann, G. J., Hughes, T. M., Thompson, J. F., Scolyer, R. A. and Kefford, R. F. (2011) Prognostic and clinicopathologic associations of oncogenic BRAF in metastatic melanoma. J Clin Oncol, 29, 1239-1246.

Ludlum, D. B. (1990) DNA alkylation by the haloethylnitrosoureas: nature of modifications produced and their enzymatic repair or removal. Mutat Res, 233, 117-126.

Ludlum, D. B. (1997) The chloroethylnitrosoureas: sensitivity and resistance to cancer chemotherapy at the molecular level. Cancer Invest, 15, 588-598.

Ma, Y., Pannicke, U., Schwarz, K. and Lieber, M. R. (2002) Hairpin opening and overhang processing by an Artemis/DNA-dependent protein kinase complex in nonhomologous end joining and V(D)J recombination. Cell, 108, 781-794.

Makharashvili, N., Tubbs, A. T., Yang, S. H., Wang, H., Barton, O., Zhou, Y., Deshpande, R. A., Lee, J. H., Lobrich, M., Sleckman, B. P., Wu, X. and Paull, T. T. (2014) Catalytic and noncatalytic roles of the CtIP endonuclease in double-strand break end resection. Mol Cell, 54, 1022-1033.

Mao, Z., Bozzella, M., Seluanov, A. and Gorbunova, V. (2008) DNA repair by nonhomologous end joining and homologous recombination during cell cycle in human cells. Cell Cycle, 7, 2902-2906.

Margison, G. P., Povey, A. C., Kaina, B. and Santibanez Koref, M. F. (2003) Variability and regulation of O6-alkylguanine-DNA alkyltransferase. Carcinogenesis, 24, 625-635.

Marteijn, J. A., Lans, H., Vermeulen, W. and Hoeijmakers, J. H. (2014) Understanding nucleotide excision repair and its roles in cancer and ageing. Nat Rev Mol Cell Biol, 15, 465-481.

Masumoto, H., Hawke, D., Kobayashi, R. and Verreault, A. (2005) A role for cell-cycle-regulated histone H3 lysine 56 acetylation in the DNA damage response. Nature, 436, 294-298.

Meredith, P. and Sarna, T. (2006) The physical and chemical properties of eumelanin. Pigment Cell Res, 19, 572-594.

Mesdjian, E., Ciesielski, L., Valli, M., Bruguerolle, B., Jadot, G., Bouyard, P. and Mandel, P. (1982) Sodium valproate: kinetic profile and effects on GABA levels in various brain areas of the rat. Prog Neuropsychopharmacol Biol Psychiatry, 6, 223-233.

Mhaidat, N. M., Zhang, X. D., Allen, J., Avery-Kiejda, K. A., Scott, R. J. and Hersey, P. (2007) Temozolomide induces senescence but not apoptosis in human melanoma cells. Br J Cancer, 97, 1225-1233.

Miller, K. M., Tjeertes, J. V., Coates, J., Legube, G., Polo, S. E., Britton, S. and Jackson, S. P. (2010) Human HDAC1 and HDAC2 function in the DNA-damage response to promote DNA nonhomologous end-joining. Nat Struct Mol Biol, 17, 1144-1151.

Minamiya, Y., Ono, T., Saito, H., Takahashi, N., Ito, M., Mitsui, M., Motoyama, S. and Ogawa, J. (2011) Expression of histone deacetylase 1 correlates with a poor prognosis in patients with adenocarcinoma of the lung. Lung Cancer, 74, 300-304.

Mladenov, E. and Iliakis, G. (2011) Induction and repair of DNA double strand breaks: the increasing spectrum of non-homologous end joining pathways. Mutat Res, 711, 61-72.

Mojas, N., Lopes, M. and Jiricny, J. (2007) Mismatch repair-dependent processing of methylation damage gives rise to persistent single-stranded gaps in newly replicated DNA. Genes Dev, 21, 3342-3355.

Moldovan, G. L. and D'Andrea, A. D. (2009) How the fanconi anemia pathway guards the genome. Annu Rev Genet, 43, 223-249.

Muniandy, P. A., Thapa, D., Thazhathveetil, A. K., Liu, S. T. and Seidman, M. M. (2009) Repair of laser-localized DNA interstrand cross-links in G1 phase mammalian cells. J Biol Chem, 284, 27908-27917.

Munshi, A., Kurland, J. F., Nishikawa, T., Tanaka, T., Hobbs, M. L., Tucker, S. L., Ismail, S., Stevens, C. and Meyn, R. E. (2005) Histone deacetylase inhibitors radiosensitize human melanoma cells by suppressing DNA repair activity. Clin Cancer Res, 11, 4912-4922.

Munshi, A., Tanaka, T., Hobbs, M. L., Tucker, S. L., Richon, V. M. and Meyn, R. E. (2006) Vorinostat, a histone deacetylase inhibitor, enhances the response of human tumor cells to ionizing radiation through prolongation of gamma-H2AX foci. Mol Cancer Ther, 5, 1967-1974.

Nakayama, Y., Igarashi, A., Kikuchi, I., Obata, Y., Fukumoto, Y. and Yamaguchi, N. (2009) Bleomycin-induced over-replication involves sustained inhibition of mitotic entry through the ATM/ATR pathway. Exp Cell Res, 315, 2515-2528.

Nanau, R. M. and Neuman, M. G. (2013) Adverse drug reactions induced by valproic acid. Clin Biochem, 46, 1323-1338.

Nau, H. and Loscher, W. (1982) Valproic acid: brain and plasma levels of the drug and its metabolites, anticonvulsant effects and gamma-aminobutyric acid (GABA) metabolism in the mouse. J Pharmacol Exp Ther, 220, 654-659.

Naumann, S. C., Roos, W. P., Jost, E., Belohlavek, C., Lennerz, V., Schmidt, C. W., Christmann, M. and Kaina, B. (2009) Temozolomide- and fotemustine-induced apoptosis in human malignant melanoma cells: response related to MGMT, MMR, DSBs, and p53. Br J Cancer, 100, 322-333.

Nebbioso, A., Clarke, N., Voltz, E., Germain, E., Ambrosino, C., Bontempo, P., Alvarez, R., Schiavone, E. M., Ferrara, F., Bresciani, F., Weisz, A., de Lera, A. R., Gronemeyer, H. and Altucci, L. (2005) Tumor-selective action of HDAC inhibitors involves TRAIL induction in acute myeloid leukemia cells. Nat Med, 11, 77-84.

Newbold, A., Salmon, J. M., Martin, B. P., Stanley, K. and Johnstone, R. W. (2014) The role of p21(waf1/cip1) and p27(Kip1) in HDACi-mediated tumor cell death and cell cycle arrest in the Emu-myc model of B-cell lymphoma. Oncogene, 33, 5415-5423.

Newlands, E. S., Stevens, M. F., Wedge, S. R., Wheelhouse, R. T. and Brock, C. (1997) Temozolomide: a review of its discovery, chemical properties, pre-clinical development and clinical trials. Cancer Treat Rev, 23, 35-61.

Nicoletti, I., Migliorati, G., Pagliacci, M. C., Grignani, F. and Riccardi, C. (1991) A rapid and simple method for measuring thymocyte apoptosis by propidium iodide staining and flow cytometry. J Immunol Methods, 139, 271-279.

Nikolova, T., Hennekes, F., Bhatti, A. and Kaina, B. (2012) Chloroethylnitrosourea-induced cell death and genotoxicity: cell cycle dependence and the role of DNA double-strand breaks, HR and NHEJ. Cell Cycle, 11, 2606-2619.

Noh, E. J. and Lee, J. S. (2003) Functional interplay between modulation of histone deacetylase activity and its regulatory role in G2-M transition. Biochem Biophys Res Commun, 310, 267-273.

Ohashi, A., Zdzienicka, M. Z., Chen, J. and Couch, F. J. (2005) Fanconi anemia complementation group D2 (FANCD2) functions independently of BRCA2- and RAD51-associated homologous recombination in response to DNA damage. J Biol Chem, 280, 14877-14883.

Ohgaki, H., Burger, P. and Kleihues, P. (2013) Definition of primary and secondary glioblastoma--response. Clin Cancer Res, 20, 2013.

Ostrom, Q. T., Gittleman, H., Farah, P., Ondracek, A., Chen, Y., Wolinsky, Y., Stroup, N. E., Kruchko, C. and Barnholtz-Sloan, J. S. (2013) CBTRUS statistical report: Primary brain

and central nervous system tumors diagnosed in the United States in 2006-2010. Neuro Oncol, 15 Suppl 2, ii1-56.

Pabla, N., Huang, S., Mi, Q. S., Daniel, R. and Dong, Z. (2008) ATR-Chk2 signaling in p53 activation and DNA damage response during cisplatin-induced apoptosis. J Biol Chem, 283, 6572-6583.

Papi, A., Ferreri, A. M., Rocchi, P., Guerra, F. and Orlandi, M. (2010) Epigenetic modifiers as anticancer drugs: effectiveness of valproic acid in neural crest-derived tumor cells. Anticancer Res, 30, 535-540.

Park, J. W. and Ames, B. N. (1988) 7-Methylguanine adducts in DNA are normally present at high levels and increase on aging: analysis by HPLC with electrochemical detection. Proc Natl Acad Sci U S A, 85, 7467-7470.

Pazin, M. J. and Kadonaga, J. T. (1997) What's up and down with histone deacetylation and transcription? Cell, 89, 325-328.

Peart, M. J., Smyth, G. K., van Laar, R. K., Bowtell, D. D., Richon, V. M., Marks, P. A., Holloway, A. J. and Johnstone, R. W. (2005) Identification and functional significance of genes regulated by structurally different histone deacetylase inhibitors. Proc Natl Acad Sci U S A, 102, 3697-3702.

Penketh, P. G., Shyam, K., Baumann, R. P., Ishiguro, K., Patridge, E. V., Zhu, R. and Sartorelli, A. C. (2012) A strategy for selective O(6)-alkylguanine-DNA alkyltransferase depletion under hypoxic conditions. Chem Biol Drug Des, 80, 279-290.

Petermann, E. and Helleday, T. (2010) Pathways of mammalian replication fork restart. Nat Rev Mol Cell Biol, 11, 683-687.

Pfeiffer, P., Goedecke, W. and Obe, G. (2000) Mechanisms of DNA double-strand break repair and their potential to induce chromosomal aberrations. Mutagenesis, 15, 289-302.

Phiel, C. J., Zhang, F., Huang, E. Y., Guenther, M. G., Lazar, M. A. and Klein, P. S. (2001) Histone deacetylase is a direct target of valproic acid, a potent anticonvulsant, mood stabilizer, and teratogen. J Biol Chem, 276, 36734-36741.

Pierce, A. J., Johnson, R. D., Thompson, L. H. and Jasin, M. (1999) XRCC3 promotes homology-directed repair of DNA damage in mammalian cells. Genes Dev, 13, 2633-2638.

Plate, K. H., Breier, G., Weich, H. A. and Risau, W. (1992) Vascular endothelial growth factor is a potential tumour angiogenesis factor in human gliomas in vivo. Nature, 359, 845-848.

Plosky, B., Samson, L., Engelward, B. P., Gold, B., Schlaen, B., Millas, T., Magnotti, M., Schor, J. and Scicchitano, D. A. (2002) Base excision repair and nucleotide excision repair contribute to the removal of N-methylpurines from active genes. DNA Repair (Amst), 1, 683-696.

Pont, L. M., Naipal, K., Kloezeman, J. J., Venkatesan, S., van den Bent, M., van Gent, D. C., Dirven, C. M., Kanaar, R., Lamfers, M. L. and Leenstra, S. (2015) DNA damage response and anti-apoptotic proteins predict radiosensitization efficacy of HDAC inhibitors SAHA and LBH589 in patient-derived glioblastoma cells. Cancer Lett, 356, 525-535.

Qi, Z., Redding, S., Lee, J. Y., Gibb, B., Kwon, Y., Niu, H., Gaines, W. A., Sung, P. and Greene, E. C. (2015) DNA sequence alignment by microhomology sampling during homologous recombination. Cell, 160, 856-869.

Quiros, S., Roos, W. P. and Kaina, B. (2010) Processing of O6-methylguanine into DNA double-strand breaks requires two rounds of replication whereas apoptosis is also induced in subsequent cell cycles. Cell Cycle, 9, 168-178.

Quiros, S., Roos, W. P. and Kaina, B. (2011) Rad51 and BRCA2--New molecular targets for sensitizing glioma cells to alkylating anticancer drugs. PLoS One, 6, e27183.

Radhakrishnan, R., Li, Y., Xiang, S., Yuan, F., Yuan, Z., Telles, E., Fang, J., Coppola, D., Shibata, D., Lane, W. S., Zhang, Y., Zhang, X. and Seto, E. (2015) Histone Deacetylase 10 Regulates DNA Mismatch Repair and May Involve the Deacetylation of MutS Homolog 2. J Biol Chem, 290, 22795-22804.

Reid, J. M., Kuffel, M. J., Miller, J. K., Rios, R. and Ames, M. M. (1999) Metabolic activation of dacarbazine by human cytochromes P450: the role of CYP1A1, CYP1A2, and CYP2E1. Clin Cancer Res, 5, 2192-2197.

Reinhardt, H. C. and Yaffe, M. B. (2009) Kinases that control the cell cycle in response to DNA damage: Chk1, Chk2, and MK2. Curr Opin Cell Biol, 21, 245-255.

Richardson, C., Moynahan, M. E. and Jasin, M. (1998) Double-strand break repair by interchromosomal recombination: suppression of chromosomal translocations. Genes Dev, 12, 3831-3842.

Rikimaru, T., Taketomi, A., Yamashita, Y., Shirabe, K., Hamatsu, T., Shimada, M. and Maehara, Y. (2007) Clinical significance of histone deacetylase 1 expression in patients with hepatocellular carcinoma. Oncology, 72, 69-74.

Roberson, R. S., Kussick, S. J., Vallieres, E., Chen, S. Y. and Wu, D. Y. (2005) Escape from therapy-induced accelerated cellular senescence in p53-null lung cancer cells and in human lung cancers. Cancer Res, 65, 2795-2803.

Robert, C., Karaszewska, B., Schachter, J., Rutkowski, P., Mackiewicz, A., Stroiakovski, D., Lichinitser, M., Dummer, R., Grange, F., Mortier, L., Chiarion-Sileni, V., Drucis, K., Krajsova, I., Hauschild, A., Lorigan, P., Wolter, P., Long, G. V., Flaherty, K., Nathan, P., Ribas, A., Martin, A. M., Sun, P., Crist, W., Legos, J., Rubin, S. D., Little, S. M. and Schadendorf, D. (2015) Improved overall survival in melanoma with combined dabrafenib and trametinib. N Engl J Med, 372, 30-39.

Robert, T., Vanoli, F., Chiolo, I., Shubassi, G., Bernstein, K. A., Rothstein, R., Botrugno, O. A., Parazzoli, D., Oldani, A., Minucci, S. and Foiani, M. (2011) HDACs link the DNA damage response, processing of double-strand breaks and autophagy. Nature, 471, 74-79.

Roberts, S. A., Strande, N., Burkhalter, M. D., Strom, C., Havener, J. M., Hasty, P. and Ramsden, D. A. (2010) Ku is a 5'-dRP/AP lyase that excises nucleotide damage near broken ends. Nature, 464, 1214-1217.

Rodier, F., Coppe, J. P., Patil, C. K., Hoeijmakers, W. A., Munoz, D. P., Raza, S. R., Freund, A., Campeau, E., Davalos, A. R. and Campisi, J. (2009) Persistent DNA damage signalling triggers senescence-associated inflammatory cytokine secretion. Nat Cell Biol, 11, 973-979.

Rogakou, E. P., Boon, C., Redon, C. and Bonner, W. M. (1999) Megabase chromatin domains involved in DNA double-strand breaks in vivo. J Cell Biol, 146, 905-916.

Rogakou, E. P., Nieves-Neira, W., Boon, C., Pommier, Y. and Bonner, W. M. (2000) Initiation of DNA fragmentation during apoptosis induces phosphorylation of H2AX histone at serine 139. J Biol Chem, 275, 9390-9395.

Roos, W., Baumgartner, M. and Kaina, B. (2004) Apoptosis triggered by DNA damage O6-methylguanine in human lymphocytes requires DNA replication and is mediated by p53 and Fas/CD95/Apo-1. Oncogene, 23, 359-367.

Roos, W. P., Batista, L. F., Naumann, S. C., Wick, W., Weller, M., Menck, C. F. and Kaina, B. (2007) Apoptosis in malignant glioma cells triggered by the temozolomide-induced DNA lesion O6-methylguanine. Oncogene, 26, 186-197.

Roos, W. P., Jost, E., Belohlavek, C., Nagel, G., Fritz, G. and Kaina, B. (2011) Intrinsic anticancer drug resistance of malignant melanoma cells is abrogated by IFN-beta and valproic acid. Cancer Res, 71, 4150-4160.

Roos, W. P. and Kaina, B. (2013) DNA damage-induced cell death: from specific DNA lesions to the DNA damage response and apoptosis. Cancer Lett, 332, 237-248.

Roos, W. P., Nikolova, T., Quiros, S., Naumann, S. C., Kiedron, O., Zdzienicka, M. Z. and Kaina, B. (2009) Brca2/Xrcc2 dependent HR, but not NHEJ, is required for protection against O(6)-methylguanine triggered apoptosis, DSBs and chromosomal aberrations by a process leading to SCEs. DNA Repair (Amst), 8, 72-86.

Roos, W. P., Quiros, S., Krumm, A., Merz, S., Switzeny, O. J., Christmann, M., Loquai, C. and Kaina, B. (2014) B-Raf inhibitor vemurafenib in combination with temozolomide and fotemustine in the killing response of malignant melanoma cells. Oncotarget, 5, 12607-12620.

Rosato, R. R., Almenara, J. A. and Grant, S. (2003) The histone deacetylase inhibitor MS-275 promotes differentiation or apoptosis in human leukemia cells through a process regulated by generation of reactive oxygen species and induction of p21CIP1/WAF1 1. Cancer Res, 63, 3637-3645.

Roy, S., Packman, K., Jeffrey, R. and Tenniswood, M. (2005) Histone deacetylase inhibitors differentially stabilize acetylated p53 and induce cell cycle arrest or apoptosis in prostate cancer cells. Cell Death Differ, 12, 482-491.

Ryan, Q. C., Headlee, D., Acharya, M., Sparreboom, A., Trepel, J. B., Ye, J., Figg, W. D., Hwang, K., Chung, E. J., Murgo, A., Melillo, G., Elsayed, Y., Monga, M., Kalnitskiy, M., Zwiebel, J. and Sausville, E. A. (2005) Phase I and pharmacokinetic study of MS-275, a histone deacetylase inhibitor, in patients with advanced and refractory solid tumors or lymphoma. J Clin Oncol, 23, 3912-3922.

Rydberg, B. and Lindahl, T. (1982) Nonenzymatic methylation of DNA by the intracellular methyl group donor S-adenosyl-L-methionine is a potentially mutagenic reaction. Embo J, 1, 211-216.

Sale, J. E. (2013) Translesion DNA synthesis and mutagenesis in eukaryotes. Cold Spring Harb Perspect Biol, 5, a012708.

Samson, L., Thomale, J. and Rajewsky, M. F. (1988) Alternative pathways for the in vivo repair of O6-alkylguanine and O4-alkylthymine in Escherichia coli: the adaptive response and nucleotide excision repair. Embo J, 7, 2261-2267.

Sandor, V., Senderowicz, A., Mertins, S., Sackett, D., Sausville, E., Blagosklonny, M. V. and Bates, S. E. (2000) P21-dependent g(1)arrest with downregulation of cyclin D1 and upregulation of cyclin E by the histone deacetylase inhibitor FR901228. Br J Cancer, 83, 817-825.

Santoro, F., Botrugno, O. A., Dal Zuffo, R., Pallavicini, I., Matthews, G. M., Cluse, L., Barozzi, I., Senese, S., Fornasari, L., Moretti, S., Altucci, L., Pelicci, P. G., Chiocca, S., Johnstone, R. W. and Minucci, S. (2013) A dual role for Hdac1: oncosuppressor in tumorigenesis, oncogene in tumor maintenance. Blood, 121, 3459-3468.

Sartori, A. A., Lukas, C., Coates, J., Mistrik, M., Fu, S., Bartek, J., Baer, R., Lukas, J. and Jackson, S. P. (2007) Human CtIP promotes DNA end resection. Nature, 450, 509-514.

Sassanfar, M., Dosanjh, M. K., Essigmann, J. M. and Samson, L. (1991) Relative efficiencies of the bacterial, yeast, and human DNA methyltransferases for the repair of O6-methylguanine and O4-methylthymine. Suggestive evidence for O4-methylthymine repair by eukaryotic methyltransferases. J Biol Chem, 266, 2767-2771.

Schärer, O. D. (2013) Nucleotide excision repair in eukaryotes. Cold Spring Harb Perspect Biol, 5, a012609.

Schlacher, K., Wu, H. and Jasin, M. (2012) A distinct replication fork protection pathway connects Fanconi anemia tumor suppressors to RAD51-BRCA1/2. Cancer Cell, 22, 106-116.

Schnell, O., Krebs, B., Wagner, E., Romagna, A., Beer, A. J., Grau, S. J., Thon, N., Goetz, C., Kretzschmar, H. A., Tonn, J. C. and Goldbrunner, R. H. (2008) Expression of integrin alphavbeta3 in gliomas correlates with tumor grade and is not restricted to tumor vasculature. Brain Pathol, 18, 378-386.

Scrima, A., Konickova, R., Czyzewski, B. K., Kawasaki, Y., Jeffrey, P. D., Groisman, R., Nakatani, Y., Iwai, S., Pavletich, N. P. and Thoma, N. H. (2008) Structural basis of UV DNA-damage recognition by the DDB1-DDB2 complex. Cell, 135, 1213-1223.

Sebesta, M., Burkovics, P., Haracska, L. and Krejci, L. (2011) Reconstitution of DNA repair synthesis in vitro and the role of polymerase and helicase activities. DNA Repair (Amst), 10, 567-576.

SEER - The Surveillance, Epidemiology, and End Results (SEER) Program of the National Cancer Institute (2015) Melanoma of the Skin (Invasive), SEER Incidence and U.S. Mortality, Age-Adjusted Rates and Trends By Race/Ethnicity and Sex. Surveillance, Epidemiology, and End Results (SEER) Program.

Serrano, M., Hannon, G. J. and Beach, D. (1993) A new regulatory motif in cell-cycle control causing specific inhibition of cyclin D/CDK4. Nature, 366, 704-707.

Shogren-Knaak, M., Ishii, H., Sun, J. M., Pazin, M. J., Davie, J. R. and Peterson, C. L. (2006) Histone H4-K16 acetylation controls chromatin structure and protein interactions. Science, 311, 844-847.

Shrivastav, N., Li, D. and Essigmann, J. M. (2010) Chemical biology of mutagenesis and DNA repair: cellular responses to DNA alkylation. Carcinogenesis, 31, 59-70.

Sonnemann, J., Marx, C., Becker, S., Wittig, S., Palani, C. D., Kramer, O. H. and Beck, J. F. (2014) p53-dependent and p53-independent anticancer effects of different histone deacetylase inhibitors. Br J Cancer, 110, 656-667.

Spange, S., Wagner, T., Heinzel, T. and Kramer, O. H. (2009) Acetylation of non-histone proteins modulates cellular signalling at multiple levels. Int J Biochem Cell Biol, 41, 185-198.

Srivenugopal, K. S., Yuan, X. H., Friedman, H. S. and Ali-Osman, F. (1996) Ubiquitination-dependent proteolysis of O6-methylguanine-DNA methyltransferase in human and murine tumor cells following inactivation with O6-benzylguanine or 1,3-bis(2-chloroethyl)-1-nitrosourea. Biochemistry, 35, 1328-1334.

Stewart, B. W., Wild, C. P., World Helath Organization and International Agency for Research on Cancer (2014) World Cancer Report 2014, World health organization, Geneva.

Stojic, L., Mojas, N., Cejka, P., Di Pietro, M., Ferrari, S., Marra, G. and Jiricny, J. (2004) Mismatch repair-dependent G2 checkpoint induced by low doses of SN1 type methylating agents requires the ATR kinase. Genes Dev, 18, 1331-1344.

Stott, F. J., Bates, S., James, M. C., McConnell, B. B., Starborg, M., Brookes, S., Palmero, I., Ryan, K., Hara, E., Vousden, K. H. and Peters, G. (1998) The alternative product from the human CDKN2A locus, p14(ARF), participates in a regulatory feedback loop with p53 and MDM2. Embo J, 17, 5001-5014.

Struhl, K. (1998) Histone acetylation and transcriptional regulatory mechanisms. Genes Dev, 12, 599-606.

Stupp, R., Brada, M., van den Bent, M. J., Tonn, J. C. and Pentheroudakis, G. (2014a) High-grade glioma: ESMO Clinical Practice Guidelines for diagnosis, treatment and follow-up. Ann Oncol, 25 Suppl 3, iii93-101.

Stupp, R., Hegi, M. E., Gorlia, T., Erridge, S. C., Perry, J., Hong, Y. K., Aldape, K. D., Lhermitte, B., Pietsch, T., Grujicic, D., Steinbach, J. P., Wick, W., Tarnawski, R., Nam, D. H., Hau, P., Weyerbrock, A., Taphoorn, M. J., Shen, C. C., Rao, N., Thurzo, L., Herrlinger, U., Gupta, T., Kortmann, R. D., Adamska, K., McBain, C., Brandes, A. A., Tonn, J. C., Schnell, O., Wiegel, T., Kim, C. Y., Nabors, L. B., Reardon, D. A., van den Bent, M. J., Hicking, C., Markivskyy, A., Picard, M. and Weller, M. (2014b) Cilengitide combined with standard treatment for patients with newly diagnosed glioblastoma with methylated MGMT promoter (CENTRIC EORTC 26071-22072 study): a multicentre, randomised, open-label, phase 3 trial. Lancet Oncol, 15, 1100-1108.

Stupp, R., Hegi, M. E., Mason, W. P., van den Bent, M. J., Taphoorn, M. J., Janzer, R. C., Ludwin, S. K., Allgeier, A., Fisher, B., Belanger, K., Hau, P., Brandes, A. A., Gijtenbeek, J., Marosi, C., Vecht, C. J., Mokhtari, K., Wesseling, P., Villa, S., Eisenhauer, E., Gorlia, T., Weller, M., Lacombe, D., Cairncross, J. G. and Mirimanoff, R. O. (2009) Effects of radiotherapy with concomitant and adjuvant temozolomide versus radiotherapy alone on survival in glioblastoma in a randomised phase III study: 5-year analysis of the EORTC-NCIC trial. Lancet Oncol, 10, 459-466.

Sugasawa, K., Okamoto, T., Shimizu, Y., Masutani, C., Iwai, S. and Hanaoka, F. (2001) A multistep damage recognition mechanism for global genomic nucleotide excision repair. Genes Dev, 15, 507-521.

Svendsen, J. M. and Harper, J. W. (2010) GEN1/Yen1 and the SLX4 complex: Solutions to the problem of Holliday junction resolution. Genes Dev, 24, 521-536.

Svilar, D., Goellner, E. M., Almeida, K. H. and Sobol, R. W. (2011) Base excision repair and lesion-dependent subpathways for repair of oxidative DNA damage. Antioxid Redox Signal, 14, 2491-2507.

Symington, L. S. (2014) End resection at double-strand breaks: mechanism and regulation. Cold Spring Harb Perspect Biol, 6.

TCGA (2015) Genomic Classification of Cutaneous Melanoma. Cell, 161, 1681-1696.

Thorslund, T., McIlwraith, M. J., Compton, S. A., Lekomtsev, S., Petronczki, M., Griffith, J. D. and West, S. C. (2010) The breast cancer tumor suppressor BRCA2 promotes the specific targeting of RAD51 to single-stranded DNA. Nat Struct Mol Biol, 17, 1263-1265.

Tjeertes, J. V., Miller, K. M. and Jackson, S. P. (2009) Screen for DNA-damage-responsive histone modifications identifies H3K9Ac and H3K56Ac in human cells. Embo J, 28, 1878-1889.

Tong, W. P., Kirk, M. C. and Ludlum, D. B. (1982) Formation of the cross-link 1-[N3-deoxycytidyl),2-[N1-deoxyguanosinyl]ethane in DNA treated with N,N'-bis(2-chloroethyl)-N-nitrosourea. Cancer Res, 42, 3102-3105.

Topalian, S. L., Sznol, M., McDermott, D. F., Kluger, H. M., Carvajal, R. D., Sharfman, W. H., Brahmer, J. R., Lawrence, D. P., Atkins, M. B., Powderly, J. D., Leming, P. D., Lipson, E. J., Puzanov, I., Smith, D. C., Taube, J. M., Wigginton, J. M., Kollia, G. D., Gupta, A., Pardoll, D. M., Sosman, J. A. and Hodi, F. S. (2014) Survival, durable tumor remission, and long-term safety in patients with advanced melanoma receiving nivolumab. J Clin Oncol, 32, 1020-1030.

Tremethick, D. J. (2007) Higher-order structures of chromatin: the elusive 30 nm fiber. Cell, 128, 651-654.

Tudek, B. (2003) Imidazole ring-opened DNA purines and their biological significance. J Biochem Mol Biol, 36, 12-19.

Tuominen, R., Jewell, R., van den Oord, J. J., Wolter, P., Stierner, U., Lindholm, C., Hertzman Johansson, C., Linden, D., Johansson, H., Frostvik Stolt, M., Walker, C., Snowden, H., Newton-Bishop, J., Hansson, J. and Egyhazi Brage, S. (2015) MGMT promoter methylation is associated with temozolomide response and prolonged progression-free survival in disseminated cutaneous melanoma. Int J Cancer, 136, 2844-2853.

Valentini, A., Gravina, P., Federici, G. and Bernardini, S. (2007) Valproic acid induces apoptosis, p16INK4A upregulation and sensitization to chemotherapy in human melanoma cells. Cancer Biol Ther, 6, 185-191.

van Gent, D. C., Hoeijmakers, J. H. and Kanaar, R. (2001) Chromosomal stability and the DNA double-stranded break connection. Nat Rev Genet, 2, 196-206.

Van Nifterik, K. A., Van den Berg, J., Slotman, B. J., Lafleur, M. V., Sminia, P. and Stalpers, L. J. (2012) Valproic acid sensitizes human glioma cells for temozolomide and gamma-radiation. J Neurooncol, 107, 61-67.

Vempati, R. K., Jayani, R. S., Notani, D., Sengupta, A., Galande, S. and Haldar, D. (2010) p300-mediated acetylation of histone H3 lysine 56 functions in DNA damage response in mammals. J Biol Chem, 285, 28553-28564.

Verhaak, R. G., Hoadley, K. A., Purdom, E., Wang, V., Qi, Y., Wilkerson, M. D., Miller, C. R., Ding, L., Golub, T., Mesirov, J. P., Alexe, G., Lawrence, M., O'Kelly, M., Tamayo, P., Weir, B. A., Gabriel, S., Winckler, W., Gupta, S., Jakkula, L., Feiler, H. S., Hodgson, J. G., James, C. D., Sarkaria, J. N., Brennan, C., Kahn, A., Spellman, P. T., Wilson, R. K., Speed, T. P., Gray, J. W., Meyerson, M., Getz, G., Perou, C. M. and Hayes, D. N. (2010) Integrated genomic analysis identifies clinically relevant subtypes of glioblastoma characterized by abnormalities in PDGFRA, IDH1, EGFR, and NF1. Cancer Cell, 17, 98-110.

Vermes, I., Haanen, C., Steffens-Nakken, H. and Reutelingsperger, C. (1995) A novel assay for apoptosis. Flow cytometric detection of phosphatidylserine expression on early apoptotic cells using fluorescein labelled Annexin V. J Immunol Methods, 184, 39-51.

Vermeulen, W. and Fousteri, M. (2013) Mammalian transcription-coupled excision repair. Cold Spring Harb Perspect Biol, 5, a012625.

Vernole, P., Pepponi, R. and D'Atri, S. (2003) Role of mismatch repair in the induction of chromosomal aberrations and sister chromatid exchanges in cells treated with different chemotherapeutic agents. Cancer Chemother Pharmacol, 52, 185-192.

Vincensi, M. R., d'Ischia, M., Napolitano, A., Procaccini, E. M., Riccio, G., Monfrecola, G., Santoianni, P. and Prota, G. (1998) Phaeomelanin versus eumelanin as a chemical indicator of ultraviolet sensitivity in fair-skinned subjects at high risk for melanoma: a pilot study. Melanoma Res, 8, 53-58.

Vrana, J. A., Decker, R. H., Johnson, C. R., Wang, Z., Jarvis, W. D., Richon, V. M., Ehinger, M., Fisher, P. B. and Grant, S. (1999) Induction of apoptosis in U937 human leukemia cells by suberoylanilide hydroxamic acid (SAHA) proceeds through pathways that are regulated by Bcl-2/Bcl-XL, c-Jun, and p21CIP1, but independent of p53. Oncogene, 18, 7016-7025.

Wagner, M., Hampel, B., Bernhard, D., Hala, M., Zwerschke, W. and Jansen-Durr, P. (2001) Replicative senescence of human endothelial cells in vitro involves G1 arrest, polyploidization and senescence-associated apoptosis. Exp Gerontol, 36, 1327-1347.

Walden, H. and Deans, A. J. (2014) The Fanconi anemia DNA repair pathway: structural and functional insights into a complex disorder. Annu Rev Biophys, 43, 257-278.

Walker, J. R., Corpina, R. A. and Goldberg, J. (2001) Structure of the Ku heterodimer bound to DNA and its implications for double-strand break repair. Nature, 412, 607-614.

Wang, Q., Wu, P. C., Dong, D. Z., Ivanova, I., Chu, E., Zeliadt, S., Vesselle, H. and Wu, D. Y. (2013) Polyploidy road to therapy-induced cellular senescence and escape. Int J Cancer, 132, 1505-1515.

Wang, X., Andreassen, P. R. and D'Andrea, A. D. (2004) Functional interaction of monoubiquitinated FANCD2 and BRCA2/FANCD1 in chromatin. Mol Cell Biol, 24, 5850-5862.

Wang, X. Q., Redpath, J. L., Fan, S. T. and Stanbridge, E. J. (2006) ATR dependent activation of Chk2. J Cell Physiol, 208, 613-619.

Waters, C. A., Strande, N. T., Wyatt, D. W., Pryor, J. M. and Ramsden, D. A. (2014) Nonhomologous end joining: a good solution for bad ends. DNA Repair (Amst), 17, 39-51.

Weichert, W., Roske, A., Gekeler, V., Beckers, T., Stephan, C., Jung, K., Fritzsche, F. R., Niesporek, S., Denkert, C., Dietel, M. and Kristiansen, G. (2008a) Histone deacetylases 1, 2 and 3 are highly expressed in prostate cancer and HDAC2 expression is associated with shorter PSA relapse time after radical prostatectomy. Br J Cancer, 98, 604-610.

Weichert, W., Roske, A., Niesporek, S., Noske, A., Buckendahl, A. C., Dietel, M., Gekeler, V., Boehm, M., Beckers, T. and Denkert, C. (2008b) Class I histone deacetylase expression has independent prognostic impact in human colorectal cancer: specific role of class I histone deacetylases in vitro and in vivo. Clin Cancer Res, 14, 1669-1677.

Weinstein, I. B. (2002) Cancer. Addiction to oncogenes--the Achilles heal of cancer. Science, 297, 63-64.

Weller, M., Gorlia, T., Cairncross, J. G., van den Bent, M. J., Mason, W., Belanger, K., Brandes, A. A., Bogdahn, U., Macdonald, D. R., Forsyth, P., Rossetti, A. O., Lacombe, D., Mirimanoff, R. O., Vecht, C. J. and Stupp, R. (2011) Prolonged survival with valproic acid use in the EORTC/NCIC temozolomide trial for glioblastoma. Neurology, 77, 1156-1164.

West, A. C. and Johnstone, R. W. (2014) New and emerging HDAC inhibitors for cancer treatment. J Clin Invest, 124, 30-39.

Westphal, M., Heese, O., Steinbach, J. P., Schnell, O., Schackert, G., Mehdorn, M., Schulz, D., Simon, M., Schlegel, U., Senft, C., Geletneky, K., Braun, C., Hartung, J. G., Reuter, D., Metz, M. W., Bach, F. and Pietsch, T. (2015) A randomised, open label phase III trial with nimotuzumab, an anti-epidermal growth factor receptor monoclonal antibody in the treatment of newly diagnosed adult glioblastoma. Eur J Cancer, 51, 522-532.

Wilson, A. J., Byun, D. S., Popova, N., Murray, L. B., L'Italien, K., Sowa, Y., Arango, D., Velcich, A., Augenlicht, L. H. and Mariadason, J. M. (2006) Histone deacetylase 3 (HDAC3) and other class I HDACs regulate colon cell maturation and p21 expression and are deregulated in human colon cancer. J Biol Chem, 281, 13548-13558.

Wood, R. D. (2010) Mammalian nucleotide excision repair proteins and interstrand crosslink repair. Environ Mol Mutagen, 51, 520-526.

Wyllie, A. H., Kerr, J. F. and Currie, A. R. (1980) Cell death: the significance of apoptosis. Int Rev Cytol, 68, 251-306.

Yang, D., McCrann, D. J., Nguyen, H., St Hilaire, C., DePinho, R. A., Jones, M. R. and Ravid, K. (2007) Increased polyploidy in aortic vascular smooth muscle cells during aging is marked by cellular senescence. Aging Cell, 6, 257-260.

Yang, X. J. and Seto, E. (2007) HATs and HDACs: from structure, function and regulation to novel strategies for therapy and prevention. Oncogene, 26, 5310-5318.

Yoshioka, K., Yoshioka, Y. and Hsieh, P. (2006) ATR kinase activation mediated by MutSalpha and MutLalpha in response to cytotoxic O6-methylguanine adducts. Mol Cell, 22, 501-510.

You, Y. H., Lee, D. H., Yoon, J. H., Nakajima, S., Yasui, A. and Pfeifer, G. P. (2001) Cyclobutane pyrimidine dimers are responsible for the vast majority of mutations induced by UVB irradiation in mammalian cells. J Biol Chem, 276, 44688-44694.

Yuan, Z., Zhang, X., Sengupta, N., Lane, W. S. and Seto, E. (2007) SIRT1 regulates the function of the Nijmegen breakage syndrome protein. Mol Cell, 27, 149-162.

Zhang, M., Xiang, S., Joo, H. Y., Wang, L., Williams, K. A., Liu, W., Hu, C., Tong, D., Haakenson, J., Wang, C., Zhang, S., Pavlovicz, R. E., Jones, A., Schmidt, K. H., Tang, J., Dong, H., Shan, B., Fang, B., Radhakrishnan, R., Glazer, P. M., Matthias, P., Koomen, J.,

Seto, E., Bepler, G., Nicosia, S. V., Chen, J., Li, C., Gu, L., Li, G. M., Bai, W., Wang, H. and Zhang, X. (2014) HDAC6 deacetylates and ubiquitinates MSH2 to maintain proper levels of MutSalpha. Mol Cell, 55, 31-46.

Zhang, X. D., Gillespie, S. K., Borrow, J. M. and Hersey, P. (2004) The histone deacetylase inhibitor suberic bishydroxamate regulates the expression of multiple apoptotic mediators and induces mitochondria-dependent apoptosis of melanoma cells. Mol Cancer Ther, 3, 425-435.

Zhao, Y., Lu, S., Wu, L., Chai, G., Wang, H., Chen, Y., Sun, J., Yu, Y., Zhou, W., Zheng, Q., Wu, M., Otterson, G. A. and Zhu, W. G. (2006) Acetylation of p53 at lysine 373/382 by the histone deacetylase inhibitor depsipeptide induces expression of p21(Waf1/Cip1). Mol Cell Biol, 26, 2782-2790.

Zhu, W., Chen, Y. and Dutta, A. (2004) Rereplication by depletion of geminin is seen regardless of p53 status and activates a G2/M checkpoint. Mol Cell Biol, 24, 7140-7150.

Zou, L. and Elledge, S. J. (2003) Sensing DNA damage through ATRIP recognition of RPA-ssDNA complexes. Science, 300, 1542-1548.

7 Supplementary information

7.1 Supplementary figures and tables

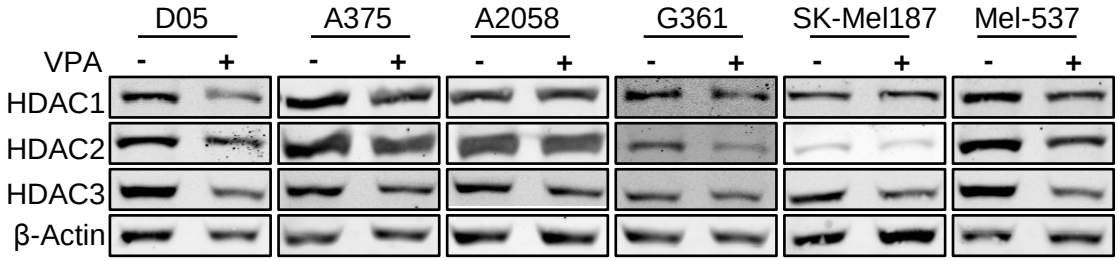

S 1 - Influence of VPA on HDAC protein levels.
Whole cell protein extracts of indicated melanoma cell lines, treated with VPA (1 mM, 168 h) or left untreated for controls, were subjected to immunoblotting.

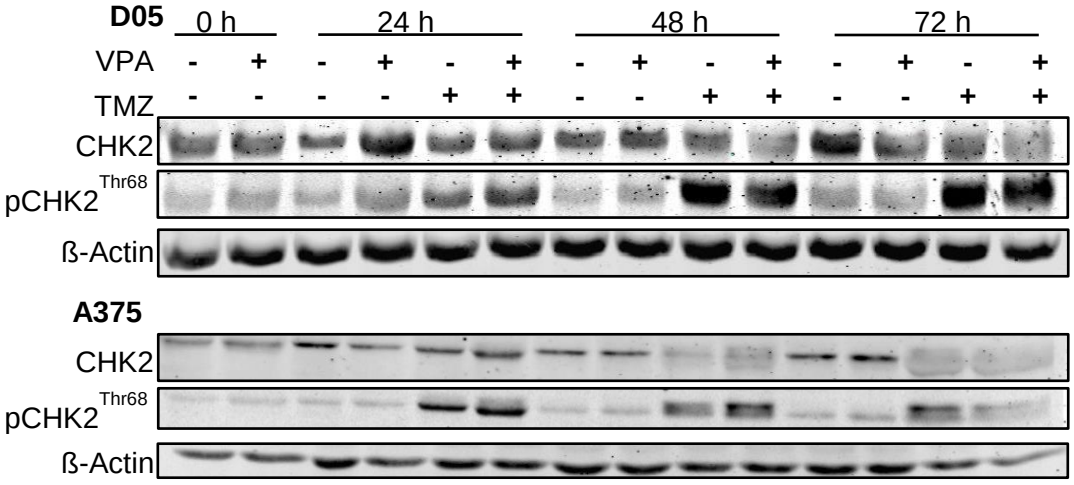

S 2 - TMZ-induced CHK2 phosphorylation in control and VPA pretreated melanoma cells.
Whole cell protein extracts of VPA pretreated (1 mM, 168 h) and untreated D05 and A375 cells were exposed to TMZ (50 µM). MGMT was depleted with O^6BG (10 µM) 1 h prior to TMZ treatment. At indicated times, total protein was extracted and subjected to immunoblotting.

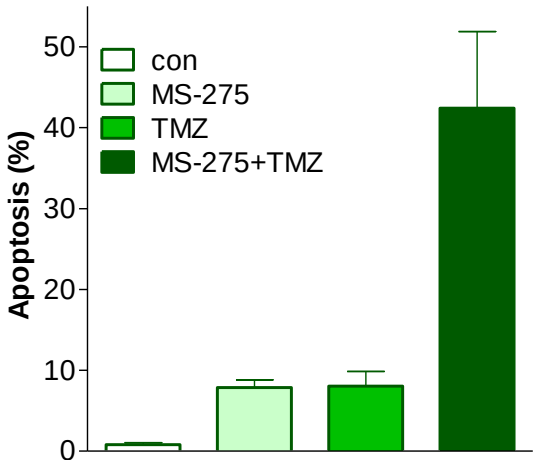

S 3 - Apoptosis induction by TMZ and late addition of MS-275.
LN229 cells were treated with TMZ (50 µM, 120 h) or additionally with MS-275 (2 µM) 24 h after TMZ treatment. Apoptosis was assessed by AnnexinV-FITC/PI staining and flow cytometry analysis.

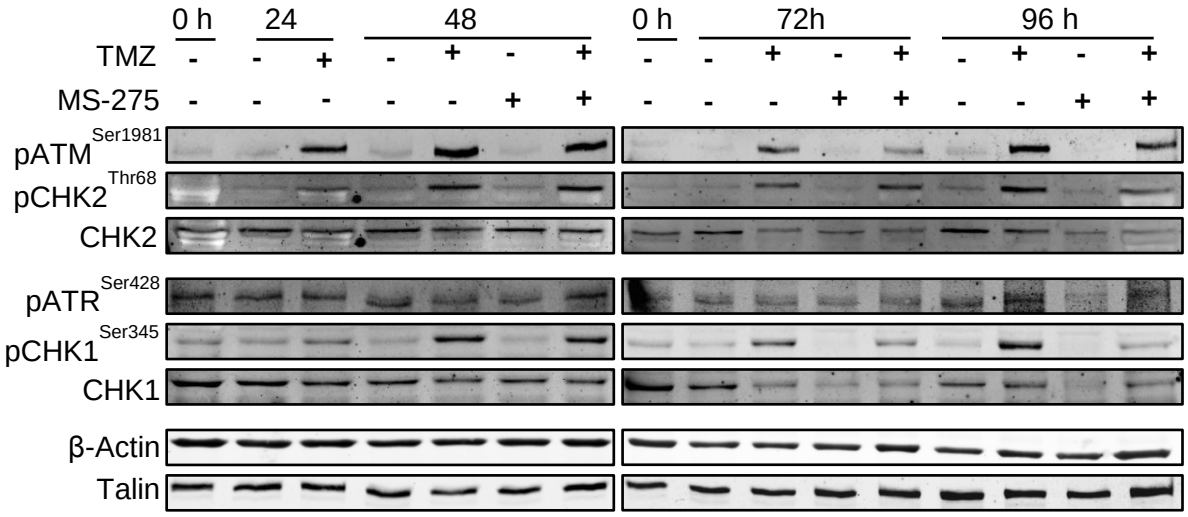

S 4 - Influence of MS-275 on TMZ-induced damage response.
Whole cell extracts of LN229 cells treated with TMZ (50 µM) and MS-275 (2 µM) 24 h later, single treated or untreated were subjected to immunoblotting to analyze damage signaling.

S 5 – VPA regulated genes.
D05 melanoma cells were treated with VPA (1 mM, 168 h) and gene expression was assessed by a real-time based PCR array. Relative expression (Rel. expression) is related to untreated controls.

Gene	Rel. expression	SD	Gene	Rel. expression	SD
ABH	0.94	± 0.33	***MMP 3***	0.17	± 0.06
APAF1	1.26	± 0.53	***MNAT1***	1.18	± 0.53
APEX 1	0.88	± 0.06	***MPG***	1.13	± 0.14
APTX	1.06	± 0.36	***MRE 11A***	1.15	± 0.23
ARTEMIS	0.89	± 0.32	***MSH 2***	1.04	± 0.18
ATG 5	1.33	± 0.12	***MSH3***	0.92	± 0.86
ATG 7	1.52	± 0.10	***MSH6***	0.83	± 0.08
ATM	1.25	± 0.70	***MTH1***	0.98	± 0.32
ATR	0.54	± 0.41	***MUS81***	1.09	± 0.13
ATRX	0.75	± 0.28	***MYH***	0.80	± 0.20
BAX	2.95	± 2.05	***NBS1***	0.71	± 0.33
BCL 2	0.66	± 0.33	***NEIL1***	0.90	± 0.45
BCL-XL	0.85	± 0.05	***NOXA***	2.59	± 0.26
BECN 1	1.52	± 0.22	***NTH1***	1.43	± 0.89
BID	1.26	± 0.21	***OGG 1***	0.97	± 0.24
BLM	0.73	± 0.38	***P21***	1.79	± 1.01
BRCA 1	0.82	± 0.16	***PARP 1***	1.03	± 0.15
BRCA 2	1.19	± 0.16	***PARP4***	1.08	± 0.46
CASP 2	1.20	± 0.49	***PCNA***	0.83	± 0.35
CCNA 1	18.29	± 5.33	***PMS2***	0.94	± 0.40
CCNE 1	1.37	± 0.21	***PNKP***	0.96	± 0.30
CCNH	0.94	± 0.34	***POLH***	0.83	± 0.16
CDC 25A	1.04	± 0.28	***POLI***	1.05	± 0.23
CDC 25B	0.77	± 0.19	***POLK***	1.49	± 1.29
CDC 25C	0.91	± 0.19	***POLQ***	0.94	± 0.32
CDK7	0.95	± 0.51	***PRKDC***	1.28	± 0.12
CDKN 1A	2.11	± 0.83	***PTEN***	1.64	± 0.17
CDKN 1B	1.73	± 0.19	***PUMA***	2.66	± 1.26
CHEK 1	1.24	± 0.33	***RAC 1***	0.35	± 0.34
CHEK 2	1.27	± 0.20	***RAD 51***	0.37	± 0.24
C-IAP 1	3.11	± 0.75	***RAD1***	1.69	± 1.90
C-JUN	1.14	± 0.30	***RAD17***	1.49	± 0.23
CSA	0.79	± 0.32	***RAD50***	1.12	± 0.59
CSB	1.02	± 0.38	***RAD51B***	1.06	± 0.69
CYP 1A1	3.46	± 0.65	***RAD51C***	1.04	± 0.44

DDB 2	1.20 ± 0.18	***RAD51D***	0.65 ± 0.10
DDIT 3	0.76 ± 0.11	***RAD52***	1.04 ± 0.64
DNMT	0.83 ± 0.31	***RAD54B***	0.68 ± 0.12
DUT	0.68 ± 0.24	***RAD9A***	1.00 ± 0.06
EME1	0.80 ± 0.22	***RB1***	0.97 ± 0.30
ERCC 1	1.95 ± 0.20	***RECQL 1***	1.12 ± 0.14
EXO1	0.97 ± 0.38	***REV 1***	1.05 ± 0.81
FAN1	0.58 ± 0.30	***REV 3***	1.28 ± 0.20
FANC C	1.49 ± 0.23	***REV7***	1.04 ± 0.71
FANCA	0.81 ± 0.35	***RHO A***	0.91 ± 0.21
FANCB	1.26 ± 0.58	***RHO B***	1.24 ± 0.19
FANCD2	0.67 ± 0.22	***RNA POL II***	0.75 ± 0.13
FANCE	0.93 ± 0.28	***SLX***	1.37 ± 0.60
FANCF	1.12 ± 0.48	***SMC 5***	1.76 ± 0.32
FANCG	0.98 ± 0.34	***SMC 6***	1.31 ± 0.18
FANCI	1.09 ± 0.25	***SMUG1***	1.91 ± 1.19
FANCJ	0.97 ± 0.66	***SOD 1***	1.01 ± 0.11
FANCL	1.31 ± 0.54	***SURVIVIN***	0.86 ± 0.21
FANCM	0.87 ± 0.76	***T53BP1***	1.03 ± 0.62
FANCN	0.89 ± 0.22	***TDG***	0.30 ± 0.34
FAS-R	0.91 ± 0.30	***TERT***	1.01 ± 0.42
FEN 1	1.08 ± 0.15	***TNKS***	1.30 ± 0.44
FOS	0.90 ± 0.06	***TOP3A***	1.11 ± 0.55
GADD 45A	2.37 ± 0.07	***TOP3B***	1.12 ± 0.37
GADD45B	0.66 ± 0.08	***TOPO II A***	0.93 ± 0.27
GPX 1	1.28 ± 0.32	***TOPO II B***	1.22 ± 0.04
GSTM 1	1.48 ± 0.55	***TRP 53***	0.80 ± 0.11
HIF 1A	1.41 ± 0.35	***TRP 73***	1.71 ± 1.39
HMOX 1	1.23 ± 0.48	***TXNRD 1***	1.70 ± 0.62
HSP 90	0.79 ± 0.24	***UNG2***	0.75 ± 0.24
HSPA 1B	0.99 ± 0.18	***WRN***	1.30 ± 0.44
HUS 1	0.97 ± 0.29	***WRNIP 1***	1.30 ± 0.38
IL 6	2.07 ± 0.50	***XIAP***	0.98 ± 0.51
KU70	0.72 ± 0.18	***XLF***	0.87 ± 0.19
KU80	0.62 ± 0.12	***XPA***	1.22 ± 0.09
LIG 3	0.90 ± 0.22	***XPB***	1.18 ± 0.46
LIG 4	1.82 ± 0.26	***XPC***	1.09 ± 0.29
MBD2	1.16 ± 0.32	***XPD***	1.01 ± 0.33
MBD4	0.94 ± 0.34	***XPF***	0.88 ± 0.28

MDM 2	1.34 ± 0.45	***XPG***	1.42 ± 0.53
MGMT	1.40 ± 0.19	***XRCC 3***	1.20 ± 0.38
MLH1	0.90 ± 0.28	***XRCC 4***	1.32 ± 0.23
MLH3	1.30 ± 0.94	***XRCC2***	1.34 ± 0.87

7.2 Abbreviations

APAF1 Apoptotic protease-activating factor 1
ADP Adenosine diphosphate
alt-EJ Alternative end joining
AP-site Apurinic/Apyrimidinic site
ATM Ataxia Telangiectasia Mutated
ATP Adenosine triphosphate
ATR Ataxia telangiectasia and Rad3-related protein
ATRIP ATR interacting protein
BER Base excision repair
BID BH3-interacting domain death agonist
BLM Bloom syndrome protein
BRAF Rapidly accelerated fibrosarcoma kinase B
BRCA2 Breast cancer type 2 susceptibility protein
BSA Bovine serum albumin
bwt Bodyweight
CAD Caspase activated Dnase
Caspase Cysteinyl-aspartate specific protease
CCNU N-(2-chloroethyl)-N'-cyclohexyl-N-nitrosourea (Lomustine)
cdc25 Cell division cycle phosphatase
CDK Cyclin-dependent kinase
CDKI CDK inhibitor
cDNA Complementary DNA
CENU Chloroethyl-nitrosourea
CHK1 Chekpoint kinase 1
CHK2 Chekpoint kinase 2
CPD Cyclobutane pyrimidine dimer
CSA Cockayne syndrome protein A
CSB Cockayne syndrome protein B
CtIP CtBP interacting protein
CTLA-4 Cytotoxic T-lymphocyte-associated antigen 4

DDB2	DNA damage-binding protein 2
DISC	Death-inducing signaling complex
DMEM	Dulbecco's modified Eagle medium
DMSO	Dimethylsulfoxide
DNA	Deoxyribonucleic acid
DNA-PKcs	DNA-dependent protein kinase catalytic subunit
DSB	DNA double-strand break
DSBR	DNA double-strand break repair
DTIC	5-(3,3-Dimethyl-1-triazenyl)imidazole-4-carboxamide (Dacarbazine)
DTT	Dithiothreitol
EDTA	Ethylenediaminetetraacetic acid
EGFR	Epidermal growth factor receptor
EME1	Essential meiotic structure-specific endonuclease 1
ERCC1	Excision repair cross-complementation group 1
ERK2	Extracellular signal-regulated kinase 2
EXO1	Exonuclease 1
FA	Fanconi anaemia
FADD	Fas-associated death domain protein
FANCD2	Fanconi anemia group D2 protein
FCS	Fetal calf serum
FITC	Fluorescein-isothiocyanate
FM	Fotemustine
GBM	Glioblastoma
GFP	Green fluorescent protein
GG-NER	Global genome nucleotide excision repair
Gy	Gray
H3ac	Acetylated histone 3
H4ac	Acetylated histone 4
HAT	Histone acetyl transferase
HDAC	Histone deacetylase
HEPES	4-(2-hydroxyethyl)-1-piperazineethanesulfonic acid
HR	Homologous recombination
ICL	Interstrand crosslink
IDH	Isocitrate dehydrogenase
IR	Ionizing radiation
LIG I	DNA ligase 1
MAPK	Mitogen-activated protein kinase

MEK	Mitogen-activated protein kinase kinase
MGMT	O^6-methylguanine-DNA methyltransferase
MMC	Mitomycin C
MMR	Mismatch repair
MNNG	N-methyl-N'-nitro-N-nitrosoguanidine
MPG	N-methylpurine-DNA glycosylase
MRE11	Meiotic recombination 11 homolog
MRN	MRE11-RAD50-NBS1-complex
mt	mutant
MTIC	3-methyl-(triazen-1-yl)imidazole-4-carboximide
N3MeA	N3-methyladenine
N7MeG	N7-methylguanine
NAD+	Nicotinamide adenine dinucleotide
NBS1	Nijmegen breakage syndrome protein 1
N-CoR	Nuclear receptor corepressor 1
NER	Nucleotide excision repair
NHEJ	Non-homologous end joining
***O*^{6}BG**	O^6-benzylguanine
***O*^{6}MeG**	O^6-methylguanine
OGG1	8-oxoguanine DNA glycosylase
PARP1	Poly (ADP-ribose) polymerase 1
PBMC	Peripheral blood mononuclear cell
PBS	Phosphate buffered saline
PCNA	Proliferating cell nuclear antigen
PD-1	Programmed cell death protein 1
PI	Propidium iodide
PNKP	Polynucleotide phosphatase/kinase
POL	Polymerase
PTEN	Phosphatase and Tensin homolog
qRT-PCR	Quantitative reverse transcription polymerase chain reaction
RFC	Replication factor C
RIPK1	Receptor-interacting serine/threonine-protein kinase 1
RNA	Ribonucleic acid
RNAPII	RNA polymerase II
ROS	reactive oxygen species
RPA	Replication protein A
RPMI	Roswell Park Memorial Institute Medium

RT	Room temperature
SCE	Sister chromatid exchange
SD	Standard deviation
SDS	Sodium dodecyl sulfate
SDSA	Synthesis-dependent strand annealing
SDS-PAGE	SDS polyacrylamide gel electrophoresis
SEM	Standard error of the mean
SIRT	Sirtuin
SMAC	Second mitochondria-derived activator of caspases
SSB	DNA single-strand break
ssDNA	Single-strand DNA
TBS-T	TRIS-buffered saline with Tween
TC-NER	Transcription coupled Nucleotide excision repair
TEMED	Tetramethylethylenediamine
TFIIH	Transcription factor IIH
TMZ	Temozolomide
TNF	Tumor necrosis factor
TRAIL	TNF-related apoptosis inducing ligand
TRIS	Tris(hydroxymethyl)aminomethane
TSG	Tumor suppressor gene
UDG	Uracil-DNA glycosylase
UV	Ultraviolet
VEGF	Vascular endothelial growth factor
VPA	Valproic acid
wt	wild type
XPA	Xeroderma pigmentosum group A-complementing protein
XPC	Xeroderma pigmentosum group C-complementing protein
XPF	Xeroderma pigmentosum group F-complementing protein
XPG	Xeroderma pigmentosum group G-complementing protein

7.3 Publications

Research papers:

Roos, W. P., Quiros, S., Krumm, A., Merz, S., Switzeny, O. J., Christmann, M., Loquai, C. and Kaina, B. (2014) *B-Raf inhibitor vemurafenib in combination with temozolomide and fotemustine in the killing response of malignant melanoma cells.* Oncotarget, 5, 12607-12620.

Krumm, A., Barckhausen, C., Kücük, P., Tomaszowski, K.-H., Loquai, C., Fahrer, J., Krämer, O. H., Kaina, B., Roos W. P. (2015) *Enhanced histone deacetylase activity in malignant melanoma provokes RAD51 and FANCD2 triggered drug resistance*. Submitted for publication.

7.4 Congresses (poster presentations)

IMB Conference – DNA Demethylation, DNA Repair and Beyond (2012) Mainz
Andrea Krumm, Christina Barckhausen, Bernd Kaina, Wynand P. Roos
Sensitization of p53 wild-type melanoma cells towards temozolomide by the histone deacetylase inhibitor valproic acid

8th World Congress of Melanoma (2013) Hamburg
Andrea Krumm, Christina Barckhausen, Bernd Kaina, Wynand P. Roos
The Histone Deacetylase Inhibitor Valproic Acid Sensitizes Melanoma Cells towards Temozolomide and Ionizing Radiation

German-French DNA Repair Meeting (2013) Strasbourg-Illkirch
Andrea Krumm, Christina Barckhausen, Bernd Kaina, Wynand P. Roos
The Histone Deacetylase Inhibitor Valproic Acid Sensitizes Melanoma Cells towards Genotoxic Stress by Downregulation of Rad51

GBS Jahrestagung (2013) Darmstadt
Andrea Krumm, Christina Barckhausen, Bernd Kaina, Wynand P. Roos
*Valproic Acid Reduces Rad51-dependent Homologous Recombination Repair thereby Sensitizing Melanoma Cells to Genotoxic Stres*s

13th Biennial Conference of the DGDR (2014) Mainz
Andrea Krumm, Christina Barckhausen, Bernd Kaina, Wynand P. Roos
Histone deacetylase inhibition by valproic acid sensitizes melanoma cells to chemotherapeutics by suppressing homologous recombination

30th Ernst Klenk Symposium in Molecular Medicine - DNA Damage Response and Repair Mechanisms in Aging and Disease (2014) Köln
Andrea Krumm, Christina Barckhausen, Bernd Kaina, Wynand P. Roos
Histone deacetylase inhibition by valproic acid sensitizes melanoma cells to chemotherapeutics by suppressing homologous recombination

18th International AEK Cancer Congress (2015) Heidelberg
Andrea Krumm, Christina Barckhausen, Pelin Küküc, Bernd Kaina, Wynand P. Roos
Inhibition of class I histone deacetylases in melanoma cells suppresses homologous recombination and sensitizes to chemotherapeutics